

8-Alkyl Adenines and Their Nucleoside Derivatives

by

Maha Abouelghit

A dissertation submitted to the Graduate Faculty of
Auburn University
in partial fulfillment of the
requirements for the Degree of
Doctor of Philosophy

Auburn, Alabama
August 6, 2011

Copyright 2011 by Maha Abouelghit

Approved by

Stewart W. Schneller, Chair, Professor of Chemistry and Biochemistry
Edward J. Parish, Professor of Chemistry and Biochemistry
Susanne Striegler, Associate Professor of Chemistry and Biochemistry
Orlando Acevedo, Assistant Professor of Chemistry and Biochemistry

Abstract

S-adenosylhomocysteine hydrolase has become an important target in the design of antiviral drugs. It is the only known enzyme in eukaryotes that is responsible for the catabolism of S-adenosylhomocysteine into adenosine and L-homocysteine. S-adenosylhomocysteine is both a product and potent feedback inhibitor of methylation reactions involving S-adenosylmethionine as a methyl donor. By inhibition of the methylation reactions responsible for formation of the mRNA 5'-cap required by most viruses for proper translation, the viral replication process is inhibited as well. Two carbocyclic nucleosides: aristeromycin and neplanocin have been shown to possess broad spectrum antiviral properties with severe toxicity. They have been used as templates for design of antiviral agents that retain the antiviral properties without the toxic side effects.

Purine ribofuranosyl nucleosides substituted in the 8-position have shown usefulness as probes for the study of nucleoside structural conformations. Based on the nature of the purine 8-substituent, the nucleoside can exist in a *syn/anti* equilibrium that shifts from a preferred *anti* arrangement towards the *syn* conformation that may become purely *syn* depending on the 8-substituent. In this research, a group of purine carbocyclic nucleosides with variable alkyl substituents were studied theoretically and synthetically with the intent of exploring their conformational parameters that could lead to correlation with biological activity. A theoretical

methodology, the density functional theory with various basis sets, was used to predict the structural parameters: phase angle of pseudorotation, the degree of pucker and the glycosyl torsion angle of the carbocyclic nucleosides. The results were compared to experimental data either obtained from the literature or generated within this research. The investigation was aimed at identifying the conformations that attribute to the observed experimental data as well as assessing the contribution of each conformation to the overall structure. The research also focused on studying the relationship between *syn/anti* conformation and the pseudorotation of the cyclopentyl moiety in carbocyclic nucleosides and extrapolating the findings from the 8-alkyl substituted carbocyclic nucleoside. A final aspect was providing the basis for uncovering a correlation between the *syn/anti* conformation and the biological activity of purine derived carbocyclic nucleosides, which was beyond the scope of this dissertation research.

To avail authentic carbocyclic nucleoside samples for this study, synthetic procedures were developed that called upon pyrimidine and cyclopentane/cyclopentene precursors. In that effort the Mitsunobu and Luche reactions and the Grubbs metathesis procedures were employed. The required compounds were obtained in overall reasonable yields and their structures verified by x-ray crystallography and a thorough NMR analysis using contemporary, multi-dimensional methods.

Acknowledgments

For this work to be accomplished, a lot of people put in a lot of their time and knowledge to help me reach this point of my life. Allowing me to join his research group in 2006, Dr. S.W. Schneller has opened a door for me into an enriched life with a lot of expectations that there will be something new to learn each and every passing day. His kind help and support combined with his immense knowledge about science as well as his philosophy about life created a journey for me that entailed a lot of learning that will shape the rest of my life. And for all that and more, he has my deepest gratitude. Stepping into this experience, allowed me the company of a lot of people whom without thinking and with a lot of energy gave me a lot of their help.

I have to express my utmost gratitude to Dr. Michael McKee and his student Tae Bum Lee. With their help and guidance, a large proportion of this work has been accomplished. I would like to express my gratitude to Drs. Susanne Striegler, Holly Ellis, Orlando Acevedo, and Edward Parish for helping me with this project. The knowledge I received in the classrooms of the Chemistry and Biochemistry Department as well as the Harrison School of Pharmacy has been immense and I thank each and everyone who contributed to this learning experience mainly Dr. Randall Clark to whom I owe a lot both on a professional as well as personal levels. I would like to thank Dr. Smita Mohanty for her help with the NMR experiments run on the 600 MHz machine. I would also like to thank Dr. John Gordon for his help with the X-ray crystallography. I would like also to thank Drs Wei Ye, Chong Liu, Olena Musiienko and Qi Chen for their help

with my lab experience. I would also like to thank Volodymyr Musiienko and Sherif Hamad for lot of help with my lab techniques. The knowledge I received in the NMR lab and the Mass Spectroscopy labs under the guidance of Drs. Michael Meadows, and Yonnie Wu is greatly appreciated. I extend my gratitude to the Department of Chemistry and Biochemistry and the National Institutes of Health for their financial support.

Finally without the love and encouragement of my family and my husband, Tamer Awad, I would not be writing this today.

Table of Contents

Abstract.....	ii
Acknowledgments	iv
List of Tables	vii
List of Figures.....	viii
List of Schemes.....	x
List of Graphs	xii
Introduction.....	1
Biological Background	1
Computational Background	16
Rational for Research	22
Chapter 1 Theoretical Investigation of Carbocyclic Nucleosides	25
Chapter 2 Synthesis of Required Precursors	43
Synthesis of the Carbocycle	43
Synthesis of the Heterocyclic Nucleobase.....	50
Chapter 3 Synthesis of 8-Alkylaristeromycin.....	61
Chapter 4 Synthesis of 8-Substituted 4'-Norneplanocin Analogues.....	68
Chapter 5 Analysis of 8-Ethylaristeromycin (2).....	74
Conclusion	84
Experimental Details	86

References	106
Appendix	114

List of Tables

Table 1 Results of initial geometry optimization of 4 compounds.....	28
Table 2 Summary of the molecules from B3LYP/3-21G	29
Table 3 PROSIT output for (A) after single point energy in solution	30
Table 4 Results shown for AA1 and AA2 based on single point energy in solution	32
Table 5 Results shown for BB1, BB3 and BB4 based on single point energy in solution	33
Table 6 Results shown for CC1 and CC4 based on single point energy in solution	34
Table 7 Results shown for DD3 and DD4 based on single point energy in solution	35
Table 8 A Comparison of experimental and theoretical spin-spin coupling constants for (A) .	37
Table 9 A Comparison of experimental and theoretical spin-spin coupling constants for (B)...	38
Table 10 A Comparison of experimental and theoretical spin-spin coupling constants for (C)	39
Table 11 A Comparison of experimental and theoretical spin-spin coupling constants for (D)	40
Table 12 Initial conformers chosen for pseudorotation study of (F)	74
Table 13 Conformations based on single point energy calculations in solution of (F)	76
Table 14 A Comparison of experimental and theoretical spin-spin coupling constants for (F)	80

List of Figures

Figure 1 Nucleotides vs. nucleosides.....	1
Figure 2 Naturally occurring nucleosides	2
Figure 3 Stereochemistry of (A) β -nucleoside, (B) α -nucleoside.....	3
Figure 4 Carbocyclic Nucleosides as a modification of ribofuranoside nucleosides	3
Figure 5 Aristeromycin and Neplanocin A.....	5
Figure 6 Structure of S-adenosyl-L-methionine (AdoMet)	6
Figure 7 AdoMet metabolism.....	7
Figure 8 First generation AdoHcy hydrolase inhibitors	12
Figure 9 Second generation AdoHcy hydrolase inhibitors.....	14
Figure 10 Purine Nucleoside numbering	17
Figure 11 Pseudorotation cycle.....	18
Figure 12 Adenosine showing <i>syn</i> and <i>anti</i> conformations.....	20
Figure 13 Classical staggered rotational isomers around C4'-C5'	21
Figure 14 Targets 1, 2	23
Figure 15 DHCA Analogues.....	24
Figure 16 Compounds involved in the study	25
Figure 17 Starting six geometries for all 4 compounds, example shown is compound A.....	27

Figure 18 Grubbs catalysts.....	47
Figure 19 Structure of 32 from X-ray analysis.	60
Figure 20 Structure of 1 from X-ray analysis.	66
Figure 21 Structure of 7 from X-ray analysis	73
Figure 22 Initial optimization of 8-ethylaristeromycin (F).....	75
Figure 23 Final geometries for F after NMR calculations.....	77
Figure 24 Portion of ¹ HNMR spectrum of F in D ₂ O showing overlapping H2'	78
Figure 25 Portion of ¹ HNMR spectrum of F in D ₂ O (327 °K) showing resolved peaks	79
Figure 26 Structure of 2 from X-ray analysis	81
Figure 27 Summary of correlation study between theoretical and experimental data.....	82

List of Schemes

Scheme 1 Effect of phosphorylases on natural and modified nucleosides	4
Scheme 2 Toxicity of Ari and NpcA due to phosphorylation	5
Scheme 3 Structure of 5'-cap of mRNA	8
Scheme 4 Formation of AdoHcy as a byproduct of methylation reaction.....	9
Scheme 5 Mechanism of action of AdoHcy hydrolase.....	11
Scheme 6 Mechanism of Type I mechanism-based AdoHcy hydrolase inhibitors	13
Scheme 7 Mechanism Type II mechanism-based AdoHcy hydrolase inhibitors	14
Scheme 8 Convergent retrosynthesis towards target compounds and their precursors	44
Scheme 9 The synthesis of cyclopentenone 15 from D-ribose.....	46
Scheme 10 Reaction mechanism of RCM	48
Scheme 11 Synthesis of precursor 17	49
Scheme 12 Synthesis of precursor 18	49
Scheme 13 Purine synthesis based on various reagents.....	51
Scheme 14 Synthesis of 6-chloro-8-methylpurine 21	52
Scheme 15 Amination of 4,6-dichloropyrimidin-5-amine.....	53
Scheme 16 Synthesis of 28 using carboxylic acid	54
Scheme 17 Synthesis of 28 using acid chloride.....	54
Scheme 18 Synthesis of 28 using orthoesters	55
Scheme 19 Intermediates 26 and 27 from the orthoester reaction.....	56

Scheme 20 Proposed reaction mechanism for the formation of 28 from intermediates 26, 27 ..	57
Scheme 21 Synthesis of 29	58
Scheme 22 Proposed mechanism for formation of 45	59
Scheme 23 Synthesis of 6-chloro-8- <i>t</i> -butylpurine using acid chloride.....	59
Scheme 24 Synthesis of 1 based on unpublished results using the linear route	62
Scheme 25 Proposed mechanism for side products	63
Scheme 26 Retro synthesis of 8-alkyl substituted Aristeromycin	64
Scheme 27 Synthesis of compound 1 by the convergent route	65
Scheme 28 Synthesis of compound 2 by the convergent route	67
Scheme 29 Retrosynthesis of targets 3, 4, 5, 6 and 7 using the convergent route	69
Scheme 30 Synthesis of targets 3, 4, 5 and 6	71
Scheme 31 Convergent synthesis of target compound 7	72

List of Graphs

Graph 1 Relative energy in solution for A	32
Graph 2 Relative energy in solution for B	33
Graph 3 Relative energy in solution for C	34
Graph 4 Relative energy in solution for D	35
Graph 5 Relative energy in solution for F	76

Introduction

Biological Background

What are Nucleosides?

Nucleic acids, elements of heredity and agents of genetic information transfer are formed from linear polymers of nucleotides. Nucleotides are biological molecules that are composed of a heterocyclic base, a five-carbon sugar (pentose) and a phosphate group (Figure 1).¹ The two main classes of nucleic acids are deoxyribonucleic acid (DNA) and ribonucleic acid (RNA). The sugar moiety for the former is 2-deoxyribose and for the latter is ribose. Nucleosides form upon attachment of the sugar to a heterocyclic nucleobase through a β -glycosidic linkage.

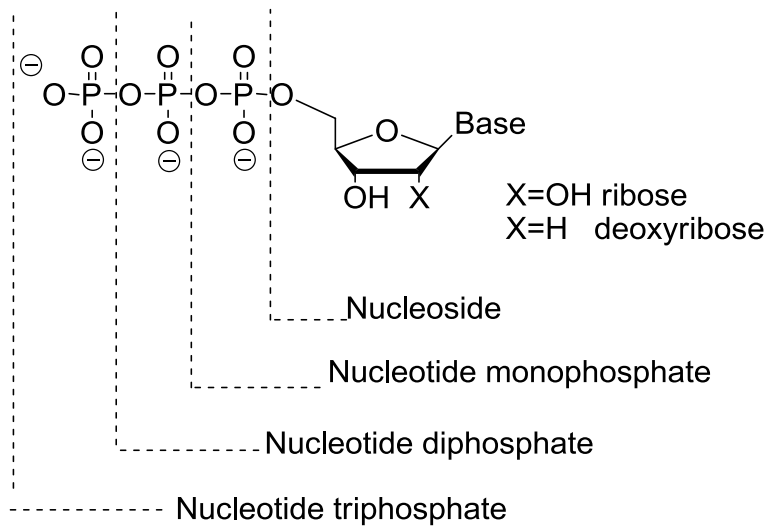


Figure 1. Nucleotides vs. nucleosides

The bases are planar aromatic heterocyclic molecules that are divided into two groups: the pyrimidine bases thymine and cytosine and in DNA the purine bases adenine and guanine with thymine being replaced with Uracil in RNA² (Figure 2).

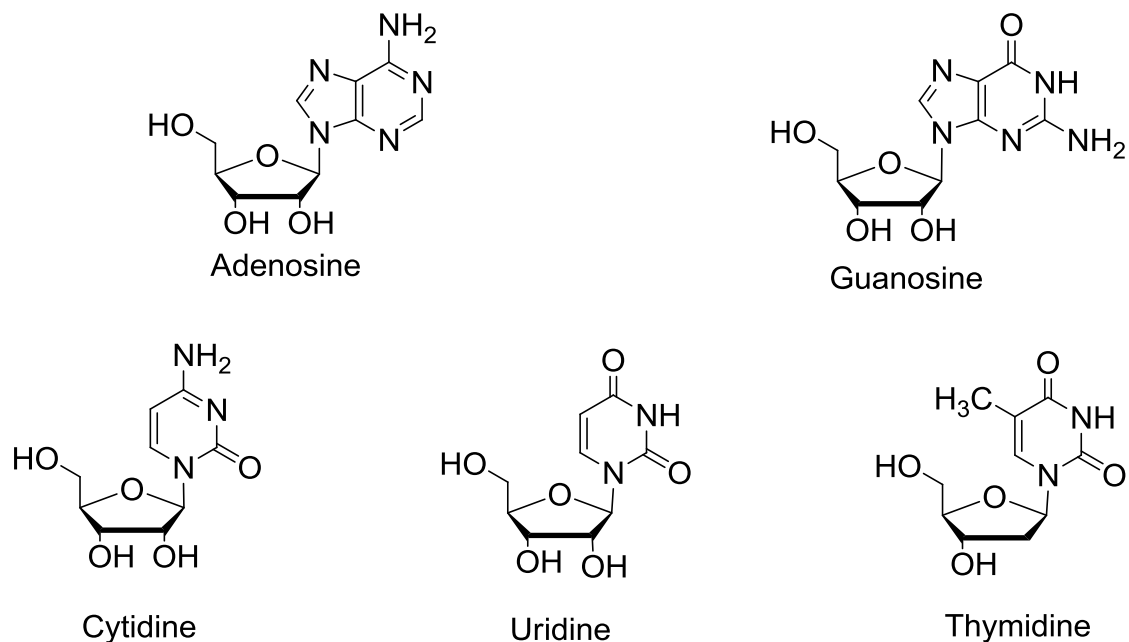


Figure 2. Naturally occurring nucleosides.

The bond between the sugar and the base is known as the glycosidic bond and its stereochemistry is β for the natural nucleic acids, which means that the base and the 4'-hydroxymethyl group are above the plane of the sugar² i.e. *cis* to each other (Figure 3). If the base is *trans* to the 4'-hydroxymethyl group, the nucleoside is considered α . Naturally occurring nucleosides and their analogues have been widely studied for their antiviral and anticancer properties.³

Purine nucleosides, in particular are of great interest chemically and pharmacologically, especially those compounds that are structurally related to adenosine (Ado) and possess

biological activity as antiviral, antitumor agents, and enzyme inhibitors.⁴ Adenosine is an intracellular modulator that mediates a wide variety of physiological functions including vasodilatation, vasoconstriction in the kidney, inhibition of platelet aggregation, inhibition of insulin release, and potentiating of histamine release.⁵

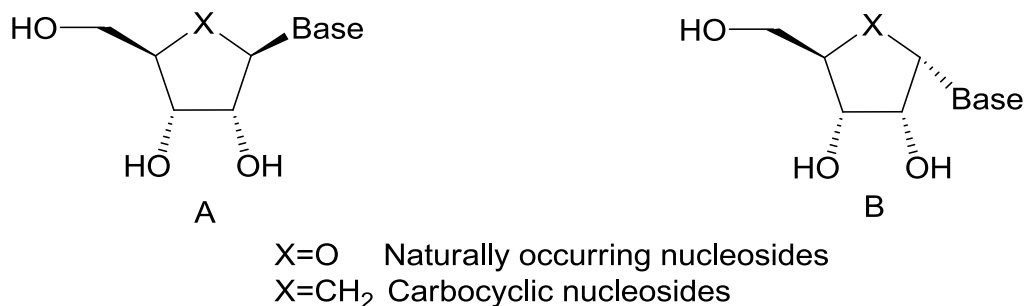


Figure 3. Stereochemistry of (A) β -nucleoside, (B) α -nucleoside

What are Carbocyclic Nucleosides?

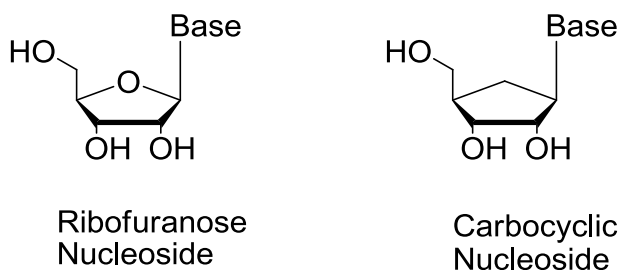
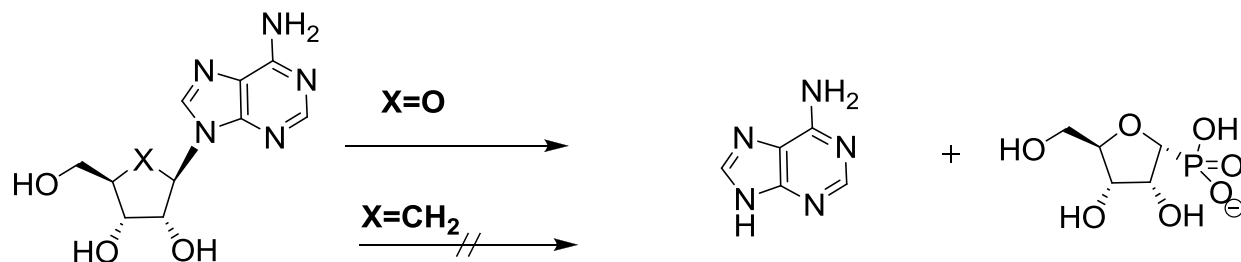


Figure 4. Carbocyclic nucleosides as a modification of ribofuranoside nucleosides

Carbocyclic nucleosides are analogues of naturally occurring nucleosides in which the furanose ring oxygen has been replaced with a methylene group (Figure 4). This modification transforms the glycosidic bond from an unstable hemiaminal to a more stable tertiary amine.⁶

This gives carbocyclic nucleosides potent metabolic stability due to resistance to phosphorylases and hydrolases that cleave the glycosidic bond of their natural counterparts (Scheme 1).⁷ These nucleoside analogues display a wide range of biological activities.⁸ The most important of which are being antiviral, antiparasitic, fungicidal and anti-tumor activities.⁹ Their activity in part is due to being recognized by the same enzymes that recognize the natural nucleosides.



Scheme 1. Effect of phosphorylases on natural and modified nucleosides

Two carbocyclic nucleosides stand out; aristeromycin (Ari) and neplanocin A (NpcA) (Figure 5). Aristeromycin was first described by Shealy and Clayton¹⁰ in 1966, two years before it was isolated as a metabolite from *Streptomyces citricolor*.¹¹ NpcA on the other hand was isolated from *Ampulariella regularis* in 1981.¹² Both compounds possess excellent chemical and metabolic stability of the glycosidic bond as well as broad-spectrum antiviral activity. In addition, both demonstrate potent inhibitory activity of S-adenosyl-L-homocysteine hydrolase (AdoHcy hydrolase). Cools and De Clerq¹³ have shown a correlation between their antiviral potency and their inhibitory effects towards AdoHcy hydrolase. AdoHcy hydrolase is an enzyme involved in the regulation of the biomethylation reactions dependent on S-adenosylmethionine, which, in turn, is crucial to viral replication.^{14,15} Severe toxicity has banned these two compounds from clinical use; however, it opened the door for a huge research area into the reasons behind their toxicity and how to modulate it for the sake of better antiviral analogues.

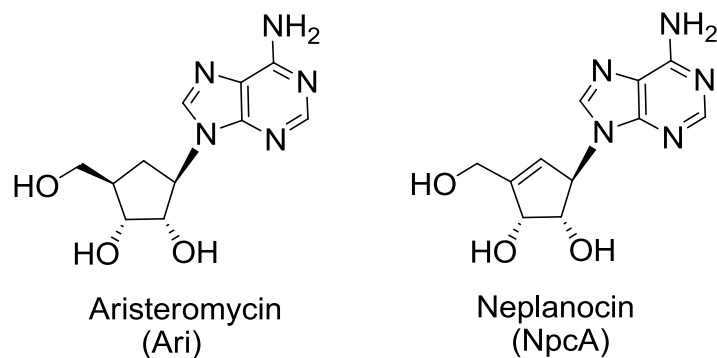
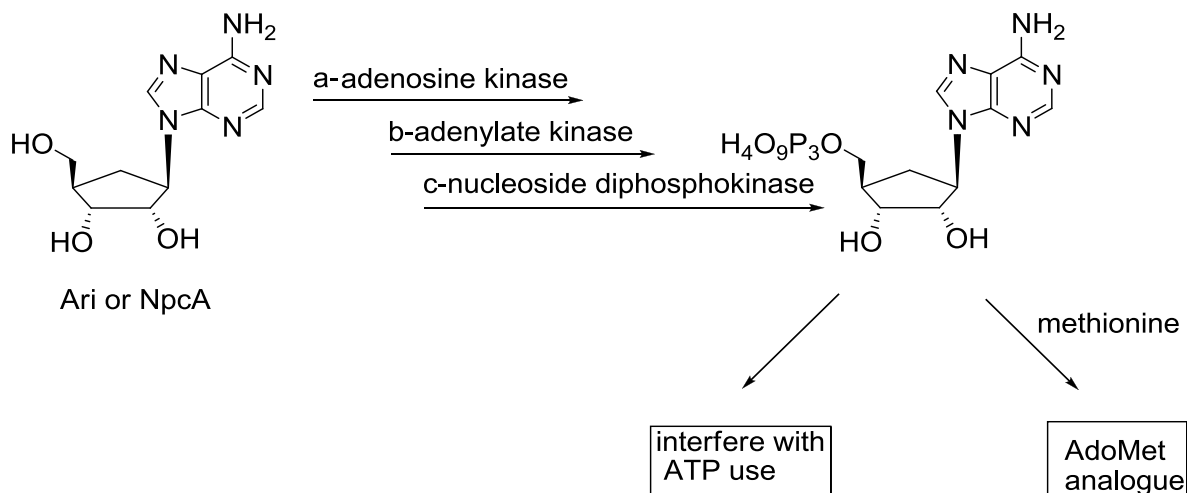


Figure 5. Aristeromycin and Neplanocin A

The cytotoxicity of Ari¹⁶ and NpcA¹⁷ is attributed to the fact that they are both substrates to adenosine kinase (Scheme 2). Interaction with kinases in the cell leads to the formation of the 5'-triphosphate analogues of the naturally occurring adenosine thus interfering with biological processes in which ATP is involved.¹⁸ Another aspect concerning NpcA⁹ toxicity is that it is converted to neplanocylmethionine¹⁹ (the AdoMet analogue) via interaction with methionine which is believed to be the mechanism by which NpcA exerts its cytotoxicity.



Scheme 2. Toxicity of Ari and NpcA due to phosphorylation.

What is SAM/AdoMet?

S-adenosyl-L-methionine (SAM, AdoMet) is one of the most versatile molecules in nature, is found in almost all phyla of living things, and is crucial for the existence of living organisms (Figure 6).

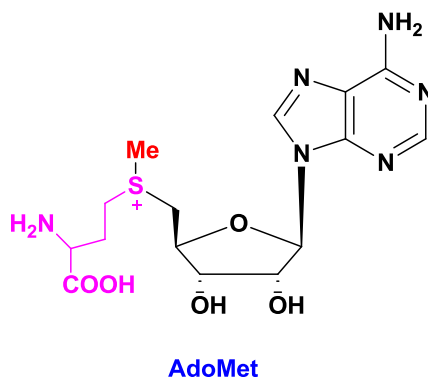


Figure 6. Structure of S-adenosyl-L-methionine (AdoMet).

First, identified by Cantoni²⁰ as a product formed from L-methionine and adenosine triphosphate (ATP) under catalysis of SAM synthetase, AdoMet is involved in a number of metabolic activities.²¹ One of the most important processes is that AdoMet serves as a cofactor methyl donor for numerous methyltransferases that catalyze the methylation of various molecules. These include macromolecules like proteins, RNA, DNA and polysaccharides as well as small molecules like phospholipids, histamines and catecholamines.¹⁹ The methylation of mRNA, has drawn a lot of attention among other methylation reactions, could happen either at the 2'-hydroxyl group of the ribose moiety or at the N-7 of the guanosine residue. Figure 7 shows the involvement of AdoMet in various biological processes.

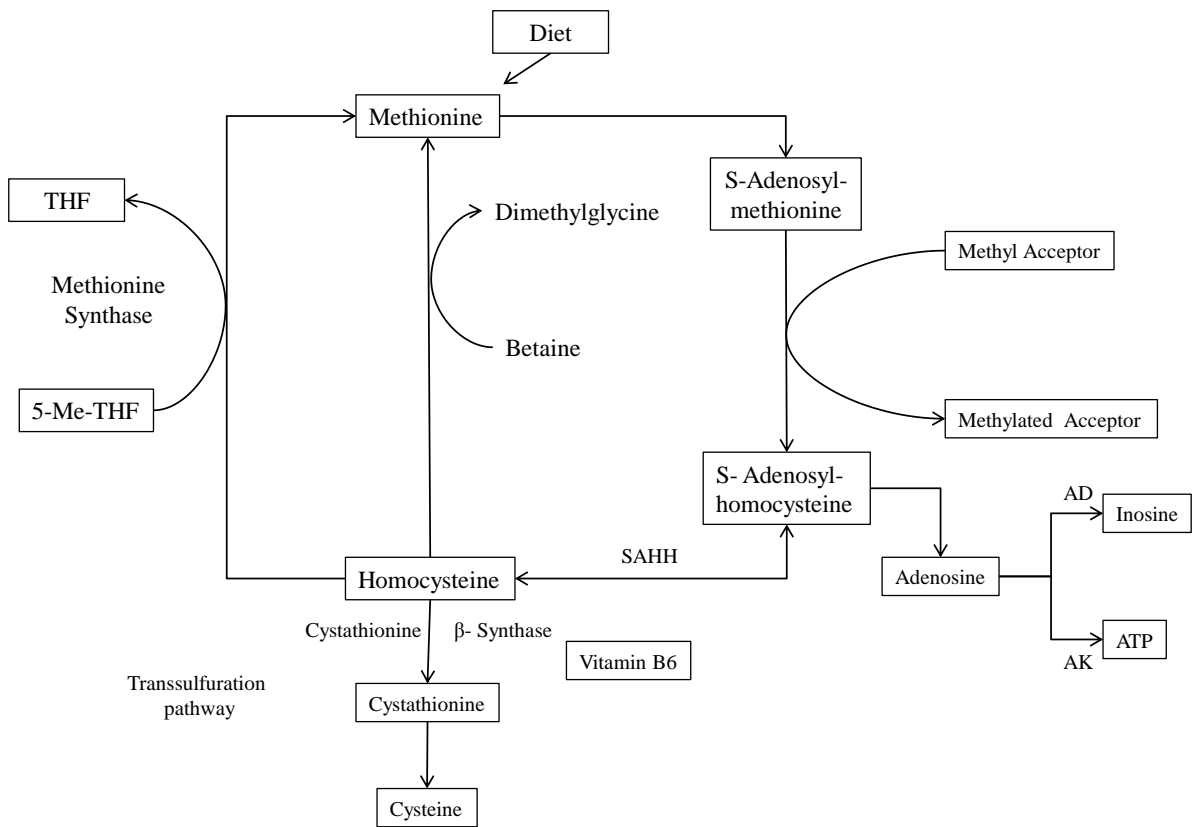
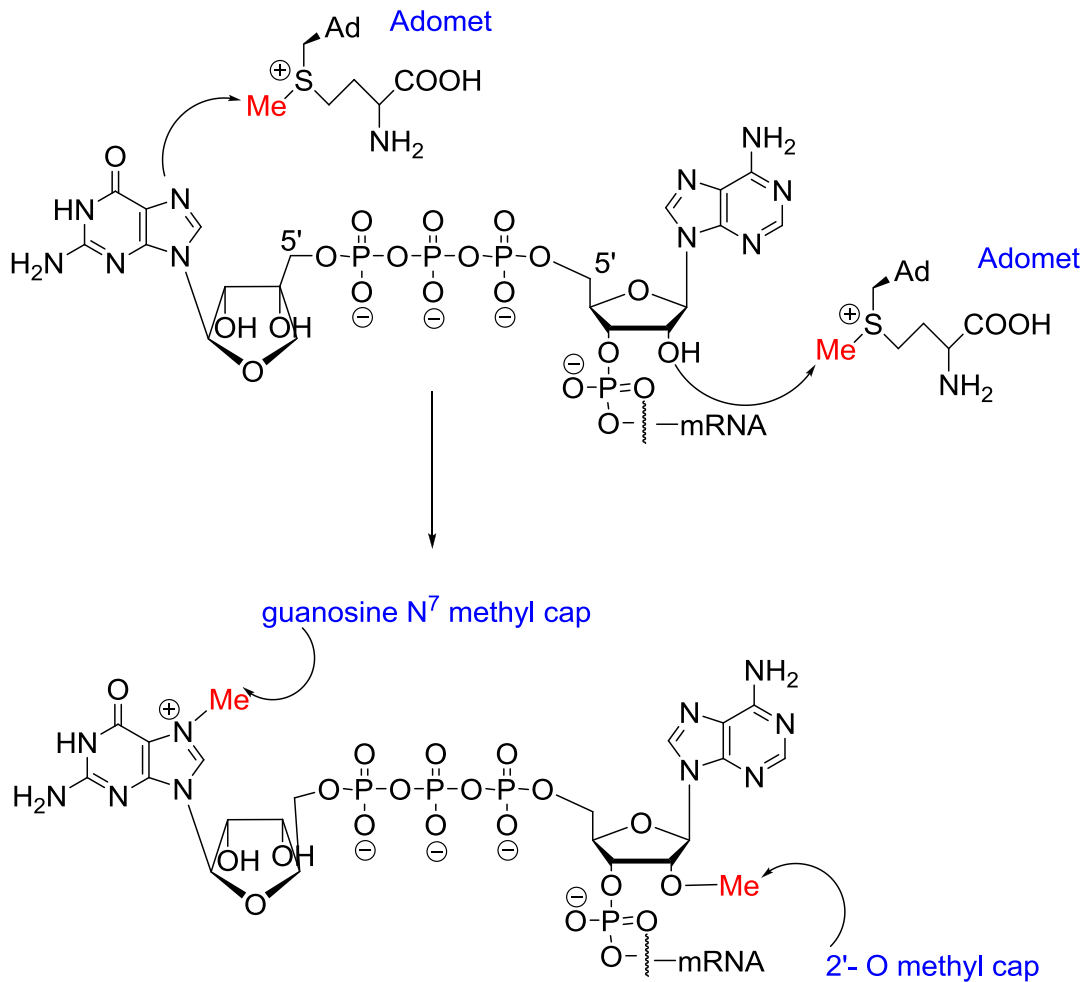


Figure 7 AdoMet Metabolism.

One of the most well-defined methylation reactions in RNA is the mRNA methylation. A variety of eukaryotic cells and viruses require enzymatic methylation of the 5'-terminal residue of their mRNA to form the 5'-methylated cap structure essential for proper translation to proteins and, subsequently, viral replication.²² In this 5'-cap (Scheme 3) a guanosine residue, transferred from guanosine triphosphate (GTP), blocks the 5'-terminal of the penultimate base of mRNA through a unique 5'-5' triphosphate linkage. Subsequently, the N-7 of the guanosine residue as well as the ribose moiety of one or more of the penultimate bases are methylated via AdoMet-dependent methylation enzymatic reactions.



Scheme 3. Structure of 5'-cap of mRNA.

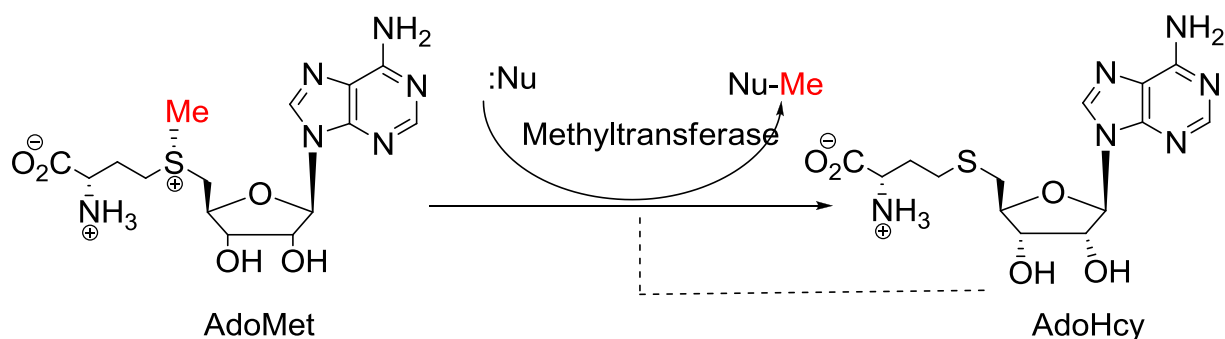
The enzymes involved in the cap formation include²³:

- (i) RNA triphosphatase: cleavage of the 5' triphosphate terminus in a transcribed RNA to a diphosphate-terminated RNA.
- (ii) mRNA guanylyltransferase: capping of the diphosphate terminus with GMP.
- (iii) mRNA (guanine-7-)methyltransferases: methylation at the N-7 position of guanine (methyl group from AdoMet).
- (iv) 2'-O-Methyltransferase: methylation of the 2'-O-ribose moiety of the penultimate nucleoside.²²

The 5'-cap structure of mRNA offers stability against phosphatases and ribonucleases hence imparting stability to the mRNA in the cell.²² It has also been recognized as playing a significant role in the interaction between mRNA and ribosomal RNA or its protein components during initiation of protein synthesis and for the promotion of splicing.¹⁴

Why has S-Adenosylhomocysteine (AdoHcy) Hydrolase (AdoHcy hydrolase; EC 3.3.1.1) become an intriguing target for antiviral drug design?¹⁴

After AdoMet participates in a methylation reaction in which an activated methyl group is being transferred to a recipient biological molecule in the cell, the product is the formation of S-adenosylhomocysteine (AdoHcy). (Scheme 4)

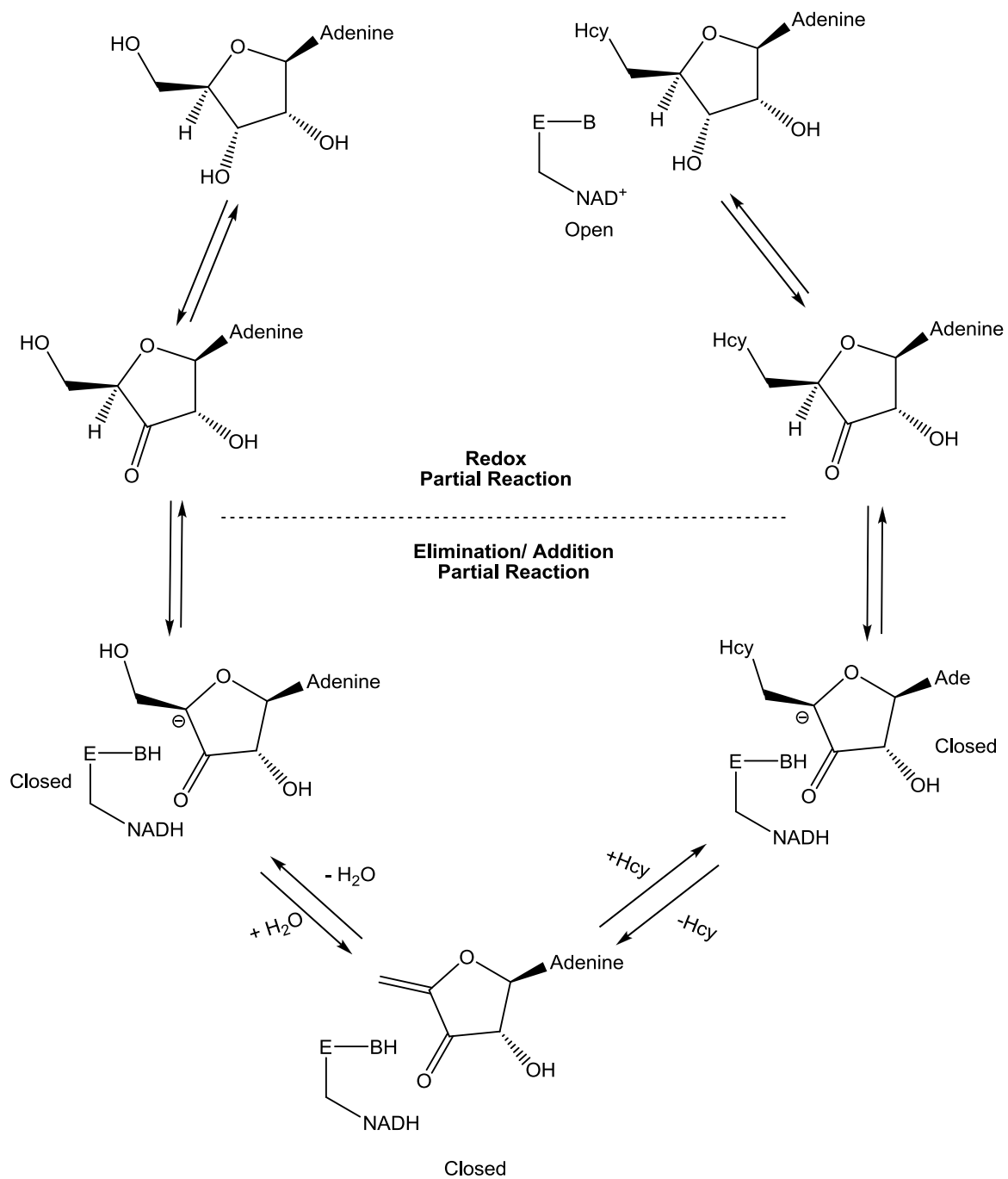


Scheme 4. Formation of AdoHcy as a byproduct of methylation reactions

AdoHcy hydrolase is the only known enzyme that catalyzes the reversible conversion of AdoHcy to adenosine (Ado) and homocysteine (Hcy). In vitro, the equilibrium of this reaction lies towards the synthetic pathway, although the reaction is pulled towards the hydrolytic direction due to efficient enzymatic removal of adenosine (Ado) and homocysteine (Hcy) under the physiological conditions.¹⁹ AdoHcy is a potent competitive feedback inhibitor of all AdoMet-

dependent methyltransferases. On the hydrolytic side, Ado is being converted via the purine degradation pathway into inosine by adenosine deaminase (ADA) or to adenosine triphosphate (ATP) by adenosine kinases (AK). On the other hand, Hcy enters the remethylation and transsulfuration pathways in a 50:50 ratio.²⁴ Remethylation of Hcy occurs via two routes: irreversible methylation via betaine (trimethyl glycine) in the liver and kidney²⁵ and the other involves a transfer of a methyl group to Hcy from 5-methyltetrahydrofolate via methionine synthase. In the transsulfuration pathway Hcy is being converted to cystathionine via cystathionine- β -synthase. Figure 6 shows an overall outlay for the position of AdoHcy hydrolase in the methionine, transmethylation and transsulfuration metabolic pathways.

The reaction mechanism of AdoHcy hydrolase has been reported by Palmer and Abeles^{26,27} (Scheme 5). The first step is the oxidation of the 3'-hydroxyl group in the enzyme-bound adenosine complex to a ketone with the concomitant reduction of the tightly bound NAD⁺ to NADH. This step results in the activation of 4'-H that is now more acidic and removed via a basic residue in the active site. This is followed by loss of homocysteine. Water adds in a Michael type fashion to the α , β -unsaturated ketone intermediate. NADH then reduces the 3'-ketone back to a hydroxyl group generating Ado, which then dissociates from the enzyme. Scheme 5 shows both the hydrolytic and synthetic pathways involved in the catalytic cycle of AdoHcy hydrolase with B being the residue responsible for accepting and returning the proton at the 4' position. There are two distinct conformations of AdoHcy hydrolase which are the open and closed forms.²⁸ In the resting state, the catalytic and the cofactor binding domains are opened to allow exposure of the active site to the environment. Upon ligand binding, the enzyme transforms to the closed conformation to allow for catalysis. Both conformations are responsible for regulation of the steps involved in the catalytic cycle.



Scheme 5. Mechanism of action of AdoHcy hydrolase²⁹

AdoHcy inhibitors can be divided into three groups based on the history of their discovery. Across the evolution of these inhibitors, the common goal was to develop more potent and more specific inhibitors.³⁰

(A) **First generation inhibitors**: include both naturally occurring carbocyclic analogues and synthetic cyclic or acyclic Ado analogues.

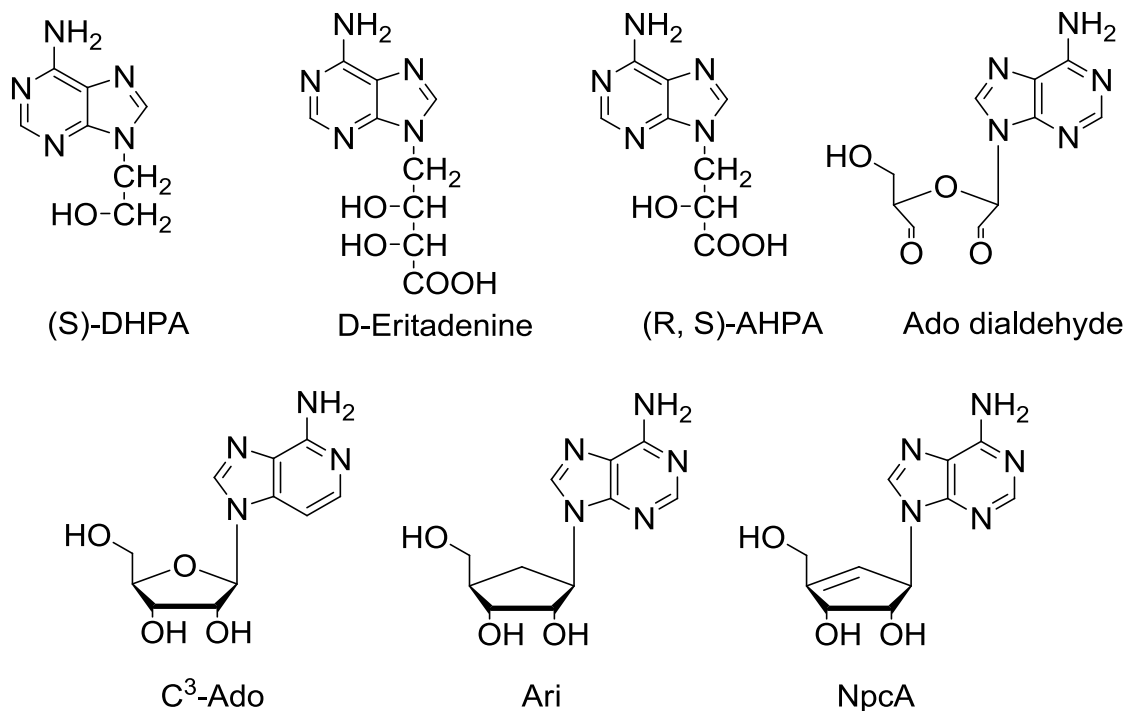
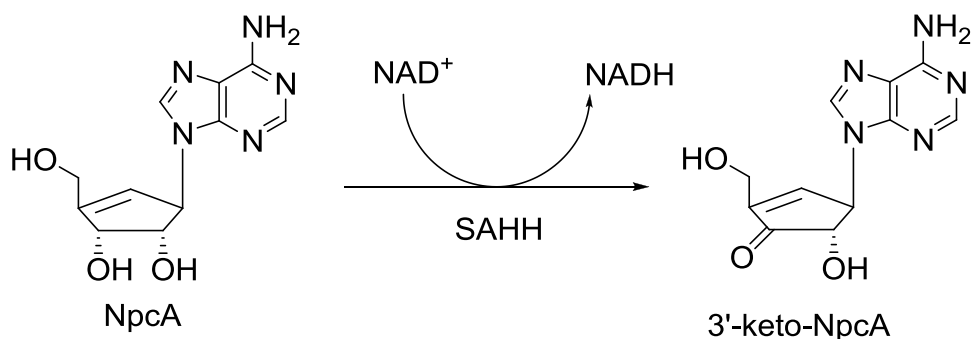


Figure 8. First Generation AdoHcy hydrolase inhibitors

Some inhibitors inactivate AdoHcy Hydrolase irreversibly and become tightly bound to the enzyme like Ado dialdehyde and NpcA, while others are reversible competitive inhibitors of the enzyme like Ari. NpcA inactivation belongs to Type-I-mechanism-based inhibitors¹⁴ where neplanocin inhibits AdoHcy hydrolase by a cofactor-depletion mechanism. After binding to the active site, the inhibitor is oxidized at the C3' position to give the 3'-keto along with the concomitant reduction of the enzyme-bound NAD⁺ leading to consumption of NAD⁺ by the

inhibitor and this leads to inactivation of the enzyme. These are exemplified by NpcA. A common feature of this generation is their cellular toxicity (Scheme 6).³⁰



Scheme 6. Mechanism of Type I mechanism-based AdoHcy hydrolase inhibitors

(B) Second Generation Inhibitors:

These were designed with an attempt to be more specific along with fewer capabilities to serve as substrates for adenosine kinase and adenosine deaminase; which is the source of their toxicity. The design was based on two directions: the first was to replace the adenine moiety in NpcA and Ari where with 3-deazaadenine (C^3 -NpcA, C^3 -Ari) and the second approach used to remove the 4'-hydroxymethyl group thus prevent 5'-phosphorylation via Ado kinase and deamination via Ado deaminase and these efforts resulted in DHCA and C^3 -DHCA and their saturated counterparts (Figure 9).^{31,32} These compounds exhibit broad-spectrum antiviral activity while their toxicity is lower than the first generation and they are not substrates for either Ado deaminase or Ado kinase. The deaza nucleosides are reversible competitive inhibitors of AdoHcy hydrolase while their truncated counterparts irreversibly inactivate the enzyme via a type I mechanism.

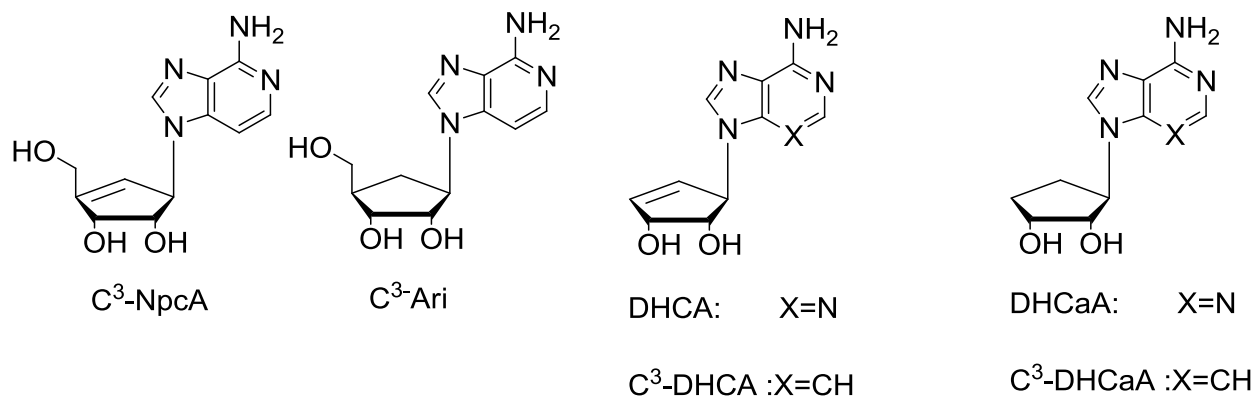
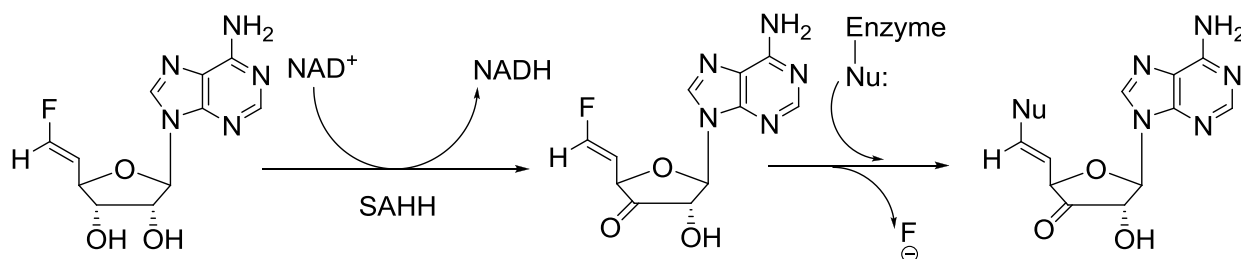


Figure 9. Second generation AdoHcy hydrolase inhibitors.

Another set of compounds was designed as part of the second generation as type II-mechanism based inhibitors of AdoHcy Hydrolase. These inhibitors are able to bind covalently at the active site of the enzyme and cause permanent irreversible inhibition in addition to causing NAD⁺ depletion. An example is (Z) 4', 5'-didehydro-5'-deoxy-5'-fluoroAdo. The type – II mechanism of inhibition is shown in Scheme 7.^{14,33}



Scheme. 7. Mechanism of Type II mechanism-based AdoHcy hydrolase inhibitors¹⁴

(C) Third Generation Inhibitors:

This generation has been designed as a prodrug that would be converted within the active site into a potent drug³³, and is based on the hydrolytic activity of AdoHcy hydrolase.

In conclusion, inhibition of AdoHcy hydrolase results in the accumulation of AdoHcy, which is both a product and a feedback inhibitor of AdoMet-dependent methylation reactions. As these methylations are important in securing the formation of the 5'-cap in viral mRNA, this capping process is being disrupted and, consequently, the viral replication is inhibited.^{14,34} AdoHcy hydrolase inhibitors are potent broad spectrum antiviral agents inhibiting an array of (-) RNA (measles, vesicular stomatitis, and parainfluenza), double stranded (\pm) RNA (i.e., reo and rotavirus) viruses and DNA poxviruses (vaccinia and African swine fever).¹⁴ They don't exhibit activity towards (+) RNA or HIV.

Computational Background:

To allow for us to understand the biological function of nucleotides and nucleic acids, we need to study their conformational characteristics.³⁵ This can be done with X-ray crystallography, spectroscopic techniques, mainly NMR, and theoretical studies. All of these methods will allow for a better understanding and characterization of the genetic materials. In addition, a ligand's activity might be correlated with its preferred structure in solution.³⁶ Research directed towards the determination of the stereochemistry of molecules in solution plays a crucial role in the understanding of interactions in both the chemical and biochemical reactions.³⁷ Defining the terms used in describing the geometry of nucleotides and nucleic acids is fundamental in understanding and explaining the results obtained via the various techniques used in their structural elucidation and giving way to a more comprehensive understanding of their properties.

The nucleotide is the basic motif in DNA and RNA. It is composed of the heterocyclic base, the sugar and the phosphate group (Figure 1).^{35,38} The conformational details of their structure has been well defined by the torsion angles $\alpha, \beta, \gamma, \delta, \epsilon$ and ζ in the phosphate backbone, $\nu_0-\nu_4$ in the furanose ring and χ for the glycosylic bond. However, due to the interdependency of those torsional angles, the shape of nucleotides (sides) can be described in terms of four parameters:

- (1) The sugar pucker.
- (2) The *syn-anti* conformation of the glycosylic bond (χ).
- (3) The orientation of the C4'-C5' (γ).
- (4) The shape of the phosphate ester bond.

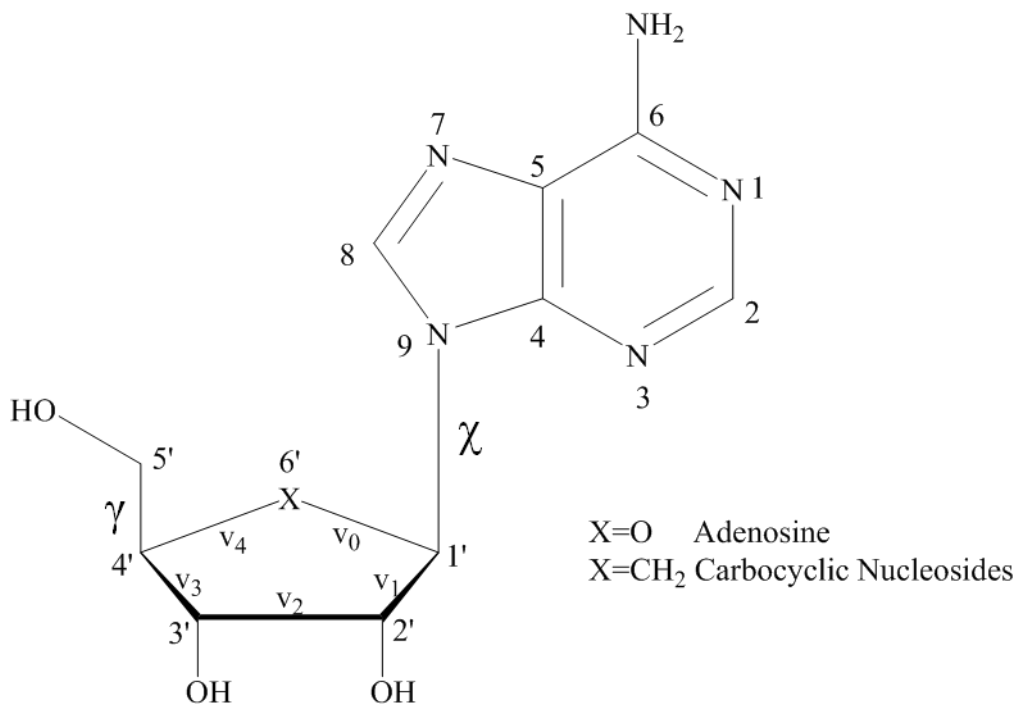


Figure 10. Purine Nucleoside numbering

The focus will be on the first three parameters because of their relevance to our study of purine nucleosides (Figure 10).

(1) The Sugar Puckering Modes: The Pseudorotation Cycle:

Planar ribose is energetically unfavorable since in such arrangement all the torsion angles would be 0° which means substituents on carbons are all eclipsed. The furanose ring twists out of plane to minimize these non-bonded interactions between substituents. Furanose can be puckered into an envelope (E) form with one atom out of plane and four atoms in a plane; or in a twist form (T) with two adjacent atoms displaced on opposite sides from the other in-plane three atoms (Figure 11). If the atom displaced from the plane is on the same side as the C5', it is referred to as *endo*, and if it is on the other side it is referred to as *exo*. *Endo* and *exo* notations

are translated into superscripts and subscripts, respectively. If the endo displacement of C2' is greater than that of C3', it is called *C2'-endo*. This corresponds to a *South* conformer along the pseudorotation cycle, the analytical representation initially introduced for cyclopentane,³⁹ extended to substituted furanose rings⁴⁰ and applied towards the study of carbocyclic nucleosides later on.⁴¹ Altona has introduced two useful parameters to describe the concept of pseudorotation in naturally occurring nucleosides^{42,43} the phase angle of pseudorotation “*P*” (0-360°) and the degree of pucker “ v_{\max} ”.

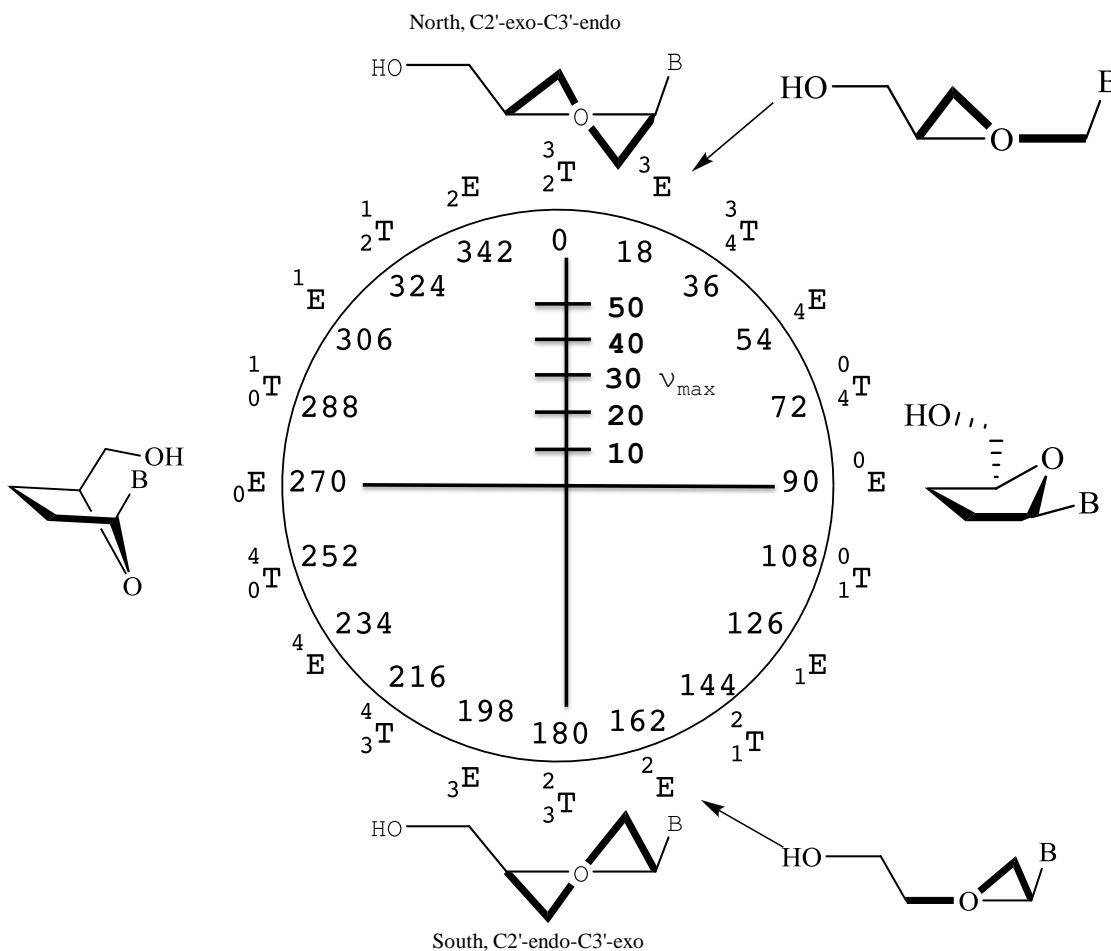


Figure 11. Pseudorotation cycle

By convention a phase angle $P=0^\circ$ corresponds to an absolute North (N) conformation having a symmetrical twist (3T_2), while a phase angle $P=180^\circ$ corresponds to the South (S) antipode with a symmetrical twist (${}^3T_2'$). The value of P depends on five torsion angles (ν_0 - ν_4) of the furanose ring (Figure 10). The relationship between these five torsion angles can be described by a simple cosine function³⁵:

$$\nu_j = \nu_{\max} \cos (P + j \delta) \quad \text{where } j = 0-4, \delta = 144^\circ \quad (\text{eq. 1})$$

And from this equation, a useful formula can be derived for the calculation of P:

$$\tan P = [(\nu_4 + \nu_1) - (\nu_3 + \nu_0)] / 2 \cdot \nu_2 \cdot (\sin 36 + \sin 72) \quad (\text{eq. 2})$$

A close inspection of the available crystallographic data for individual nucleosides reveals that the puckering modes of the furanose ring cluster in two antipodal domains around a C3'-*endo* (3E , N) and a C2'-*endo* (2E , S) envelope conformations. However, in solution, the sugar puckering fluctuates rapidly between these two conformational extremes. In the N conformation, the P values are found in a range between 342° and 18° [${}^2E \rightarrow {}^3T_2 \rightarrow {}^3E$ (C3'-*endo*)], whereas in the antipodal S conformation the range is between 162° and 198° [${}^2E \rightarrow {}^3T_2' \rightarrow {}^3E$ (C2'-*endo*)].^{42,44}

The average magnitude of equilibrium can be estimated via the 3J NMR coupling constants ${}^3J_{1'2'}$ and ${}^3J_{3'4'}$ (Equation 3, 4, 5^{45,42,46}) which gives the relative population of N/S conformations. The equilibrium is influenced mainly by the preference of the substituents at the C2' and C3' for axial orientation as well as the orientation of the base (usually C3'-*endo* is preferred for *anti* and C2'-*endo* prefers *syn*).⁴⁴

$$J_{1'2'} = 9.3(1 - X_N) = 9.3X_S \quad (\text{eq. 3})$$

$$J_{3'4'} = 9.3X_N \quad (\text{eq. 4})$$

$$\% \text{ C2'-endo} = [J_{1'2'} / (J_{1'2'} + J_{3'4'})] \times 100 \quad (\text{eq. 5})$$

(2) The *syn-anti* conformation of the glycosyl bond (χ):

Although the sugar pucker is the main conformational determinant in nucleosides, an important associated parameter is the glycosyl torsion angle χ (defined by X-C1'-N9-C4) (Figure 10). The value of χ determines the *syn* and *anti* disposition of the base relative to the sugar moiety.⁴⁴ In the *syn* conformer, the N-3 of the purine lies above the plane of the sugar moiety, while in the *anti* conformer the H-8 of purine lies in the same position (Figure 12). According to the currently accepted IUPAC definition of the angle χ , the torsion angle range of $180^\circ \pm 90^\circ$ is generally referred to as *anti* while the range $0^\circ \pm 90^\circ$ is referred to as *syn*.^{44,47} The *syn-anti* conformation of nucleosides is one of the most important conformational aspects used in the study of nucleoside-enzyme interactions.⁴⁸

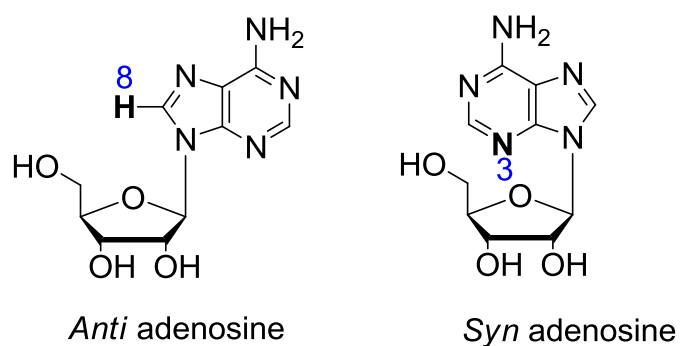


Figure 12. Adenosine showing *Syn* and *Anti* conformations.

In solution, the energy barrier between different conformations is around (25 kJ/mol)^{36,49} and normally the different conformations can be described by two-state models (*syn-anti*; N/S-type sugar pucker).⁴⁴ Stolarski et al.⁵⁰ demonstrated that the chemical shifts (δ) of H2' in purine nucleosides can be used as an indicator of the *syn/anti* orientation. Typical values of δ (H2') in DMSO are 5.2 ppm for *syn* and 4.2 ppm for *anti* conformations. The big difference between the

two values can be explained in terms of the influence exerted by N-3 on the H2' in the *syn* conformation. Adenosine has a reported value for H2' of 4.62 ppm which demonstrates that it exists in equilibrium between the *syn* and *anti* conformations.⁵⁰

(3) The orientation of the C4'-C5' (γ):

The conformation of the C4'-C5' determines the orientation of the hydroxyl group in nucleosides or the 5'-phosphate in nucleotides relative to the sugar ring. There are three favored conformers shown in Figure 13. In purines +*sc* and *ap* are equally populated.

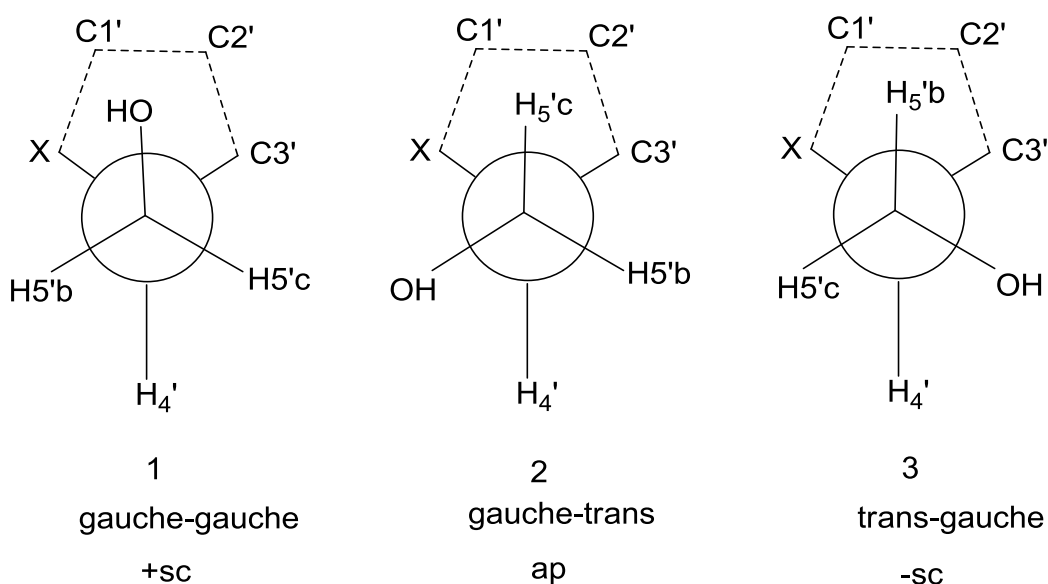


Figure 13. Classical staggered rotational isomers around C4'-C5'.^{46,51}

Rosemeyer et al⁵² used equations based on coupling between H4' and H5' as well as H5'' to calculate the population of each conformer as shown in Equations (7,8 and 9).

$$\% \gamma^{g^+} = \{1.46 - ({}^3J_{4'5'} + {}^3J_{4'5''}) / 8.9\} \times 100 \quad (\text{eq. 7})$$

$$\% \gamma^t = \{({}^3J_{4'5''} / 8.9) - 0.23\} \times 100 \quad (\text{eq. 8})$$

$$\% \gamma^{g^-} = \{({}^3J_{4'5'} / 8.9) - 0.23\} \times 100 \quad (\text{eq. 9})$$

Rational for Research

(A) 8-Alkylaristeromycin

The search for useful therapeutic agents is controlled by various factors. One aspect that makes carbocyclic nucleosides appealing is that they are highly resistant to phosphorylases, which cleaves the glycosidic bond, while still good substrates for cellular kinases.⁵³ The broad spectrum activity for both Ari and NpcA coupled with their toxicity, resulted into modification of those two important nucleosides to retain antiviral activity and lower toxicity has been done. An important consideration in nucleoside chemistry is the structural orientation of the base and sugar and its effect on the activity of nucleoside as well as the information it can provide for a better design of structural analogues. Purine nucleosides with no substitutions at the 8 position preferentially exist in the anti conformation.⁴⁴ Analogues with 8-substitution with bromo, fluoro, or methyl substituents⁵⁴ have been studied via circular dichroism and NMR spectroscopy⁵⁵ and have been assigned as *syn* conformations. It was confirmed spectroscopically that due to the rapid equilibrium between *syn-anti* that those C8-substituted nucleosides still afford access to the *anti* conformer in solution,⁵⁰ which would allow binding at the enzyme active site.⁵⁶

For carbocyclic nucleosides, especially aristeromycin, the 8-alkyl substitution has not been well explored. However, various studies regarding adenosine and its analogues have been published,^{57,58} with a variety of substituents in the 8 position. Alkylation of the 2-, 6, and 8-positions of adenosine and its deoxy analogues was accomplished and their biological activity was reported. Of the 8-substituted adenosine analogues, 8-methyladenosine exhibits a 50-60 % *syn*⁵⁰ conformations and it shows high selective inhibition against vaccinia virus.⁵⁷ They have also been studied theoretically for structural conformation.⁵⁹

So in an attempt to gain more insight into the effect of 8-alkylation on the structural and chemical aspects of carbocyclic nucleoside, mainly aristeromycin, two targets (Figure 14) were synthesized, 8-methylaristeromycin (**1**) and 8-ethylaristeromycin (**2**) within this part of the research.

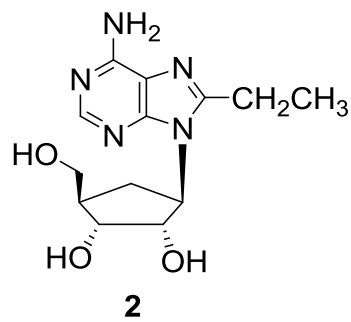
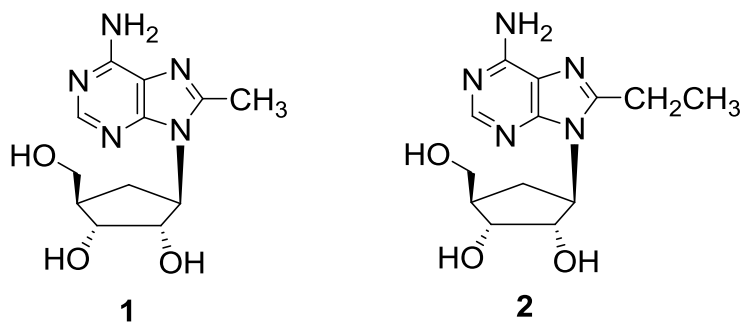


Figure 14. Targets 1, 2.

(B) Neplanocin Analogues

As mentioned before NpcA is an antiviral agent effective against a broad range of viruses, in particular (-) RNA strand viruses (vesicular stomatitis, parainfluenza, and measles),^{34,60} and whose effect is mediated by its inhibition of AdoHcy hydrolase, whilst its toxicity is mediated by its phosphorylation via adenosine kinase and subsequent transformation into S-neplanocylmethionine.⁶¹ Borhardt et al.,^{32,60} designed truncated analogues of NpcA that retained the inhibitory activity towards AdoHcy hydrolase (antiviral activity) while lacking substrate properties towards cellular adenosine kinase and deaminase (reduced cellular toxicity) via removal of the 4' hydroxymethyl group hence the term 4'-norneplanocin.

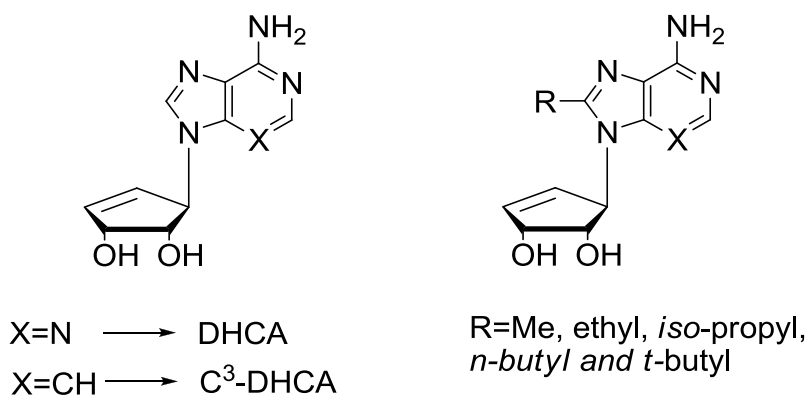


Figure 15. DHCA analogues

As part of the synthetic research, five target compounds were designed and synthesized based on the DHCA framework and are shown in Figure 15.

Chapter 1. Theoretical Investigation of Carbocyclic Nucleosides

The computational study involved five compounds:

(A) Adenosine

(B) Aristeromycin

(C) 8-methylaristeromycin (Target 1)

(D) 3-deazaaristeromycin

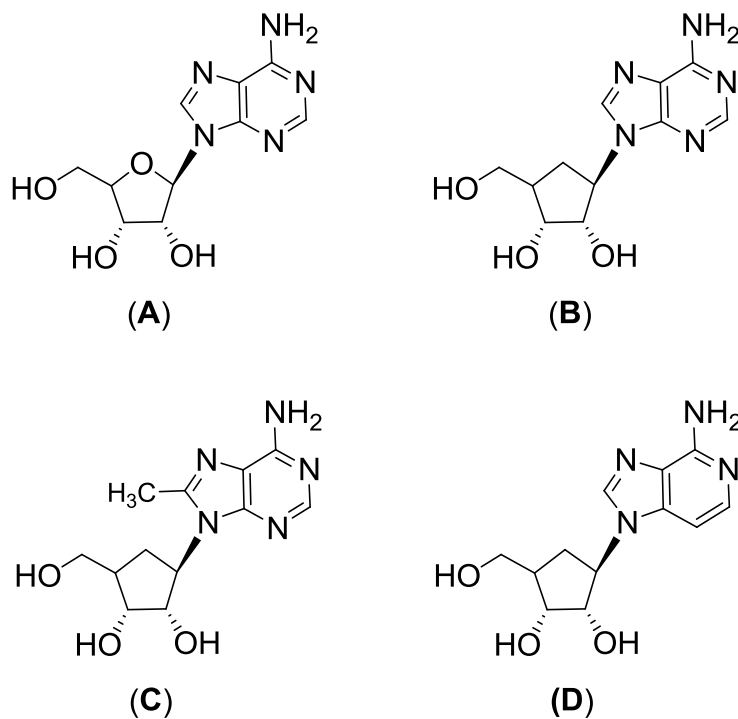


Figure 16. Compounds involved in the study

Methods:

All density functional calculations were carried out with the Gaussian program⁶² using the computational resources available through the Alabama Supercomputer Authority. Full geometry

optimizations were carried out with the Becke three-parameter exchange functional⁶³ with the nonlocal correlation functional of Lee, Yang and Parr and the 6-31G(d) basis set.⁶⁴ The PCM continuum solvation model⁶⁵ was utilized to approximate the solvent effect (water) via single point energy evaluations on the optimized gas phase structures. Further optimizations in solution using different basis set namely the augmented correlation-consistent double-zeta⁶⁶ (aug-cc-pVDZ) level of theory, was followed by NMR calculation using the mixed method at the same level.

The study aims at investigating a group of carbocyclic nucleosides (A, B, C, D) with the objective of studying the relationship between pseudorotation and the glycosyl torsion angle as well as identifying the conformations that contribute to the overall structure of the nucleoside through NMR coupling constants. This will involve optimization of molecules in the gas phase followed by stepwise constraints on the P angle and ν_{\max} and further optimization in the gas phase as well as single point energy calculations in the gas phase and in solution {using both B3LYP/3-21G and B3LYP/6-31G(d)}. The final step will involve optimization in solution and NMR calculations both with the same level of theory (B3LYP/aug-cc-pVDZ, B3LYP/aug-cc-pVDZ nmr = mixed).

The search for the lowest energy conformations for a compounds **A**, **B**, **C** and **D** (Figure 16) was based on work done by Akdag⁶⁷ as a starting point for geometry optimization. The sampling was based on variation of the torsion angle χ (X-C1'-N9-C4) (see Figure 2 for definition) as well as the orientation of the substituents on the five-membered ring. This included various combinations of North/South and *syn/anti* conformations. This led to the generation of six starting conformations (Figure 17, compound A is shown as example with AA1, AA2, AA3, AA4, AA5 and AA6 in order). These conformations were optimized using the Density

Functional Theory (DFT). They were initially optimized at the B3LYP/3-21G level^{63,64} followed by B3LYP/6-31G (d) and the results are shown in (Table 1). The conformers were checked and their χ , P and v_{\max} were tabulated as well.

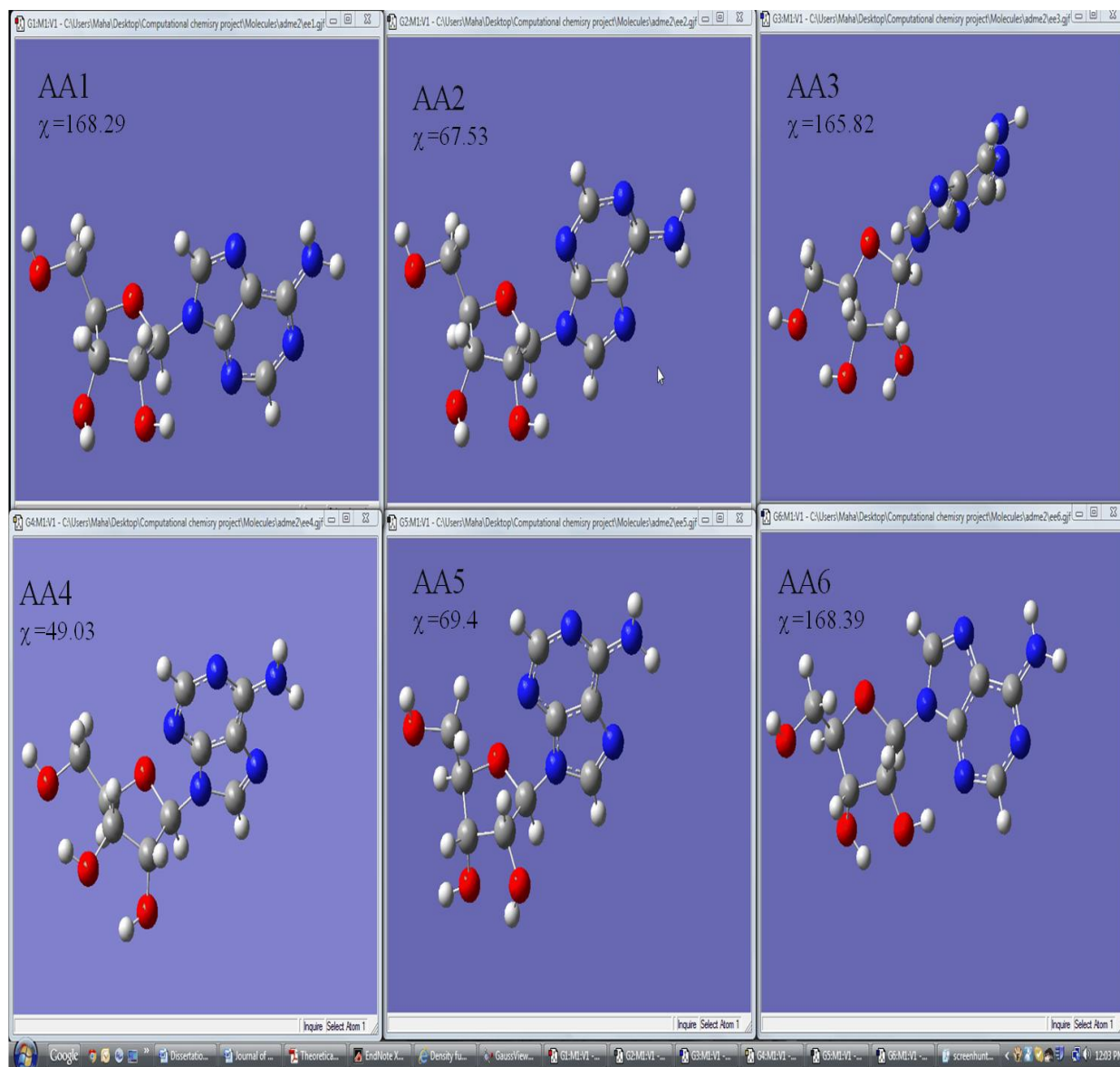


Figure 17. Starting six geometries for all 4 compounds, example shown is compound A.

Table 1. Results of initial geometry optimization of 4 compounds:

Conformer	χ	P	v_{\max}	ΔE^*		
				3-21G	6-31G(d)	
AA1	168.29	160.46	40.98	0.00	0.00	
AA2	67.53	174.11	38.64	10.23	5.97	
AA3	165.82	14.40	41.62	4.20	4.67	
AA4	49.03	19.75	38.48	1.93	2.61	
AA5	69.40	181.22	33.11	8.16	4.63	
AA6	168.39	160.43	40.98	0.00	0.00	→ AA1
BB1	162.63	153.61	45.78	0.92	0.00	
BB2	63.29	178.92	43.51	9.14	4.55	
BB3	250.49	37.49	46.14	3.82	2.16	
BB4	55.42	37.09	46.10	0.00	0.24	
BB5	61.98	181.40	39.24	7.76	3.59	
BB6	162.63	153.63	45.77	0.92	0.00	→ BB1
CC1	145.82	154.05	46.78	4.09	2.69	
CC2	63.35	178.65	43.76	9.13	4.41	
CC3	249.95	44.51	46.62	5.52	3.72	
CC4	54.86	38.04	46.18	0.00	0.00	
CC5	38.71	184.18	38.68	5.44	4.28	
CC6	145.88	154.10	46.77	4.09	2.69	→ CC1
DD1	191.50	151.39	47.03	7.58	3.40	
DD2	59.20	160.10	45.53	8.53	3.16	
DD3	250.55	38.22	46.05	0.35	0.29	
DD4	60.88	45.07	46.27	0.00	0.00	
DD5	58.32	161.29	41.15	8.66	3.01	
DD6	127.39	156.49	46.73	10.12	6.22	

* ΔE (kcal/mol)

After the 3-21G optimization, the relative energy (kcal/mol) for each set was calculated from the returned SCF of optimized molecules. Conformers within relative energy of 4 kcal/mol were chosen to go to the next level of the pseudorotation study. Some of the conformers collapsed after this initial optimization (See Table 1). At this point and further on, PROSIT⁶⁸ the online

interactive tool for pseudorotation was used and molecules were uploaded and analyzed for various data including the glycosyl torsion angle, P , ν_{\max} , and endocyclic torsion angles. This gave way to the data presented in Table 1.

Table 2. Summary of the molecules from B3LYP/3-21G.

Conformer	P	χ	ΔE^* 3-21G
AA1	S	ANTI	0.0
AA4	N	SYN	1.9
BB1	S	ANTI	0.9
BB3	N	ANTI	3.8
BB4	N	SYN	0.0
CC1	S	ANTI	4.1
CC4	N	SYN	0.0
DD4	N	ANTI	0.4
DD4	N	SYN	0.0

After the initial optimization via the B3LYP/3-21G level of theory, the conformers returned are considered our starting geometries for the pseudorotational study and they are summarized in Table 2. It is worth mentioning here that, at a later step, another level of theory 6-31G(d) had been applied to the original 6 conformations in addition to the B3LYP/3-21G. The goal was to confirm the accuracy of choice of conformers within more refined limitations.

Based on equations 1 and 2, restriction of the pseudorotation phase angle “ P ” across the five-membered ring was constrained in 30° increments with “ ν_{\max} ” taken as average of the initial six conformations from Table 1. This resulted in 12 new molecules with restricted phase angles. These restricted molecules were subjected to geometry optimization in the gas phase at the B3LYP/3-21G level followed by single point energy calculation at the B3LYP/6-31G (d) both in the gas phase and in solution.

Using SCF and information from PROSIT, data were tabulated for each compound showing P , χ , and relative energies (kcal/mol). A typical output of this online tool is displayed in (Table 3) confirming our 30° stepwise constraint for the phase angle as well as giving the corresponding constrained values for the endocyclic torsion angles (v_0 - v_4). It also lists χ thus determining the *syn* or *anti* disposition of the base and the sugar as well as the torsion angle γ , which defines the orientation of the 5'-OH. And the last column describes the type of the molecule submitted in terms of the characteristic north, east, west and south designation, which reflects the value of “ P ” on the pseudorotation cycle (See Figure 11).

Table 3. PROSIT output for (A) after single point energy in solution.

(A)	v_0	v_1	v_2	v_3	v_4	P	v_{\max}	χ	γ	TYPE
AA1_0	12.51	-32.30	39.94	-32.41	12.43	0.01	39.94	164.52	-69.62	ade, C3'-endo
AA1_30	-8.11	-16.22	34.53	-39.82	29.88	30.09	39.91	174.73	-71.82	ade, C3'-endo
AA1_60	-26.69	4.05	19.77	-36.62	39.23	60.29	39.88	178.83	-65.70	ade, C4'-exo
AA1_90	-38.16	23.39	0.08	-23.33	38.11	89.88	39.96	171.90	-57.19	ade, O4'-endo
AA1_120	-39.21	36.54	-19.75	-3.87	26.88	119.72	39.84	165.46	-57.15	ade, C1'-exo
AA1_150	-29.78	39.78	-34.50	16.43	8.36	149.93	39.87	165.54	-61.60	ade, C2'-endo
AA1_180	-12.46	32.35	-39.89	32.44	-12.41	180.02	39.89	170.68	-62.62	ade, C3'-exo
AA1_210	8.48	16.35	-34.72	39.70	-29.66	209.92	40.06	175.89	-62.28	ade, C3'-exo
AA1_240	26.93	-4.04	-20.02	36.46	-39.09	239.96	39.98	181.20	-64.00	ade, C4'-endo
AA1_270	38.11	-23.51	-0.13	23.36	-38.07	269.82	39.98	147.71	-65.17	ade, O4'-exo
AA1_300	39.13	-36.52	19.86	3.93	-26.92	299.84	39.90	147.77	-61.17	ade, C1'-endo
AA1_330	29.78	-39.73	34.56	-16.43	-8.39	329.98	39.92	154.65	-62.20	ade, C2'-exo

The relative energy for each series based upon SCF from the single point energy calculation in solution (all arranged with respect to the most stable in the series; highlighted in Tables (4-7)).

This arrangement led to construction of a graph for each compound to pick the molecules that will undergo total optimization in solution and NMR calculations. The criteria for choosing were molecules that are minima on the energy surface and that their relative energy was 4 kcal/mol or less. The results for each compound are listed in Tables 4-7 and Graphs 1-4 with the chosen molecules being pinpointed (single point energy optimization in solution).

Table 4. Results shown for AA1 and AA2 based on single point energy in solution.

Adenosine AA1	χ	ΔE kcal/mol	AA4	χ	ΔE kcal/mol
0	164.52 A	0.00	0	50.34 S	8.20
30	174.73 A	1.73	30	50.42 S	8.05
60	178.83 A	8.26	60	64.03 S	8.19
90	171.9 A	7.86	90	71.77 S	7.24
120	165.46 A	7.70	120	67.36 S	3.19
150	165.54 A	7.02	150	58.81 S	2.41
180	170.68 A	5.46	180	67.24 S	0.60
210	175.89 A	5.73	210	84.27 S	1.99
240	181.2 A	8.76	240	105.30 A	5.47
270	147.71 A	5.99	270	142.85 A	6.45
300	147.77 A	2.88	300	103.29 A	8.19
330	154.65 A	0.10	330	70.08 S	10.72

Graph 1. Relative energy in solution for A

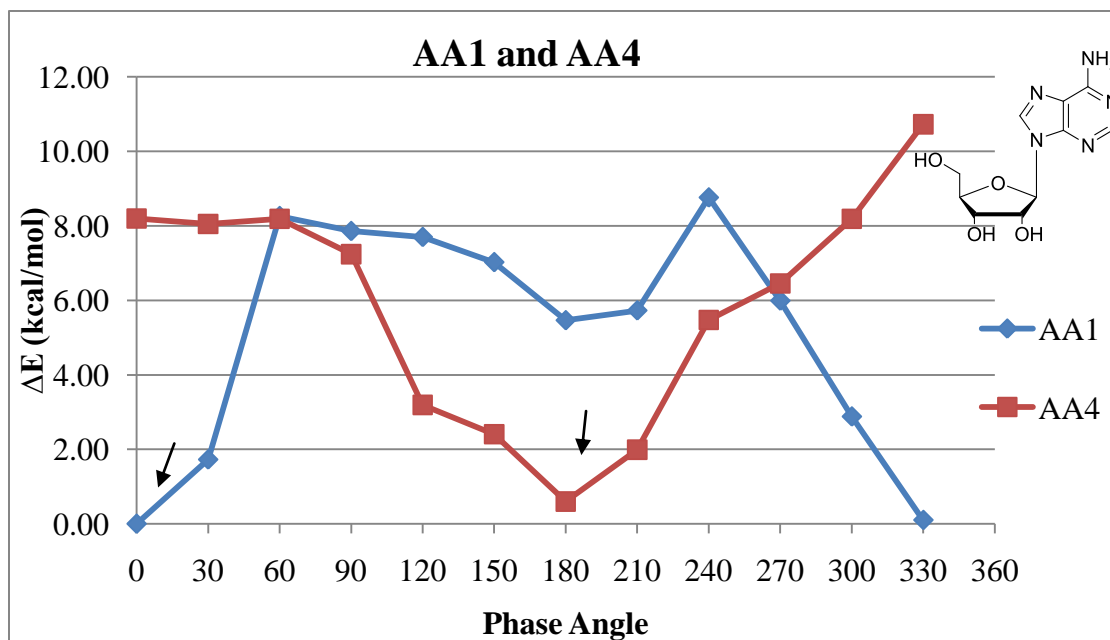


Table 5. Results shown for BB1, BB3 and BB4 based on single point energy in solution.

BB1	χ	ΔE kcal/mol	BB3	χ	ΔE kcal/mol	BB4	χ	ΔE kcal/mol
0	209.63 A	3.64	0	222.35 A	8.29	0	36.36 S	12.66
30	185.25 A	5.57	30	249.01 A	5.23	30	52.81 S	9.60
60	178.86 A	8.29	60	251.17 A	4.23	60	56.52 S	8.04
90	169.68 A	5.80	90	247.27 A	4.99	90	52.88 S	8.44
120	163.29 A	5.73	120	247.55 A	2.61	120	53.59 S	5.68
150	161.82 A	6.70	150	243.52 A	0.00	150	54.04 S	4.05
180	166.66 A	8.49	180	241.17 A	1.43	180	60.80 S	5.85
210	177.07 A	10.19	210	245.92 A	4.53	210	81.63 S	8.41
240	180.67 A	14.67	240	346.25 S	12.17	240	107.97 A	12.22
270	143.71 A	11.60	270	329.12 S	14.64	270	117.60 A	13.41
300	134.42 A	7.67	300	308.09 S	11.71	300	116.40 A	13.60
330	161.68 A	5.09	330	225.32 A	13.00	330	55.40 S	18.60

Graph 2. Relative energy in solution for B.

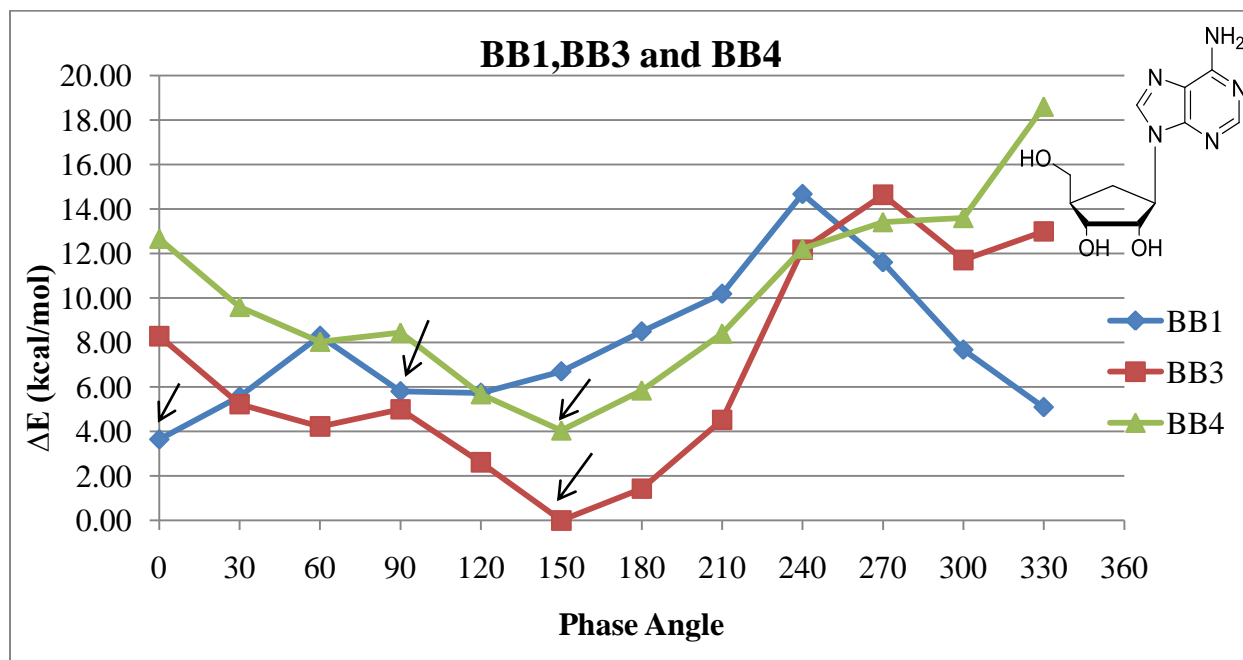


Table 6. Results shown for CC1 and CC4 based on single point energy in solution.

CC1	χ		ΔE kcal/mol	CC4	χ		ΔE kcal/mol
0	200.41	A	1.94	0	35.22	S	7.70
30	191.33	A	6.25	30	52.20	S	5.09
60	180.86	A	4.03	60	30.10	S	3.99
90	169.91	A	2.40	90	31.05	S	4.60
120	154.69	A	3.08	120	29.59	S	1.46
150	145.59	A	3.39	150	30.78	S	0.00
180	151.85	A	5.02	180	38.14	S	1.81
210	182.91	A	8.02	210	25.10	S	3.54
240	178.94	A	11.83	240	106.29	A	6.67
270	113.51	A	6.34	270	110.41	A	8.50
300	116.83	A	2.38	300	106.93	A	9.17
330	120.62	A	1.08	330	52.37	S	15.14

Graph 3. Relative energy in solution for C

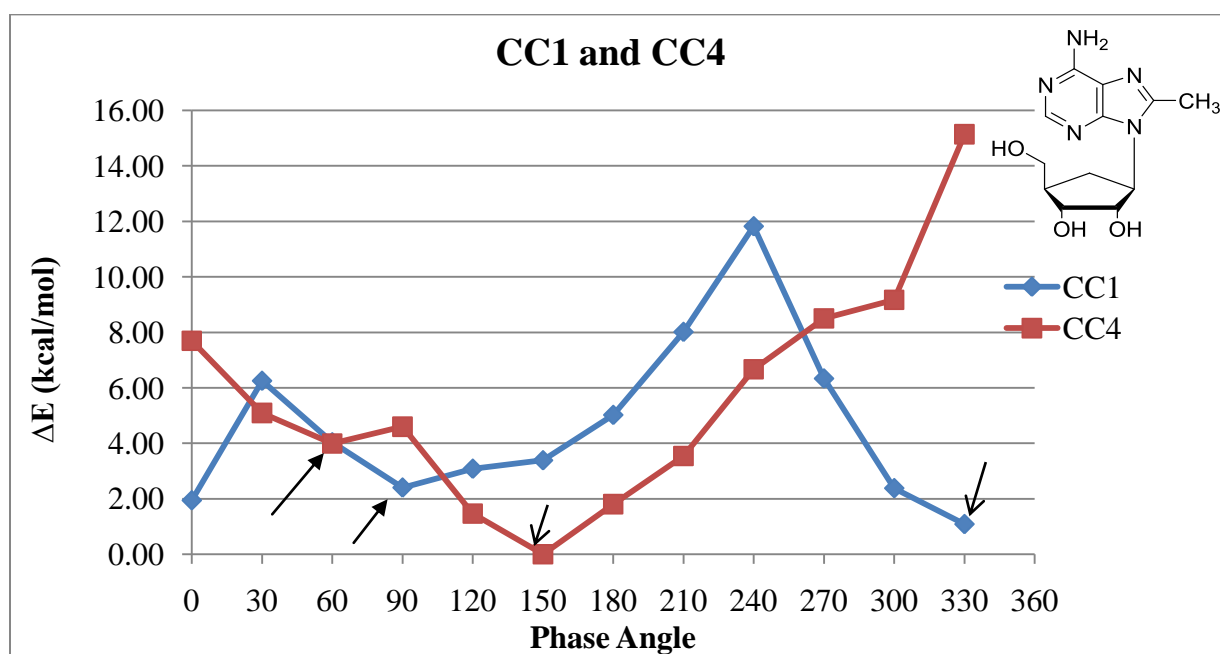
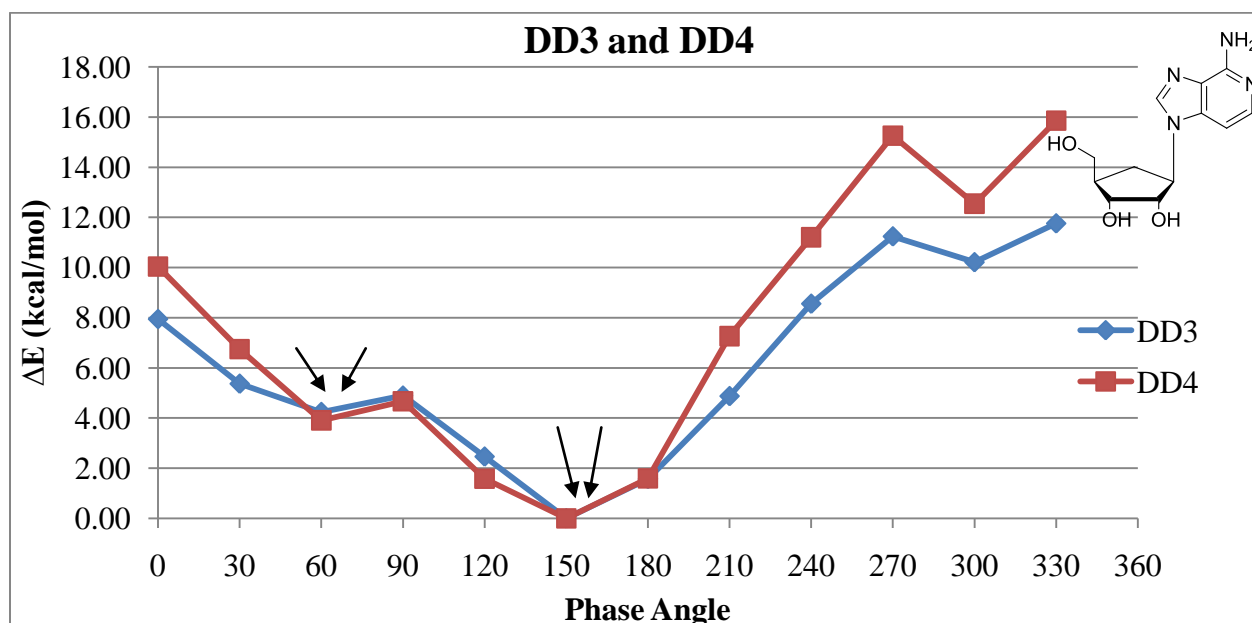


Table 7. Results shown for DD3 and DD4 based on single point energy in solution.

DD3	χ		ΔE kcal/mol	DD4	χ		ΔE kcal/mol
0	205.3	A	7.95	0	37.05	S	10.04
30	250	A	5.37	30	52.43	S	6.75
60	245	A	4.24	60	62.38	S	3.91
90	240.3	A	4.89	90	57.92	S	4.67
120	258.3	A	2.46	120	56.22	S	1.58
150	262.84	A	0.00	150	57.24	S	0.00
180	238.9	A	1.57	180	56.58	S	1.59
210	177.75	A	4.88	210	329.1	S	7.27
240	297.16	A	8.56	240	99.47	A	11.21
270	294.85	A	11.25	270	104.99	A	15.26
300	291.91	A	10.22	300	118.72	A	12.55
330	182.4	A	11.76	330	57.67	S	15.86

Graph 4. Relative energy in solution for D



From the above graphs, these are the molecules chosen for the full optimization in solution followed by NMR calculations (also showing their final designation based on lowest in energy):

I- AA1_0 (**A1**), AA4_180 (**A2**).

II- BB1_0 (**B3**), BB1_90 (**B1**), BB3_150 (**B2**), BB4_150 (**B4**).

III- CC1_90 (**C1**), CC1_330 (**C2**), CC4_60 (**C3**), CC4_150 (**C4**).

IV- DD3_60 (**D3**), DD3_150 (**D1**), DD4_60 (**D2**), DD4_150 (**D4**).

For the selected conformers, geometry optimizations in solution using B3LYP/aug-cc-pVDZ level of theory with conductor-like polarizable continuum model (CPCM) with universal force field (UFF) cavity set is applied and the spin-spin coupling constants for each conformer are determined by the same level of theory. Spin-spin coupling constants were collected, and data for final molecules were tabulated and compared with experimental data in Tables 8-11. The best fit between experimental and theoretical data was obtained via linear regression as shown in Appendix.

Table 8. A Comparison of experimental and theoretical spin-spin coupling constants for Adenosine (A)

Adenosine (A)	${}^3J_{1'-2'}$	${}^3J_{2'-3'}$	${}^3J_{3'-4'}$	P	v_{\max}	χ	ΔE^c	$C_{2'-endo}^d$	$\delta H_{2'}^e$
Exp. ⁶⁹ (D ₂ O)	6.1	5.3	3.4					64	4.6
Calc. ^a	A1	7.8	6.4	-0.2	163.8	36.3	S	0.0	3.9
	A2	0.0	6.1	7.8	0.5	33.5	A	0.8	5.0
Linear Regression ^f		5.1	6.3	2.8				64.6	4.3
		(1.1) ^b	(1.2)	(0.6)					

^aThe spin-spin coupling constant by *ab initio* calculation was done in aqueous solution. ^bThe value in parentheses is the difference between experimental data and linear regression results. ^c ΔE is the energy difference from the most stable conformer (kcal/mol). ^d $C_{2'-endo}$ is the relative population of the South conformer and is given by $[{}^3J_{1'-2'}/({}^3J_{1'-2'}+{}^3J_{3'-4'})]*100$. ^e $\delta H_{2'}$ is the chemical shift of the in ppm.⁷⁰ ^fLinear regression equation = $0.66*(\mathbf{A1})+0.34*(\mathbf{A2})$

Adenosine (A) prefers an anti conformation with 65% in DMSO and 75% in water.⁵⁰ While according to other studies based on 1D ¹H NOE, it exists as a *syn* conformation with 60% preference.³⁶ However, most of the studies refer to Ado as possessing roughly equal equilibrium between both conformations.⁵⁹ Also, the population of the C2'-*endo* (South conformation) was determined, from the coupling constants with the aid of the two-state model of Altona,⁴³ calculated to be 67% in DMSO⁷¹ and 63% in water.⁶⁹ By comparing these experimental data with our theoretical ones, we find that we have a *syn* \rightleftharpoons *anti* conformation of 66% \rightleftharpoons 34% shifted towards the *syn* conformer which conforms to literature findings. In terms of pseudorotation, we find that the percentage of population of the C2'-*endo* is within 0.6% difference which is in good

agreement with the reported values. The δ H_{2'} chemical shift is averaged at 4.3 ppm, which is within 0.3 ppm difference from the literature. This calculated chemical reflects a more preference to the anti conformations⁵⁰ even though our best fit comes mainly from the *syn* conformation. In addition the ³J spin-spin coupling constants agree well within Δ 1.2 Hz.

Table 9. A Comparison of experimental and theoretical spin-spin coupling constants for Aristeromycin (**B**)

Aristeromycin (B)	³ J _{1'-2'}	³ J _{2'-3'}	³ J _{3'-4'}	P	v _{max}	χ	ΔE^c	C _{2'} - <i>endo</i> ^d	δH_2^e
Exp ⁷² .(D ₂ O)	9.3	5.9	3.4			A		73.2	4.5
B1	10.8	7.4	0.6	136.5	43.4	A	0.0		3.9
B2	10.9	6.6	0.1	140.4	42.9	A	0.3		3.9
B3	1.1	7.5	10.0	47.0	42.8	A	1.5		4.0
B4	10.3	6.6	0.0	147.6	42.4	S	2.8		5.0
Linear Regression ^f	8.5 (0.8) ^b	6.8 (0.9)	2.6 (0.6)					76.6	4.0

^aThe spin-spin coupling constant by *ab initio* calculation was done in aqueous solution. ^bThe value in parentheses is the difference between experimental results and linear regression results. ^c ΔE is the relative energy difference from the most stable conformer (kcal/mol). ^dC_{2'}-*endo* is the relative population of the South conformer and is given by [³J_{1'-2'} / (³J_{1'-2'} + ³J_{3'-4'})]*100. ^e δH_2 is the chemical shift in ppm. ^fLinear regression equation = 0.75*(**B2**)+0.25*(**B3**)

For aristeromycin (**B**), the ³J spin-spin coupling constants⁷³ compare well within only a Δ 0.9 Hz. The % C_{2'}-*endo* differs from experiment by Δ 3.4% which is still in good agreement

signifying that the major conformer is the C2'-endo. δ H2' is averaged at 4.0 ppm which is 0.5 ppm different from the experimental and which indicates the preference of aristeromycin for *anti* conformation. Also, based on the linear regression of the coupling constants it shows major contributions from B2 and B3 which coincides with the experimental preference for *anti*.

Table 10. A Comparison of experimental and theoretical spin-spin coupling constants for 8-methylaristeromycin (C)

8-methyl Aristeromycin (C)	$^3J_{1'-2'}$	$^3J_{2'-3'}$	$^3J_{3'-4'}$	P	ν_{\max}	χ	ΔE^c	$C_{2'-endo}^d$	$\delta H_{2'}^e$
Exp.(D ₂ O)	9.1	5.6	2.8			S		76.5	4.9
C1	2.6	7.4	9.9	53.6	42.8	A	0.0		4.5
C2	1.2	7.7	10.3	49.7	42.4	S	0.7		4.3
C3	1.2	7.2	9.8	50.1	43.4	S	2.1		4.4
C4	10.3	6.9	0.2	143.5	42.8	S	2.1		5.2
Linear Regression ^f	8.6 (0.5) ^b	7.0 (1.4)	2.3 (0.5)					78.9	5.0

^aThe spin-spin coupling constant by *ab initio* calculation was done in aqueous solution. ^bThe value in parentheses is the difference between experimental results and linear regression results. ^c ΔE is the energy difference from the most stable conformers (kcal/mol). ^d $C_{2'-endo}$ is the relative population of the South conformer and is given by $[\frac{^3J_{1'-2'}}{(^3J_{1'-2'}+^3J_{3'-4'})}] * 100$. ^e $\delta H_{2'}$ is the chemical shift in ppm. ^fLinear regression equation = $0.22*(C1)+0.78*(C4)$

8-methylaristeromycin (C): By looking at Table 10, we find that the difference between experimental and calculated spin-spin coupling constants for $^3J_{1'-2'}$ and $^3J_{3'-4'}$ is 0.5 Hz whereas

the difference is higher for ${}^3J_{2'-3'}$ (1.4 Hz). The C2'-*endo* population agrees with experiment to a Δ of 2.4%. The theoretical δ H2' is 5.0 ppm which is only 0.1 ppm difference from the experimental value obtained from the NMR experiments (4.9 ppm). This indicates that **C** exists as the *syn* conformer.

Table 11. A Comparison of experimental and theoretical spin-spin coupling constants for 3-deazaaristeromycin (**D**)

3-deaza Aristeromycin(D)	${}^3J_{1'-2'}$	${}^3J_{2'-3'}$	${}^3J_{3'-4'}$	P	ν_{\max}	χ	ΔE^c	C2'- <i>endo</i> ^d	$\delta H_{2'}^e$
Exp ^{74,75} .(DMSO)	9.3	5.4	2.8					76.9	4.2
D1	10.5	6.9	0.3	150.0	46.2	A	0.0		3.9
D2	1.8	7.7	9.7	60.2	46.1	S	0.4		4.4
D3	1.3	7.3	9.6	60.2	46.1	A	0.9		4.1
D4	10.6	6.3	0.0	150.0	46.2	S	1.2		4.5
Linear Regression ^f	8.6	6.5	2.0					81.1	4.4
	0.7	1.1	0.8						

^aThe spin-spin coupling constant by *ab initio* calculation was done in aqueous solution while experimental data was derived from DMSO data. ^bThe value in parentheses is the difference between experimental results and linear regression results. ^c ΔE is the energy difference from the most stable conformer (kcal/mol). ^dC2'-*endo* is the relative population of the South conformer and is given by $[{}^3J_{1'-2'}/({}^3J_{1'-2'}+{}^3J_{3'-4'})]*100$. ^e $\delta H_{2'}$ is the chemical shift in ppm. ^fLinear regression equation = $0.21*(\mathbf{D3})+0.79*(\mathbf{D4})$

For 3-deazaaristeromycin (**D**): The coupling constants agree well to a difference of 1.1 Hz with experimental. δ H2' chemical shift at 4.4 ppm is within 0.2 ppm difference from experiment and it coincides with a preference to the *anti* conformation. The population of the C2-*endo* is within 4.2 % difference from experiment but still reflects the preference of (**D**) for the South conformation.

Again here we see, like (**A**) that the major contributor is **D4** which is *syn* while the second contributor is **D3** which is *anti* which constitutes a controversy for this compound.

Results

The orientation of the base relative to the sugar moiety has been analyzed in different ways including but not limited to: spin relaxation times, NOE effects, chemical shifts perturbation, Karplus-like dependence of the $^3J(\text{C-8}, \text{H1}')$ coupling constant on χ .³⁶ All methods have been aiming at gaining reliable information regarding the dynamic equilibrium between *syn* and *anti* conformation as well as the conformation around the five-membered ring(North/South).

This theoretical study started with three known nucleosides that represent three nucleosides classes and for which information is available for comparison and validation of the methodology adopted. These nucleosides are: Adenosine (**A**) represents the ribofuranoside nucleoside, Aristeromycin (**B**) as a representative of the carbocyclic nucleosides with the oxygen of the tetrahydrofuran of adenosine being replaced with a methylene group and finally 3-deazaaristeromycin (**D**) where it lacks the N3 nitrogen. Our targets for the study were the 8-methyl and 8-ethyl Aristeromycin (**C**) and (**F**).

The developed methodology has good agreements in terms of the C2'-*endo* population in cases of A, B, C and D.

*In terms of prediction of the *syn-anti* conformer, it has been inconsistent with the predictions of which is the lowest energy conformer.

*In terms of predicting the spin-spin coupling constants, with the exception of E, it was in good agreement with the experimental data.

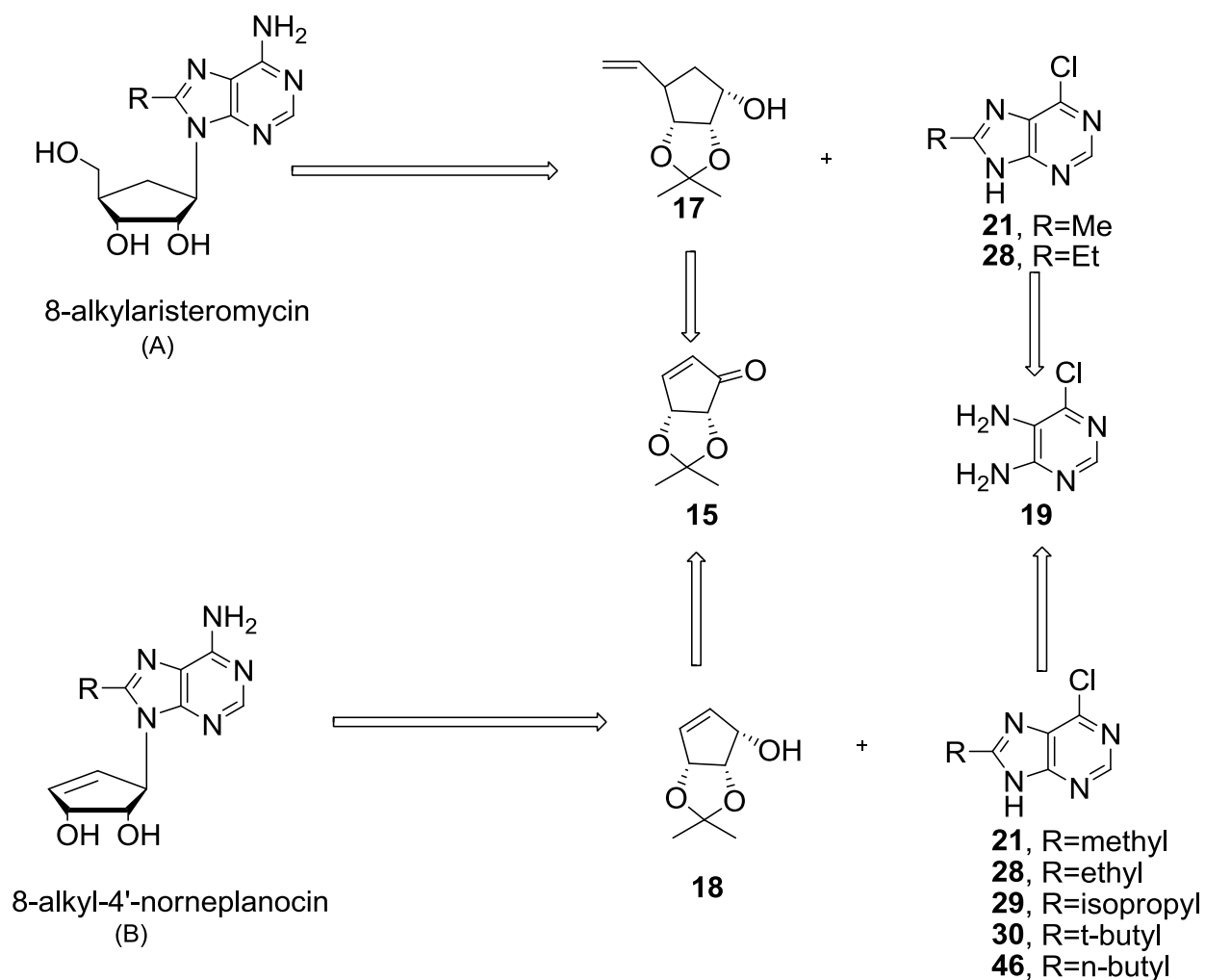
More refinement into the conditions of the calculations may be needed to increase the precision of the methodology and address the issues of description of the conformation around the glycosidic torsion angle.

Chapter 2. Synthesis of Required Precursors

Synthesis of the Carbocycle:

The synthesis of carbocyclic nucleosides depends mainly on the condensation of the heterocyclic nucleobase and the pseudo cyclopentyl sugar.⁷⁶ This can be done via one of two methods: a convergent or a linear route. In the former, an intact nucleobase is coupled directly to an activated carbocycle, while the latter depends on the construction of the heterocyclic nucleobase onto a suitable chiral cyclopentylamine.⁸ Both routes have been studied extensively for their advantages and disadvantages. The convergent route is generally less tedious than the linear one and hence was utilized throughout this research.

In this regard, whether the target is A or B (Scheme 8), the convergent synthesis will follow a pathway outlined by attaching a functionalized heterocyclic base with an appropriately constructed version of intermediate **15** (Scheme 8). The direct substitution can be accomplished via several methods^{3,53} including: (a) palladium catalyzed displacement of an allylic ester or carbonate, (b) Mitsunobu coupling with a cycloalkanol, (c) nucleophilic displacement of a halide ion or activated hydroxyl such as mesylate or triflate, (d) ring opening of an epoxide, (e) Michael addition to an olefin activated by a carbonyl or other electron withdrawing group.

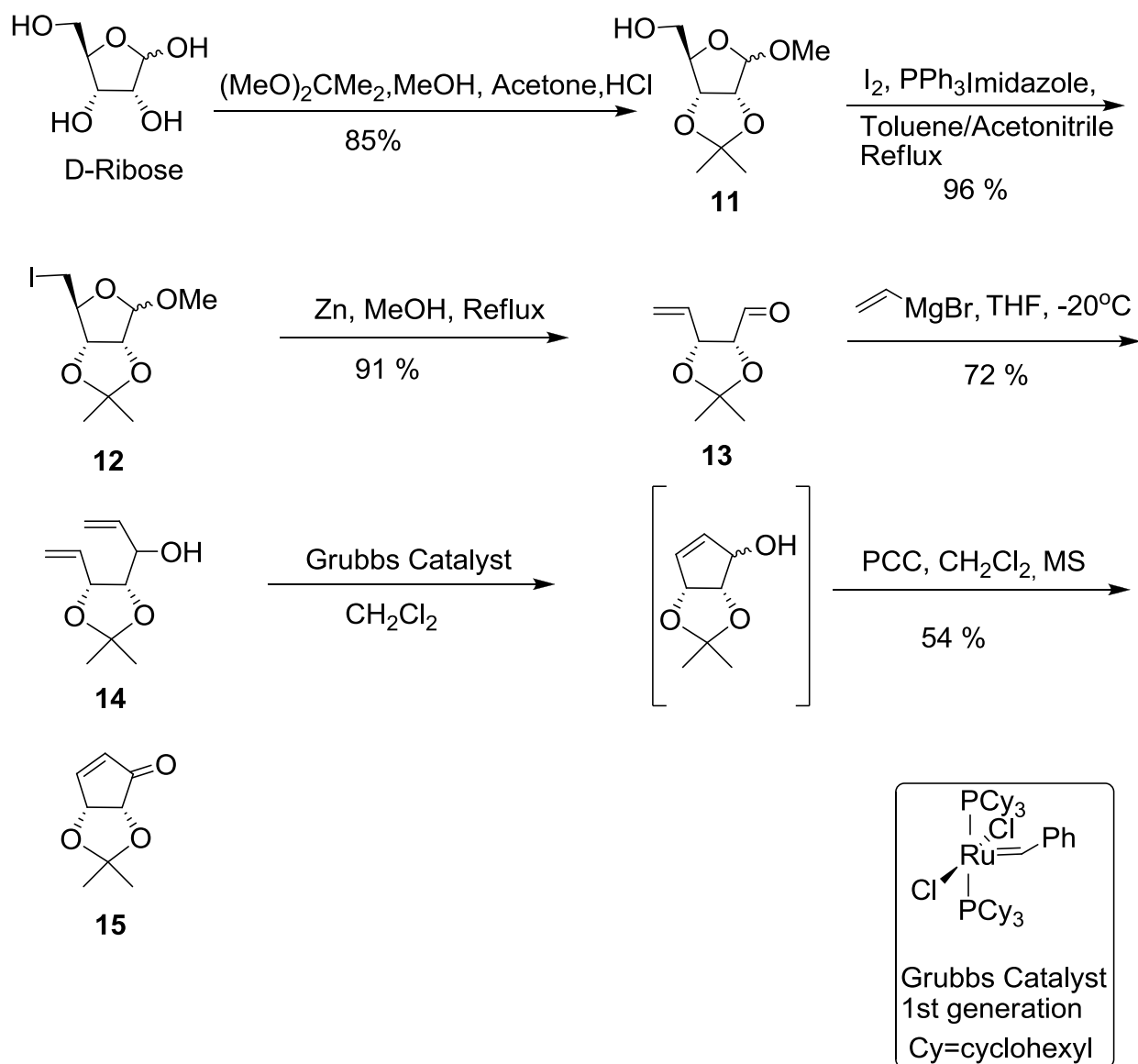


Scheme 8. Convergent retrosynthesis towards target compounds.

One of the most useful common methods is the Mitsunobu coupling. It depends on activation of a hydroxyl group by a complex formed from an azodicarboxylate and triphenylphosphine which allows for direct substitution of the alcohol. The relative high acidity of the NH- on the aromatic base makes it a useful partner in the coupling.⁵³ A major drawback of this reaction is the poor atom economy displayed by the use of triphenylphosphine (PPh₃) and diisopropyl azodicarboxylate (DIAD) only for hydroxyl group activation and resulting inevitably

in the formation of by-products insoluble in aqueous media and need to be removed via chromatography.⁷⁶ And although the yield for the Mitsunobu coupling was low, it was still a more desirable practical step that avoided the lengthy linear route of building the purine base in a stepwise fashion.⁷⁷ The requisite cyclopentenone **15** has been synthesized previously via various pathways.^{32,78-80} Adaptation of a concise and efficient method developed in the Schneller group⁸¹ was called on for this research.

The synthesis of cyclopentenone **15** is outlined in Scheme 9. The preparation of this important intermediate started with commercially available D-ribose by its reaction with 2, 2-dimethoxypropane, methanol and hydrochloric acid to achieve 2, 3- ketal protection and methylation of the anomeric hydroxyl group in **11**. This was followed by transformation of the primary hydroxyl group of **11** into the iodide site via reaction with triphenylphosphine and iodine to give compound **12**.⁷⁸ Reductive cleavage of **12** using activated zinc in methanol gave the ring opened aldehyde **13**.⁸⁰ This aldehyde underwent a Grignard 1,2-addition process using vinylmagnesium bromide to yield diene **14**. The compound **14** was subjected to a ring closing metathesis using Grubbs first generation catalyst (Figure 18) resulting in the formation of the allylic alcohol, which was oxidized directly, and without purification, using pyridinium chlorochromate to give **15** (in 30 % overall yield over five steps from D-ribose).



Scheme 9. The synthesis of cyclopentenone 15 from D-Ribose

Olefin metathesis has emerged as a powerful tool in C-C bond formation⁸² and was called upon here for the necessary ring-closing metathesis (RCM) whereby medium or large sized rings are constructed from acyclic diene precursors. It has been an efficient approved tool in the total

synthesis of natural products^{83,84} and nucleoside chemistry.⁸⁵ The ruthenium olefin metathesis catalysts (Grubbs catalysts) offer high activity, functional group tolerance and adequate air and moisture stability for this purpose.⁸⁶ In 2005, Yves Chauvin, Robert Grubbs and Richard Schrock received the Nobel Prize for their contributions and the development of metatheses reactions.⁸⁷

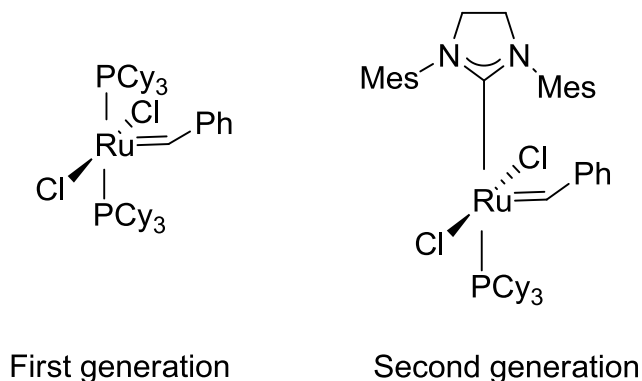
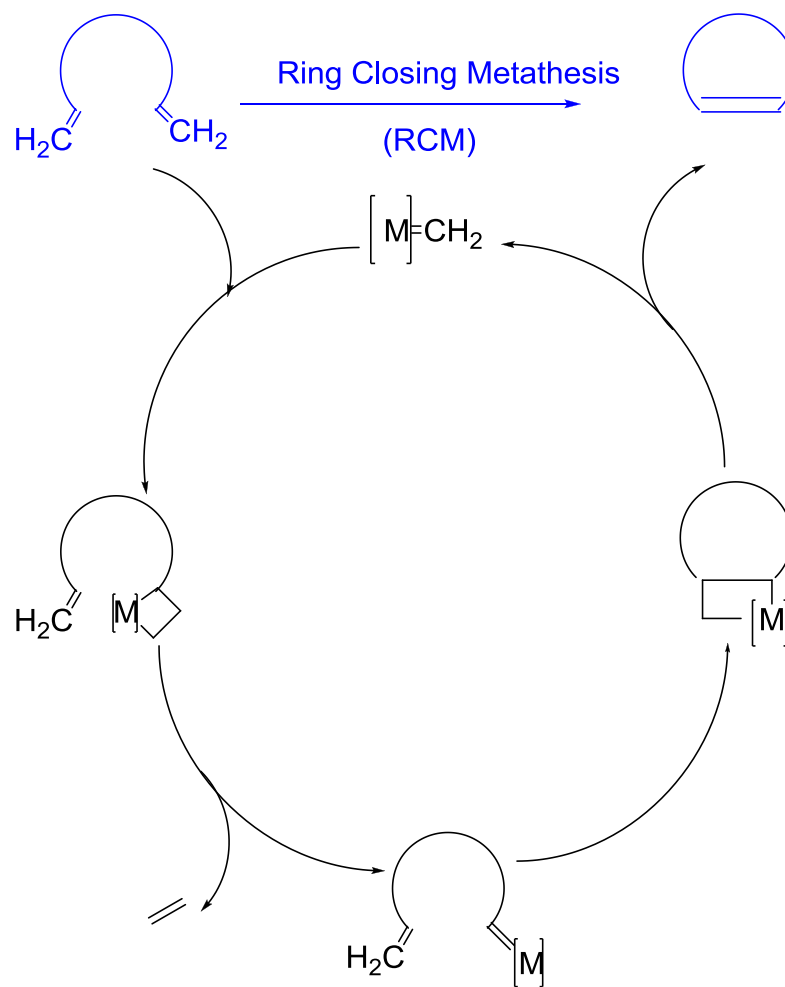


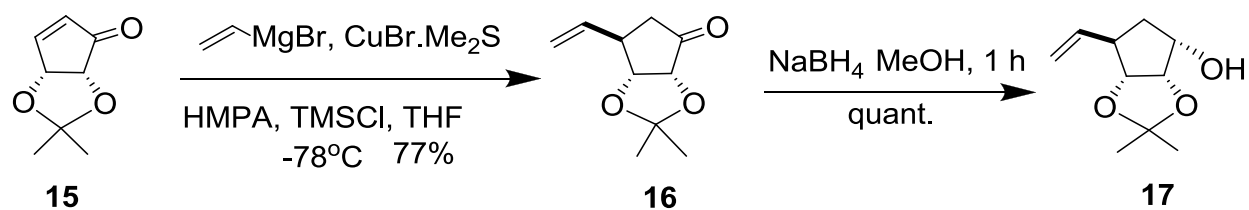
Figure 18. Grubbs catalysts

The mechanism of action^{88,89} as shown in Scheme 10 was proposed by Chauvin where a metal alkylidene reacts with an olefin leading to the formation of the metallocyclobutane intermediate. The newly formed metal alkylidene reacts with the other olefinic group resulting in another metallocyclobutane intermediate which upon decomposition yields the product and the metal alkylidene which is ready for another catalytic cycle.



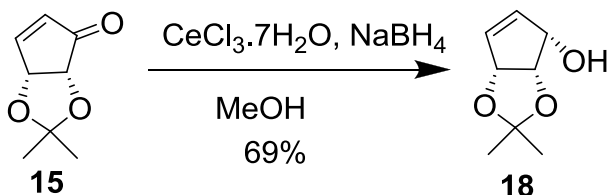
Scheme 10. Reaction mechanism of RCM

Having the enone **15** in hand allowed for its functionalization to yield all the required targets. For target A (Scheme 8), the enone was transformed into compound **16** through a 1, 2-Michael addition of vinylmagnesium bromide to **15**. Reduction of the vinyl ketone using lithium aluminum hydride gave the vinyl alcohol **17** in 92% yield. (Scheme 11)



Scheme 11. Synthesis of precursor 17

Cyclopentenone **15** was also employed to build up the needed precursor **18**, which also illustrated the versatility of **15** for the synthesis of carbocyclic nucleosides. Thus cyclopentenone **15** was reduced to allylic alcohol **18** under the stereoselective Luche reduction conditions⁶ employing sodium borohydride and cerium(III)chloride heptahydrate (Scheme 12).

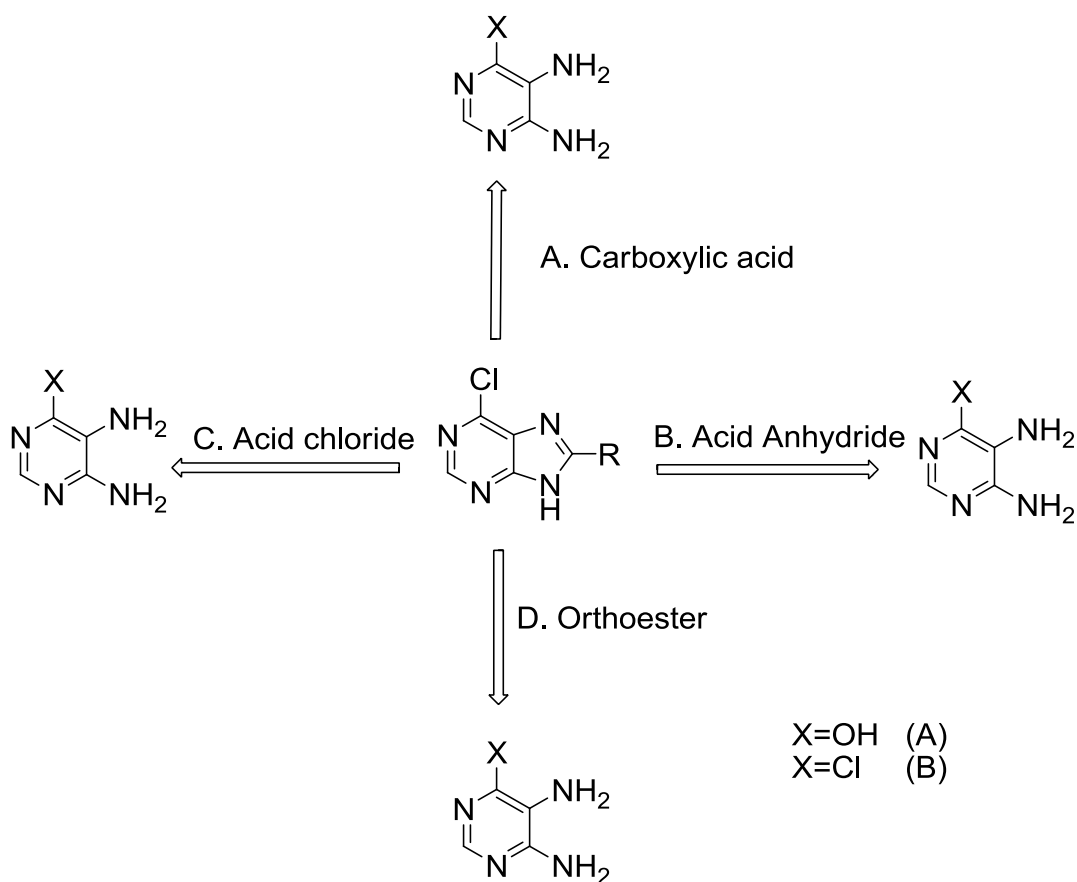


Scheme 12. Synthesis of precursor 18

Synthesis of the Heterocyclic Nucleobase:

Attention turned to the synthesis of the C-8 substituted heterocyclic nucleobase. The literature shows that a large number of purines are synthesized from pyrimidine precursors. For example the Traube synthesis of 2,4,5-triamino-1,6-dihydro-6-oxopyrimidine with formic acid and a wide variety of cyclizing agents provide a versatile and efficient route to numerous substituted purines.⁹⁰ This approach is based on introduction of a one-carbon fragment to bridge the nitrogens of the amino groups at the 4 and 5 positions of the pyrimidine. Some of the cyclizing agents used are carboxylic acids, acid chlorides, acid anhydride, orthoesters, ureas and amidines.

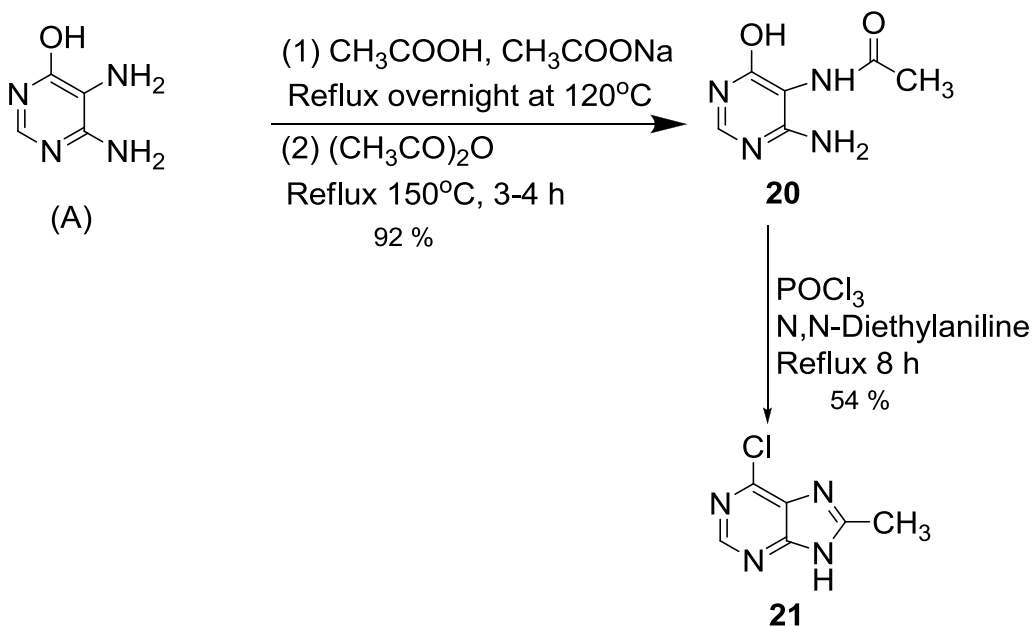
Almost all chloropurines that appear in the literature come from chlorination of purinones with phosphorus oxychloride (POCl_3) and with or without a tertiary β -amine resulting in variable yields and unpredictability of formation of the chloropurine.⁹¹ Other methods involve the use of chloro-4, 5-diaminopyrimidines with conventional reagents as formic acid which leads to hydrolysis of the chlorine atom. The use of chloro-4, 5-diaminopyrimidines with orthoesters and anhydride mixtures leads to the formation of chloropurines and N-acetyl purines. The N-acetyl purines are hydrolyzed to the corresponding purines upon dissolution in 10% NaOH solution for 5-10 minutes.



Scheme 13. Purine synthesis based on various reagents agents

In Scheme 13, four routes to the synthesis of purines via the Traube method were attempted based on compatibility, availability and efficiency. The first starting material tried was the commercially available 5, 6-diaminopyrimidin-4-ol that is supplied as a hemisulfate salt (A, Scheme 14). Treatment of the hemisulfate salt with acetic anhydride at refluxing conditions followed literature conditions,⁹² failed to produce any products. Alternatively the salt was treated with acetic acid and sodium acetate, and was refluxed overnight. The excess acetic acid was distilled off under reduced pressure (Scheme 14), and the residue treated with acetic anhydride

under refluxing conditions to produce **20**.⁹² Refluxing **20** in phosphorus oxychloride in the presence of N, N-diethylaniline afforded **21**.

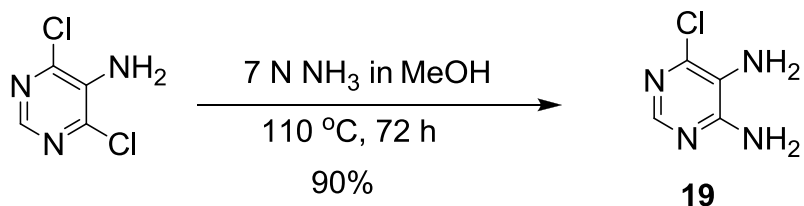


Scheme 14. Synthesis of 6-chloro-8-methylpurine 21.

Failure of the hemisulfate to give ring closed products without treatment with acetic acid and sodium acetate may be attributed to the stability of the salt and the reduced nucleophilicity of the amino nitrogens. Hence, this procedure was eliminated for optimization towards other alkyl substituents at the purine-8-position.

Looking back at Scheme 13, 4, 6-dichloropyrimidin-5-amine (B) arose as a promising possibility for the desired syntheses of the 8-alkyl-6-chloropurines. Thus the less expensive

reagent available 4, 6-dichloropyrimidin-5-amine was transformed with methanolic ammonia into **19** in high yields (Scheme 15).



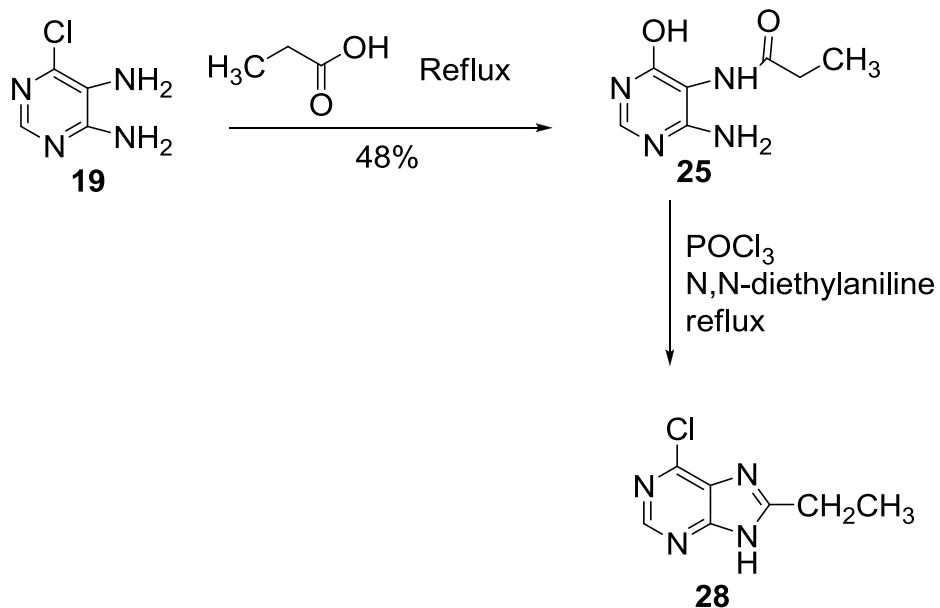
Scheme 15. Amination of 4, 6-dichloropyrimidin-5-amine

Using **19** as a starting material, an optimization study using different routes as described in Scheme 12 was conducted towards the synthesis of 6-chloro-8-ethyl-9H-purine.

Synthesis of 6-chloro-8-ethyl-9H-purine:

(A) Synthesis based on use of carboxylic acids:

This route was based on using carboxylic acids with **19** under refluxing conditions (Scheme 16).⁹³ Use of propionic acid led to the formation of the monoacylated product with concomitant displacement of the chlorine atom. Cyclization and chlorination were achieved with phosphorus oxychloride in the presence of N,N-diethylaniline.⁹² This reaction has been inconsistent and at times the chlorination step didn't occur simultaneously with cyclization which led to exploring other routes for cyclization and alkylation at the 8-position of the purine.

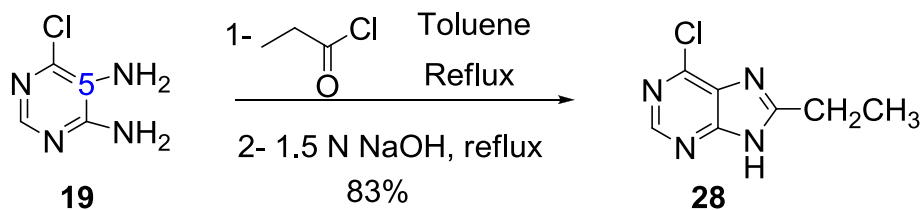


Scheme 16. Synthesis of 28 using carboxylic acid

(B) Synthesis based on use of acid anhydrides:

Reaction of **19** with propionic anhydride under reflux gave **28** in very low yield along with the formation of unidentified byproducts.

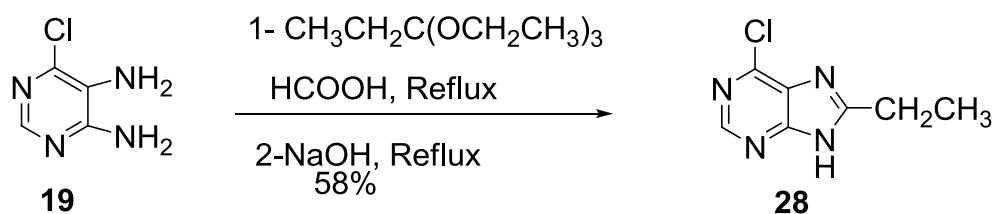
(C) Synthesis based on use of acid chlorides:



Scheme 17. Synthesis of 28 using acid chloride.

Heating **19** with propionyl chloride in toluene led to acylation of the amino group at the 5 position of **19** and the cyclized product **28**. These conditions also caused displacement of the chlorine atom. However, maintaining anhydrous conditions for the reaction and using a low concentration of sodium hydroxide in the second step and refluxing for a short time produced a good yield of **28** (Scheme 17).

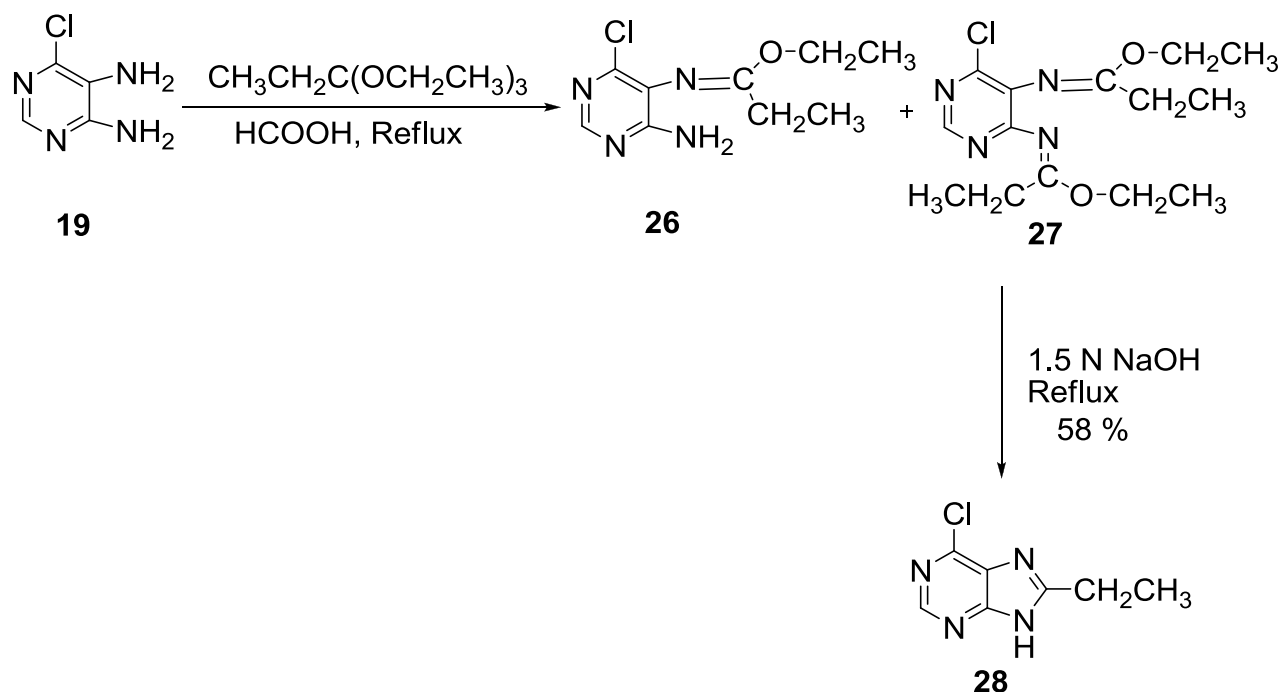
(D) Synthesis based on use of orthoesters:



Scheme 18. Synthesis of 28 using orthoesters.

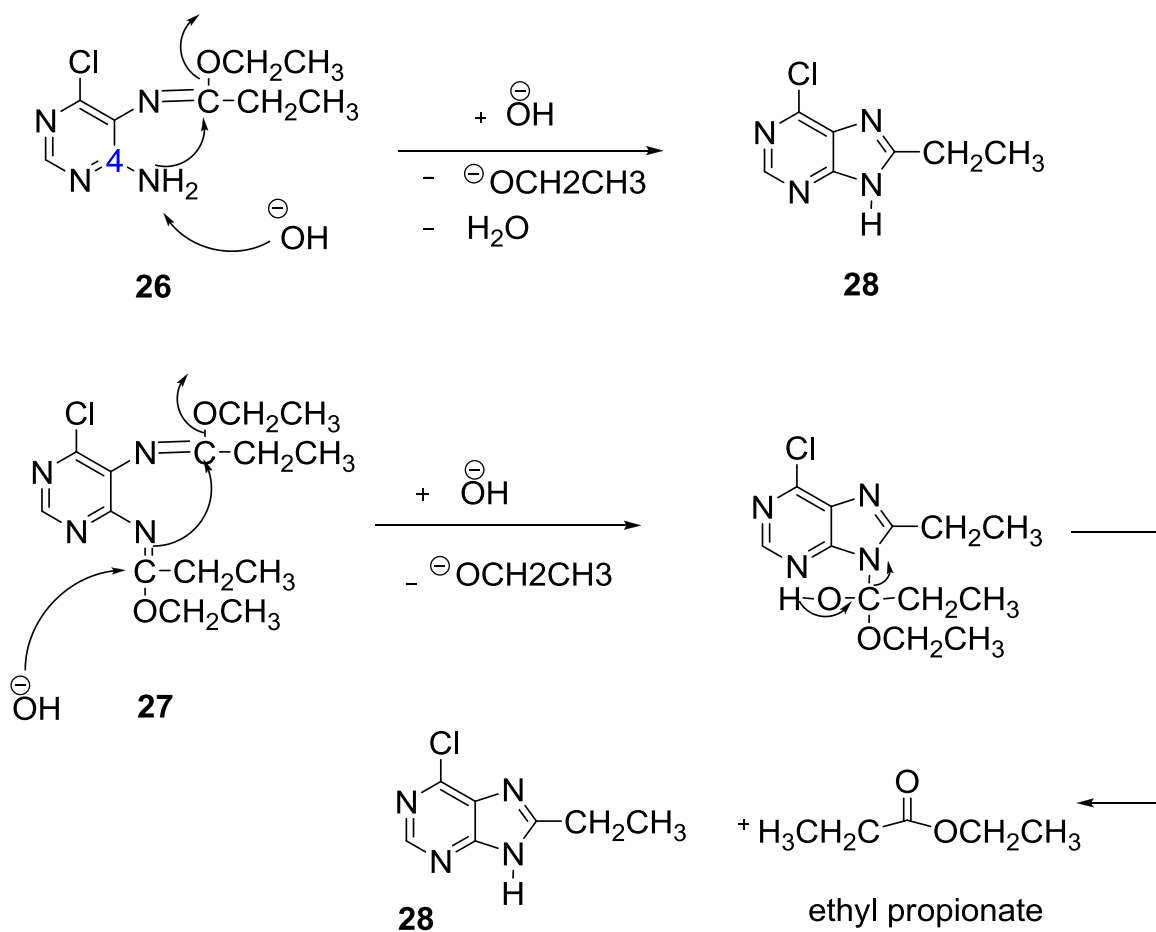
It is known that direct cyclization of diamino pyrimidines is possible with various combinations of orthoesters and acid mixtures or acid anhydrides with desired purine functionalization guiding reagent choice.^{90,94} Thus reacting **19** with triethyl orthopropionate in the presence of a catalytic amount of formic acid gave a crude mixture of mono- **26** and diimino **27** substituted intermediates as well as **28** (Scheme 18). After the reaction was done, as evident by disappearance of starting material as shown via thin layer chromatography and LC/MS, both compounds were separated and refluxed in NaOH separately. Compound **26** was cyclized in less than 30 min of reflux. On the other hand, compound **27** took longer to cyclize into **28**. Upon repetition of this synthesis it was apparent that separation of 26 and 27 and cyclization in NaOH

didn't improve the yields. Hence the crude mixture, without separation, was refluxed in sodium hydroxide for short periods of time to furnish **21** in 58% yield.



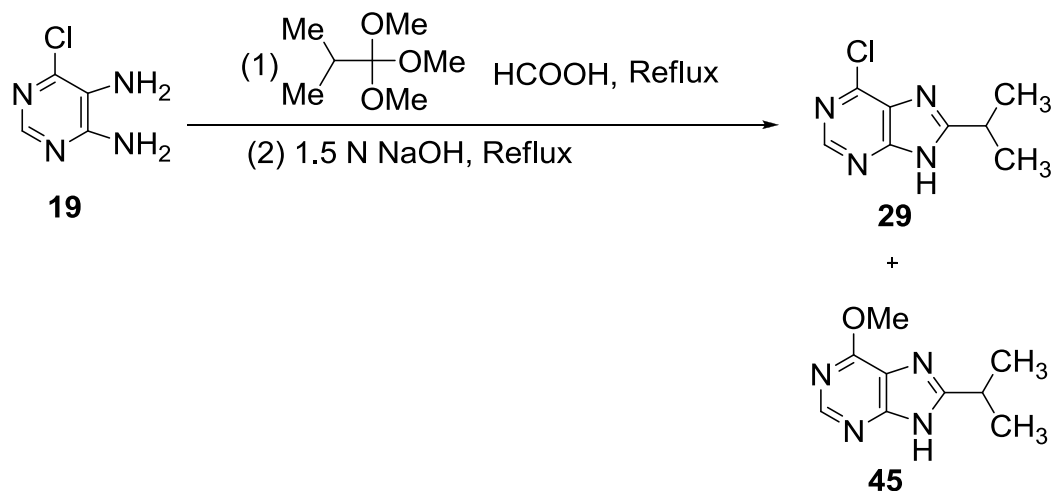
Scheme 19. Intermediates 26 and 27 from the orthoester reaction.

A proposal for the reaction mechanism is outlined in Scheme 20. For compound **26**, NaOH abstracts a proton from the amino group at the 4-position of the pyrimidine ring leading to a nucleophilic attack on the imine carbon and subsequent loss of ethanol leading to the cyclized product **28**. Cyclization of compound **27** follows a similar mechanism with the subsequent loss of ethanol and ethyl propionate.



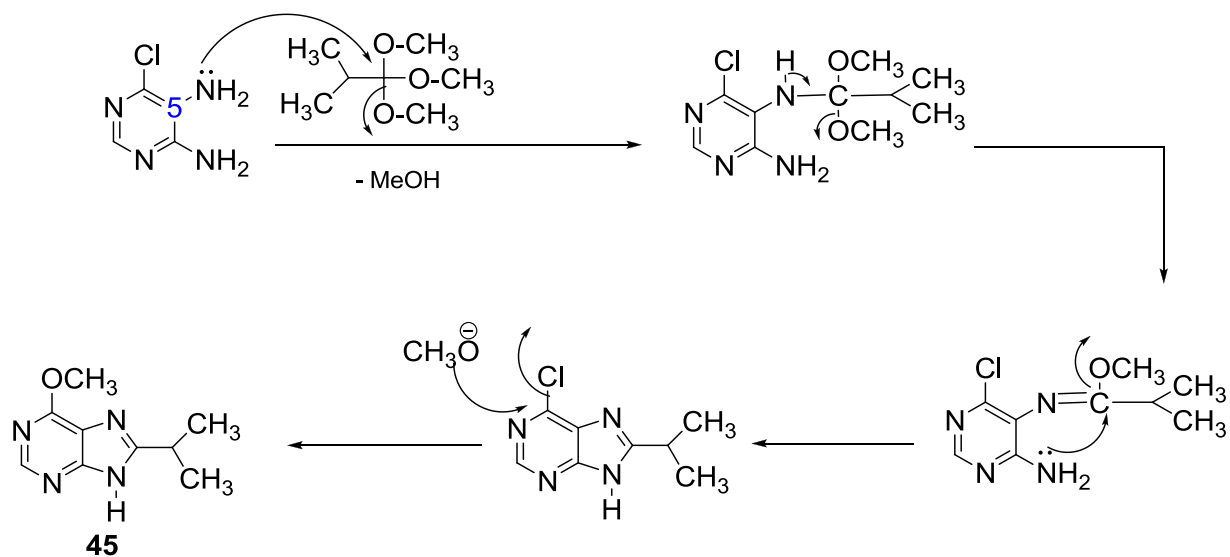
Scheme 20. Proposed reaction mechanism for the formation of 28 from intermediates 26, 27.

Synthesis of 6-chloro-8-isopropyl-9H-purine using orthoesters:



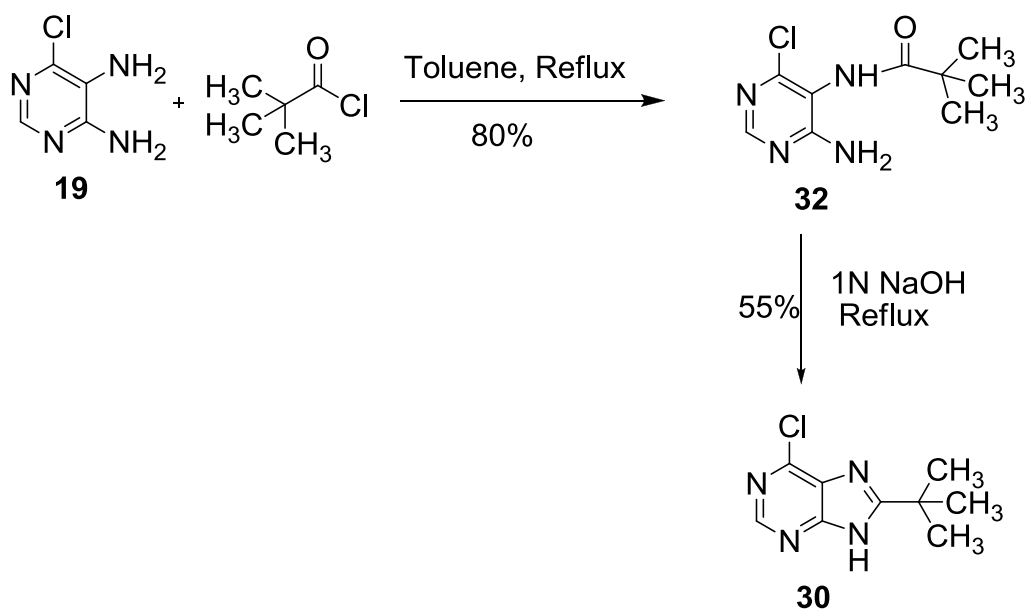
Scheme 21. Synthesis of 29

Due to the availability of the orthoester that furnishes the isopropyl substitution at the 8-position of the purine ring, **19** was reacted with trimethyl orthoisobutyrate [(CH₃)₂CHC(OCH₃)₃] in the presence of formic acid (Scheme 21). The crude mixture then refluxed in sodium hydroxide to provide **29** which occurred in low yield with the appearance of a side-product **45** which is believed to be a cyclization product following displacement of the chlorine atom. The proposed mechanism is outlined in Scheme 22. A nucleophilic attack of the pyrimidine amino group at the 5-position happened at the orthoester with concomitant loss of methanol. This was followed with imine formation and loss of another methanol. Nucleophilic attack at the imine carbon coupled with loss of another methanol furnished the cyclized product **29**, which under these reaction conditions caused a nucleophilic aromatic substitution of the chlorine resulting in **45** resulting in low yields of **29**.



Scheme 22. Proposed mechanism for formation of 45

Synthesis of 8-tert-butyl-6-chloro-9H-purine:



Scheme 23. Synthesis of 6-chloro-8-*t*-butylpurine using acid chloride

Due to the fact that longer chain orthoesters are either unavailable or very expensive, to realize compound **30**, trimethylacetyl chloride was the reagent of choice (Scheme 23). Refluxing **19** with this acid chloride gave the monoacylated product **32** as a hydrochloride salt. **Figure 19** shows structure of **32** from analysis of a single crystal by X-ray spectroscopy and it serves as a confirmation as to which amino group (at the C5 of the pyrimidine, ortho to chlorine atom) was involved in the acylation reaction. Upon refluxing of **32** with sodium hydroxide for 2 h, the cyclized product **30** was obtained as a hydrochloride salt in 55% yield.

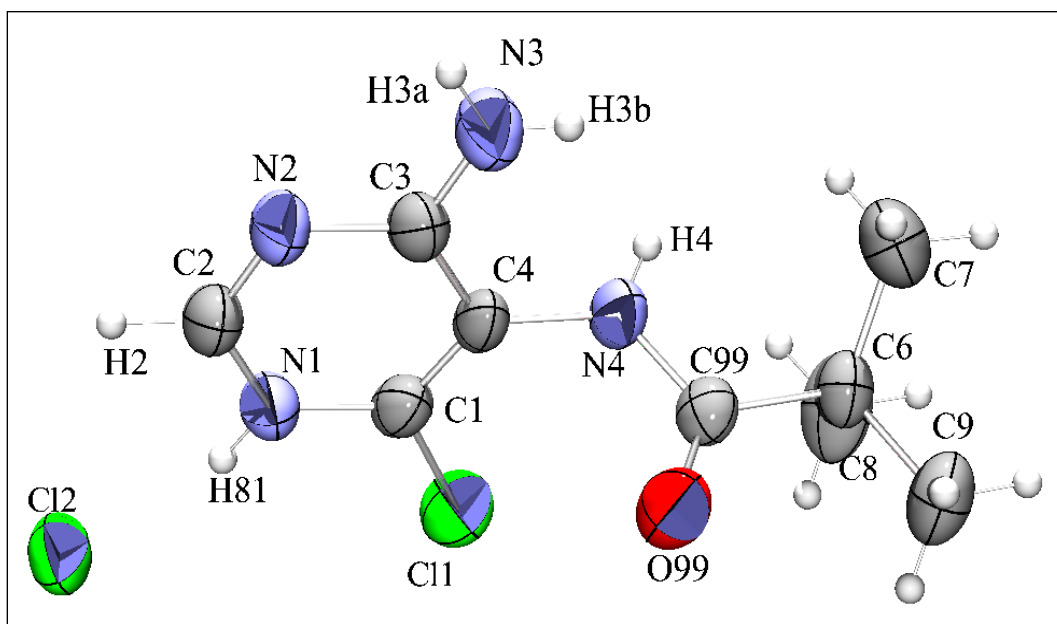
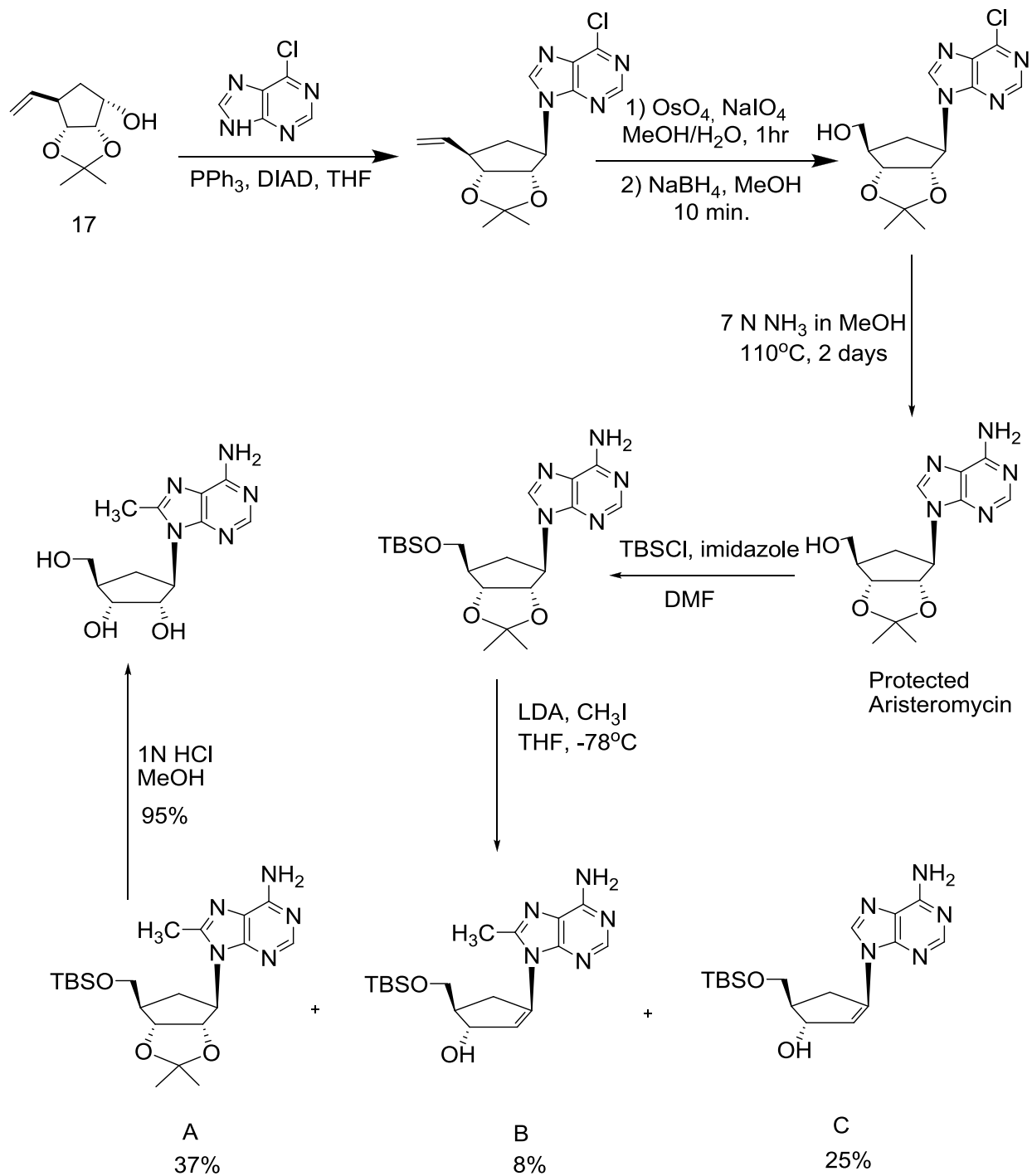


Figure 19. Structure of **32** from X-ray analysis.

Chapter 3. Synthesis of 8-Alkyaristeromycin

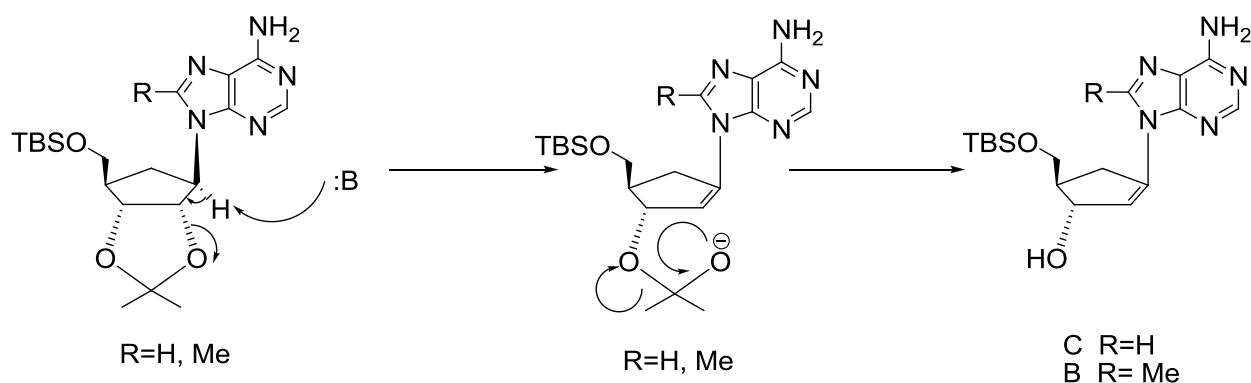
Based on the computational analysis described in chapter 1, two compounds were chosen for preparation as prototypes for the experimental of 8-substituted aristeromycin. Once obtained, these two compounds were analyzed and the data collected to measure the precision of the methodology developed from the theoretical calculations (spin-spin coupling constants, *syn/anti*, N/S, and relevant chemical shifts).

The synthesis will depend on the convergent route to carbocyclic nucleosides. Alkylation of the 8-position of purine nucleosides has been extensively studied.⁵⁷ One of the routes used to accomplish this, is C-8 bromination followed by nucleophilic displacement.^{95,96} However, this pathway is time consuming and offers low yields. Another route to this alkylation is lithiation at C-8 followed by reaction with a desired electrophile.^{97,98} Based on some unpublished results by Dr. Wei Ye from our labs, the latter linear route was adopted as shown in Scheme 24 as a way of synthesis.



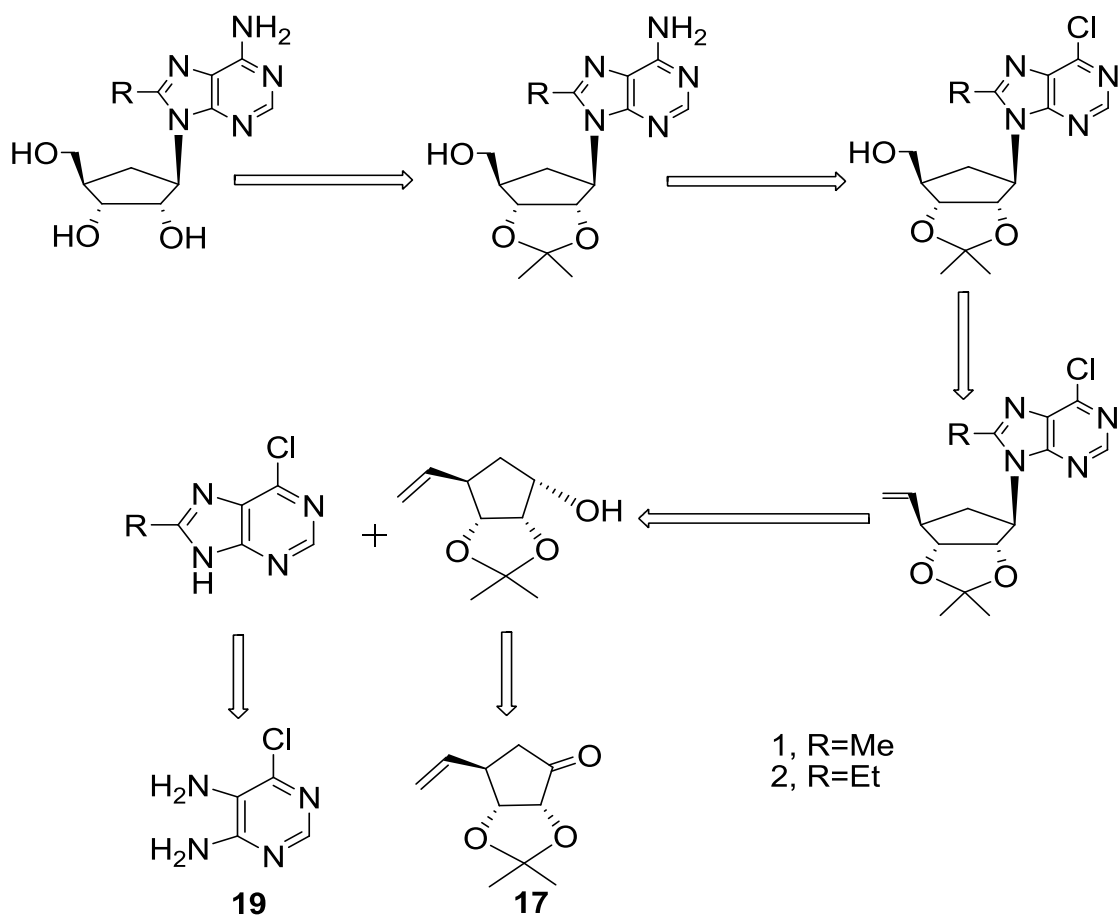
Scheme 24. Synthesis of 1 based on unpublished results using the linear route.

The synthesis was based on obtaining the protected aristeromycin then protecting the primary hydroxyl group with a t-butyldimethyl silyl group and subjecting it to lithiation using 5 equivalents of lithium diisopropylamide (LDA) and finally quenching with iodomethane. This step resulted in the formation of the desired product in addition to two other side products as well as recovering some starting material. The side products obtained B and C were studied, and a mechanism was proposed for their formation as shown in (Scheme 25). This is based on the abstraction of H1' via LDA and the formation of the C1'-C2' double bond, followed by opening of the isopropylidene and subsequent loss of acetone.



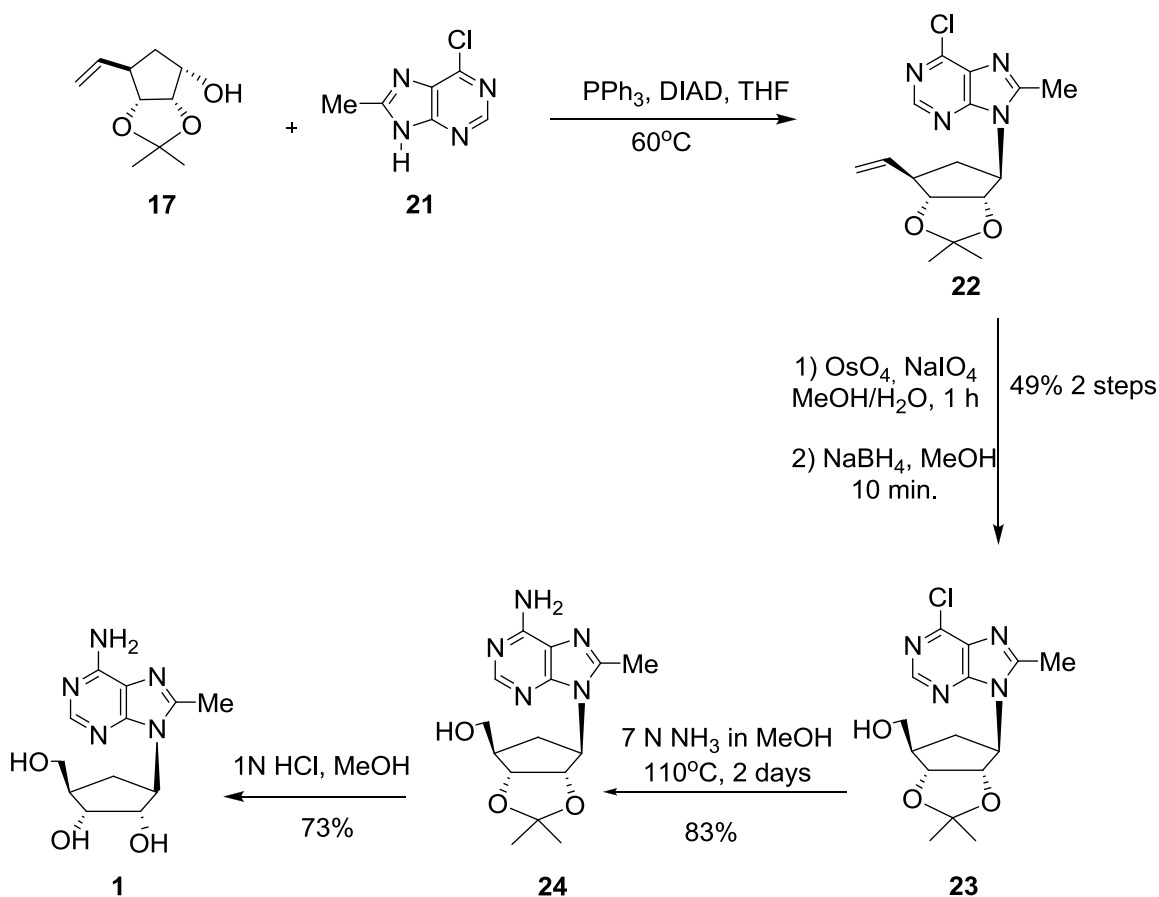
Scheme 25. Proposed mechanism for side products.

Based on these results, optimization of this procedure was undertaken. The convergent route provides advantages for this purpose as being shorter and more efficient. The proposed retro synthesis of 8-alkylaristeromycin is presented in (Scheme 26) where R = methyl or ethyl.



Scheme 26. Retro synthesis of 8-alkyl substituted Aristeromycin

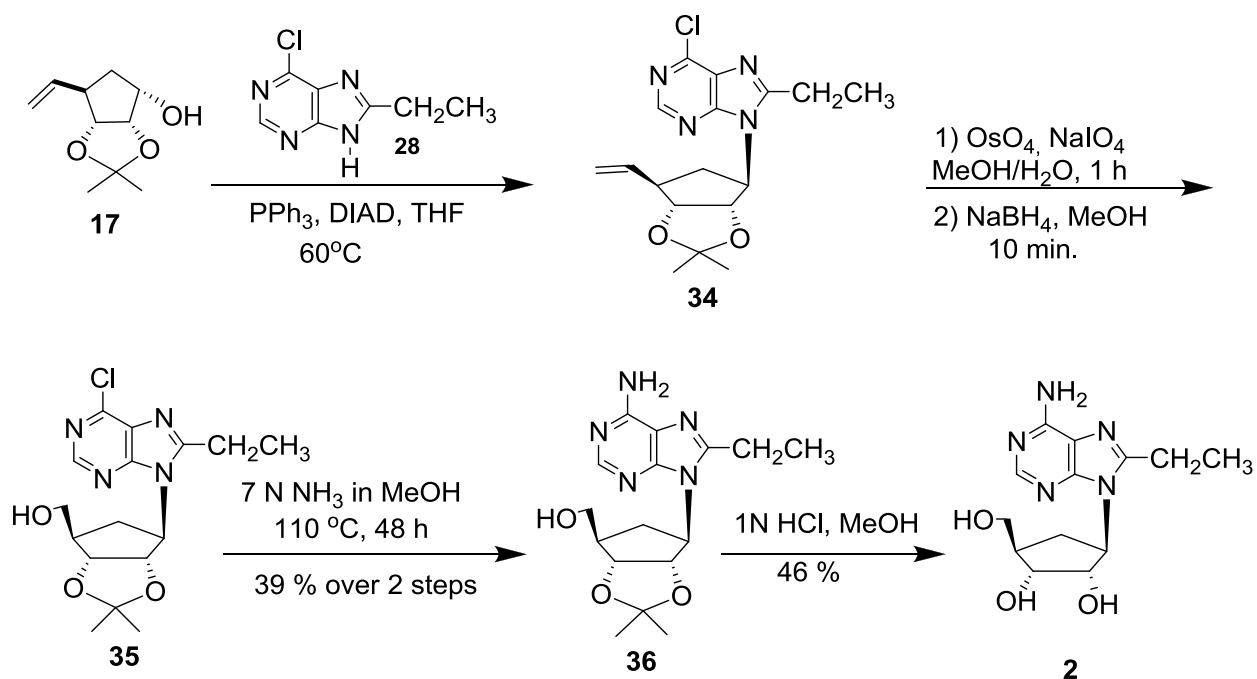
The synthesis (Scheme 27) starts with precursor **17** (Scheme 11) and 6-chloro-8-methyl-purine **21** in (Scheme 14) with a Mitsunobu coupling in the presence of triphenylphosphine and diisopropyl azodicarboxylate yielded **22**. Manipulation of the vinyl group in **22** to the requisite hydroxymethyl side chain was accomplished in two steps⁸¹: (i) oxidative cleavage with osmium tetroxide and sodium periodate gave an intermediate aldehyde, (ii) direct reduction of the aldehyde, without separation, with sodium borohydride into the alcohol giving **23** in 49% yield over two steps.



Scheme 27. Synthesis of compound 1 by the convergent route.

Treatment of **23** with methanolic ammonia at 110 °C for two days gave **24** in good yield. Finally, deprotection of the isopropylidene group under acidic conditions followed by chromatographic purification afforded target **1** which was confirmed with X-ray crystallography. Target **1** was characterized via NMR spectroscopy and LC/MS. Both the NMR data and the X-ray crystallography show a *syn* conformation of compound **1**.

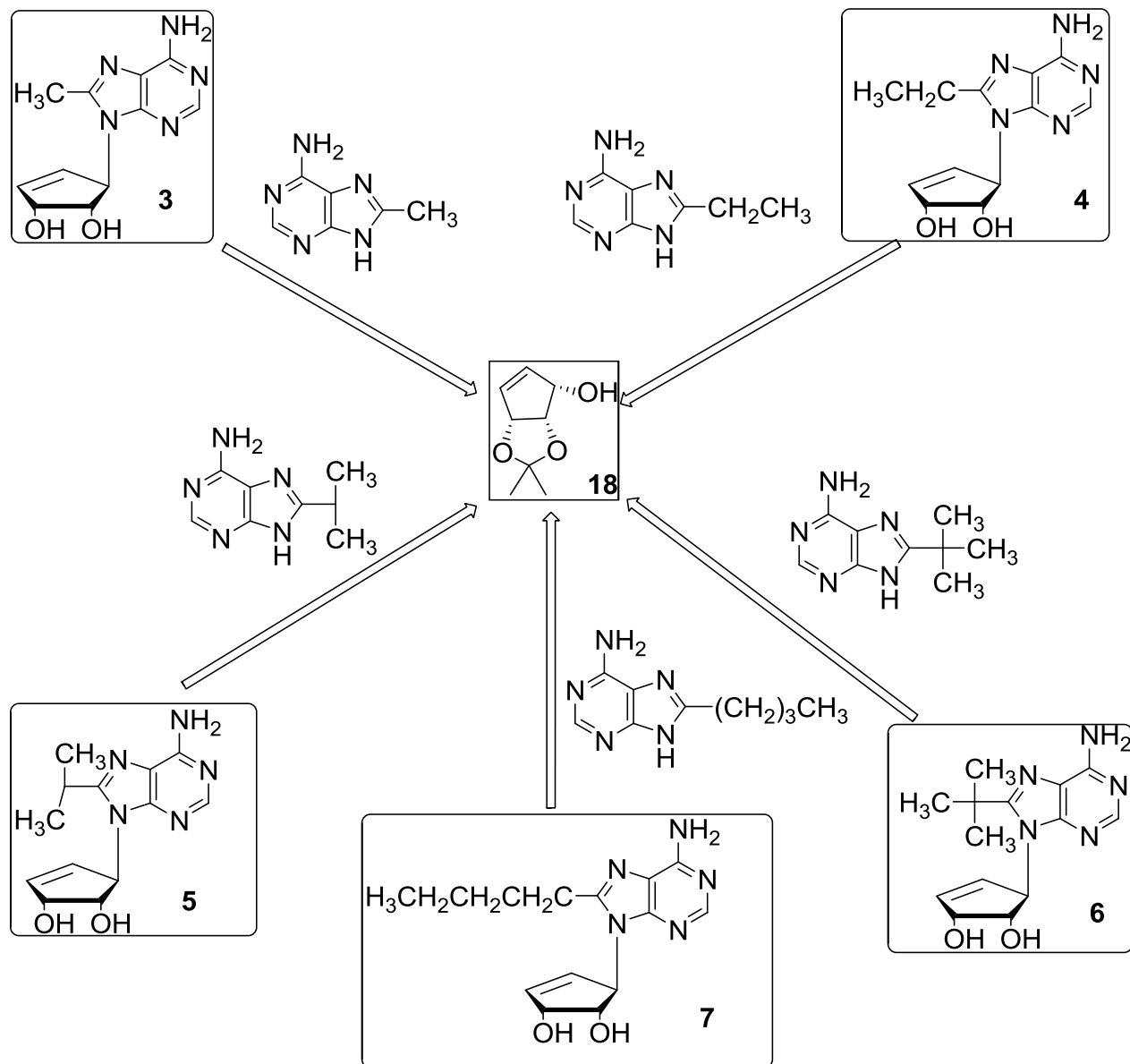
The preparation of target **2** followed the retro synthesis outlined in Scheme 25. Thus, a Mitsunobu coupling between **17** and **28** (Scheme 28) was carried out. The crude mixture of **34**, contaminated with diisopropylhydrazine dicarboxylate, was subjected to oxidative cleavage with osmium tetroxide followed by reduction with sodium borohydride to yield **35**. Ammonolysis of **35** with methanolic ammonia furnished **36** in 39 % over two steps. Deprotection of **36** with 1 N HCl gave target **2** in 46% yield.



Scheme 28. Synthesis of compound 2 by the convergent route.

Chapter 4. Synthesis of 8-Substituted 4'-Norneplanocin Analogues

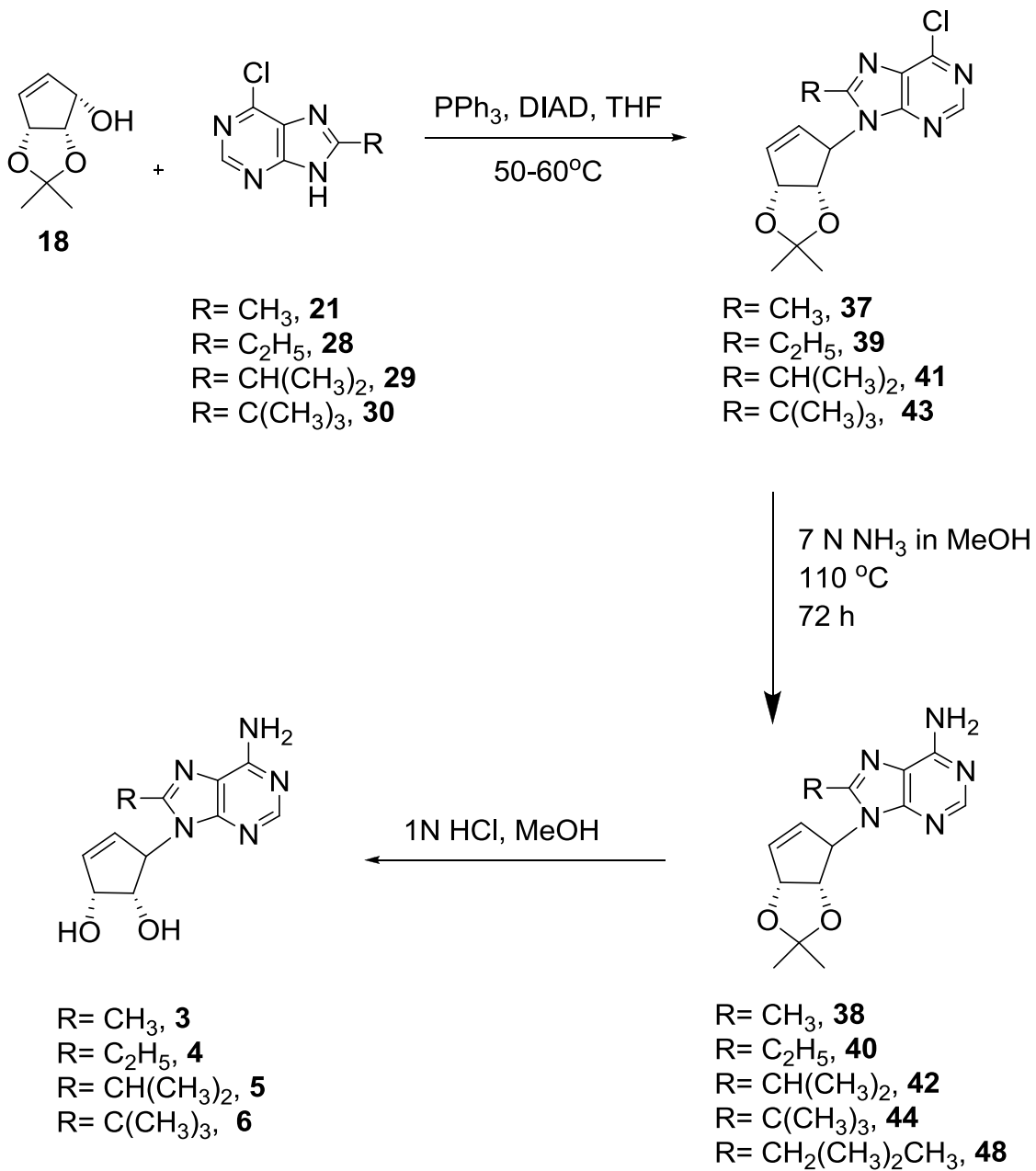
This chapter will describe the investigations into alkyl substitution at the 8 position of purine bases within the framework of 4'-norneplanocin. The synthetic approach made use of the convergent pathway of synthesis of carbocyclic nucleosides stressing the versatility of this route. The efficiency of this route became more evident in instances where the series of nucleosides built on a specific carbocycle or specific heterocycle is required for building libraries of nucleosides for biological screenings.⁷⁶ In this research the synthetic investigation of 8-alkyl-4'-norneplanocin depended on the common allylic alcohol **18** with the preformed heterocycles: **21**, **28**, **29**, **30** and **46**. Target compounds **3**, **4**, **5**, **6** and **7** pursued are shown in Scheme 29.



Scheme 29. Retrosynthesis of targets 3, 4, 5, 6 and 7 using the convergent route.

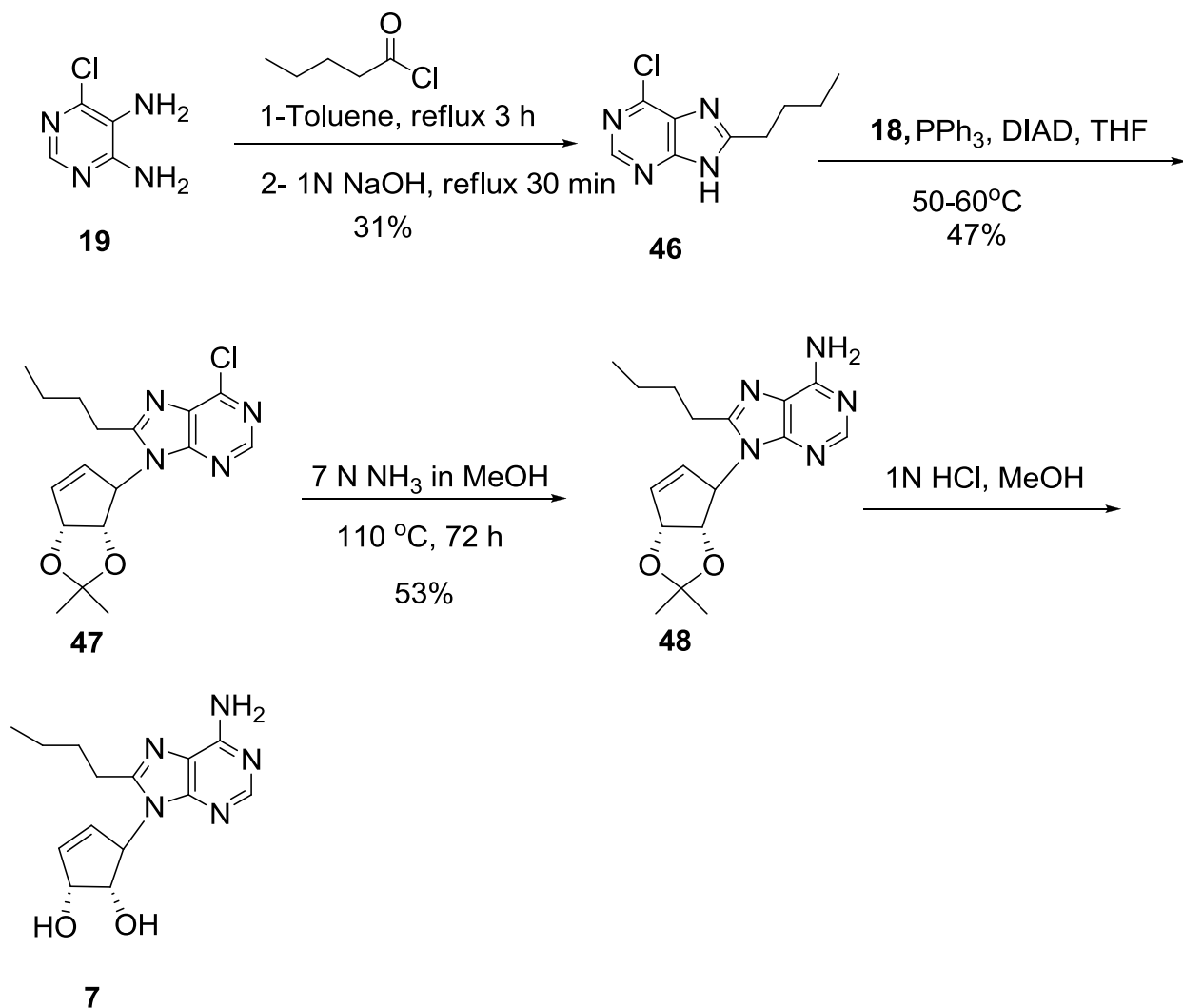
The synthesis of target nucleosides made use of the allylic alcohol **18** described earlier in Scheme 12. One of the most common and useful methods for joining the heterocycle and the carbocycle is the afore described Mitsunobu coupling reaction. However, one of the drawbacks of this process is the formation of side products, namely, triphenylphosphine oxide and the diisopropyl hydrazine dicarboxylate (DIAD by-product). In this case, the closeness of the retention factor R_f between diisopropyl hydrazine dicarboxylate and the coupled product led to problematic separations of the coupled adducts i.e. **37**, **39**, **41**, **43** and **47**. Fortunately, the next step in the synthesis was not affected by the use of the crude material in the ammonolysis reaction. For **43**, the reaction required longer heating during the Mitsunobu coupling step, up to 5 days, and only a minor portion of **30** reacted as demonstrated by its 90 % recovery. This suggests that the bulky t-butyl is interfering with the S_N2 reaction of the Mitsunobu coupling.

Having prepared the heterocyclic bases **21**, **28**, **29** and **30** allowed coupling under regular Mitsunobu conditions with **18** and the adduct products (**37**, **39**, **41** and **43**) were confirmed via mass spectrometry as well as NMR spectroscopy (Scheme 29). However, due to contamination with the diisopropyl hydrazine dicarboxylate (DIAD by-product), the NMR spectra were sometimes difficult to reconcile. Consequently, the crude material was subjected to amination under standard methanolic ammonia conditions to furnish the protected nucleoside (**38**, **40**, **42** and **44**). A final deprotection under acidic conditions followed with purification with column chromatography gave target compounds **3**, **4**, **5** and **6** (Scheme 30) for which verification via NMR spectroscopy and mass spectrometry was accomplished.



Scheme 30. Synthesis of targets 3, 4, 5, and 6

In order to summarize the conditions used for both the synthesis of the heterocycle and the convergent route used in this research, a final target compound **7** was pursued showing the consequence of synthetic optimization in Scheme 31.



Scheme 31. Convergent Synthesis of target compound 7

The synthesis of **46** proceeded via the use of valeroyl chloride under refluxing conditions. This reaction required anhydrous conditions to circumvent displacement of the chlorine atom. Upon reflux, a mixture of acylated products (mono- and di- acylation at the 4 and 5 positions of

the pyrimidine ring) resulted which upon treatment with NaOH under reflux yielded **46** in 31 % yield. The Mitsunobu coupling proceeded smoothly in 47 % yield. This was followed by standard amination with methanolic ammonia giving **48** in 53% yield then deprotection under acidic conditions furnished target **7** in quantitative yield. X-ray crystallography, NMR spectroscopy and LC/MS were used for identification of target **7** and its x-ray crystal structure is show in Figure 21 as a *syn* conformer.

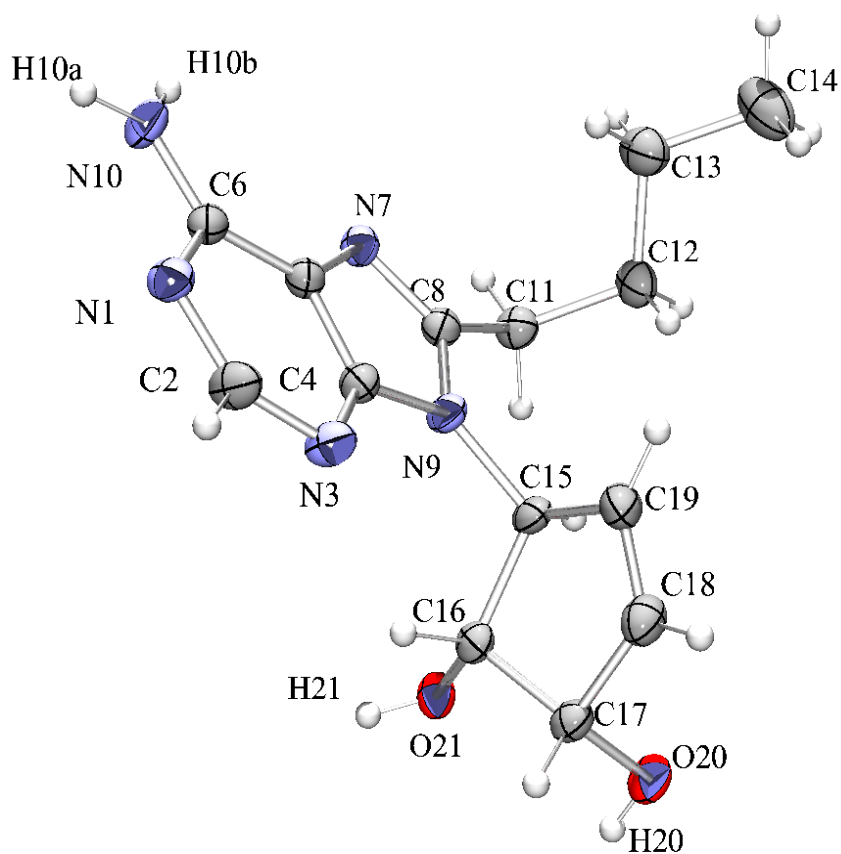


Figure 21. Structure of 7 from X-ray analysis

Chapter 5. Analysis of 8-Ethylaristeromycin (2)

Target **2** (referred to as **F** for the theoretical study) was the second probe to test the theoretical methodology developed in this research. For this target, the molecule was optimized according to the method described in Chapter 2 and all data generated for this molecule were collected. The NMR calculations were done in water and the coupling constants were gathered.

The optimization started with six geometries for **2** that were optimized using both the 3-21G and the 6-31G (d) level of theory. This resulted in three conformations that were being chosen based on our choice of 4 kcal/mol in relative energy (Table 12).

Table 12. Initial conformers chosen for pseudorotation study of (**F**).

Conformer	ΔE 3-21G kcal/mol	ΔE 631G(d) kcal/mol	P	ν_{\max}	χ
FF1	4.2	2.9	152.9	47.2	144.2
FF2	9.1	4.2	177.1	43.9	61.4
FF3	5.4	3.8	43.9	46.6	248.6
FF4	0.0	0.0	37.7	46.0	55.7
FF5	5.4	4.3	183.6	38.5	38.7
FF6	4.2	2.9	152.9	47.2	144.2

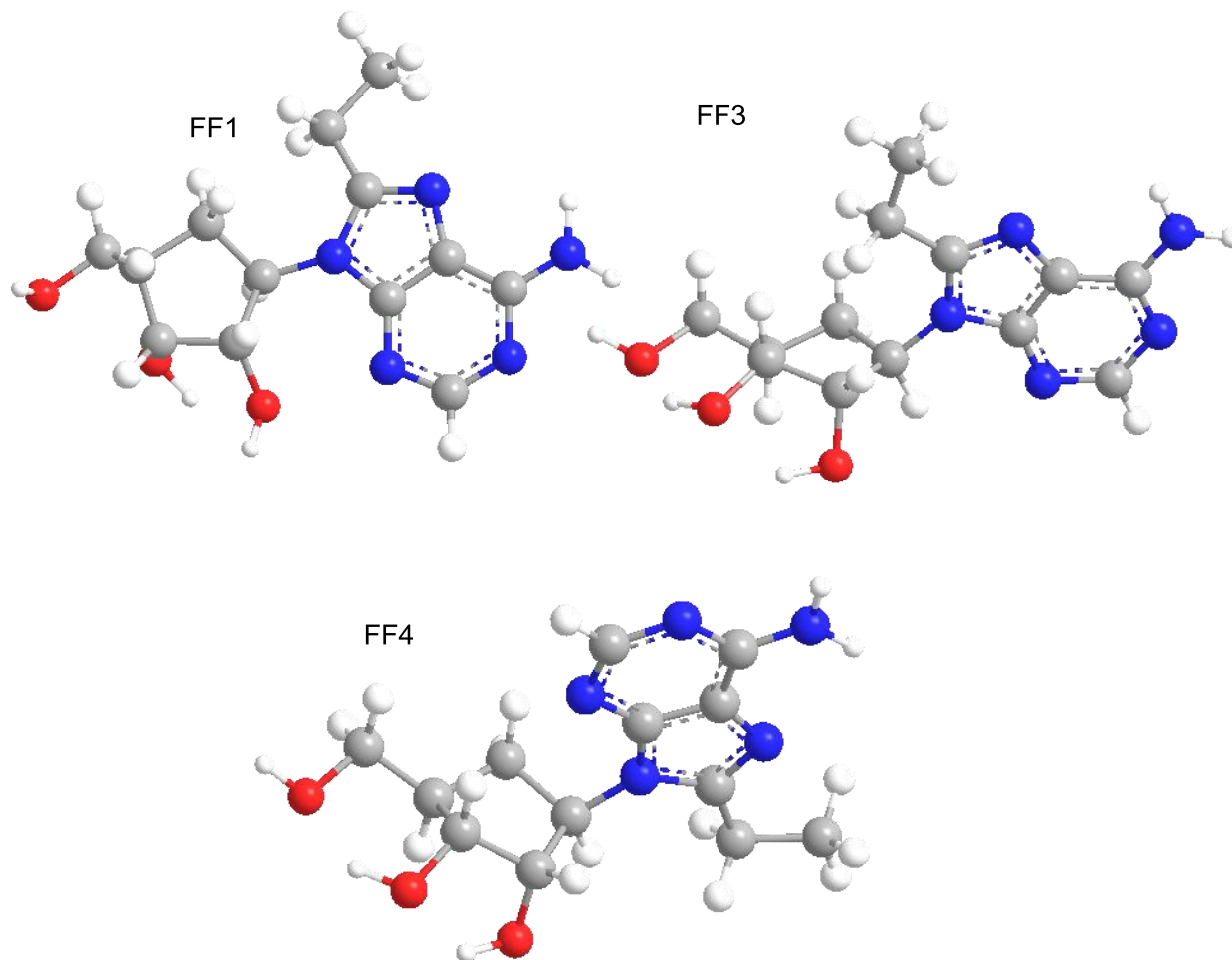


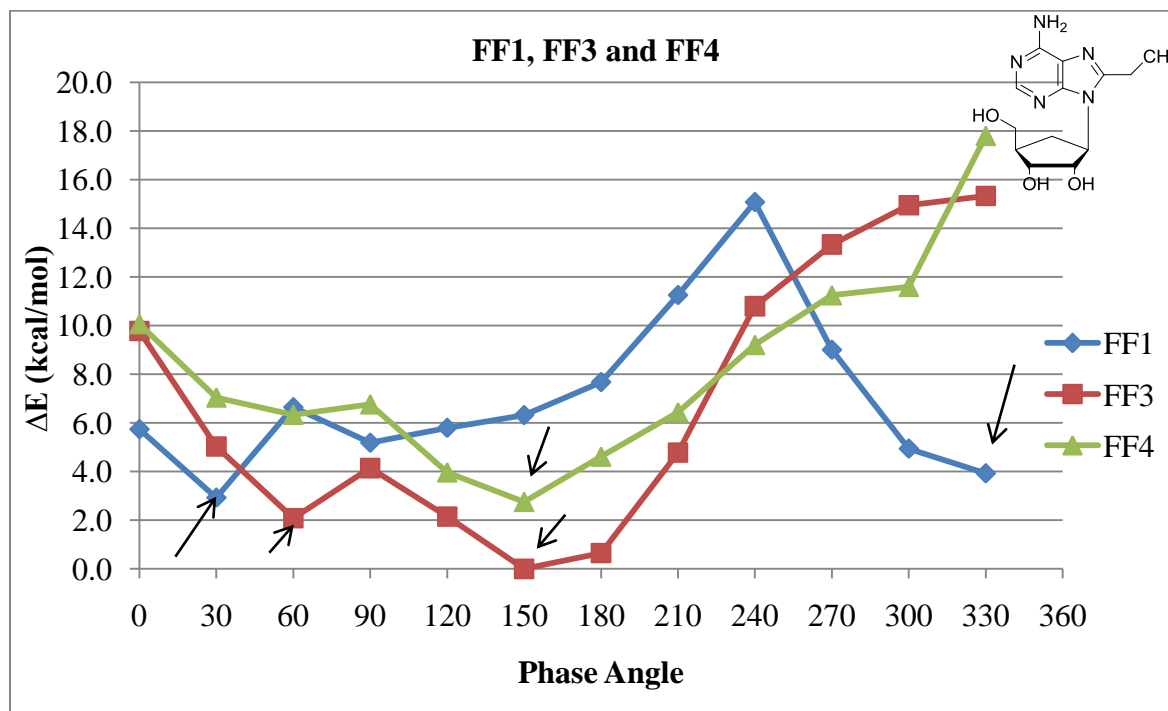
Figure 22. Initial optimization of 8-ethylaristeromycin (F).

For each of FF1, FF3 and FF4 shown in Figure 22, the phase angle has been constrained in 30° increments to generate 12 structures that were fully optimized under the 3-21G in the gas phase followed by single point energy calculations in the gas phase and in solution via the 6-31G (d) level of theory. A graph was constructed to choose the final conformations for total solvation optimization and NMR calculations.

Table 13. Conformations based on single point energy calculations in solution of (F).

FF1	χ		ΔE (kcal/mol)	FF3	χ		ΔE (kcal/mol)	FF4	χ		ΔE (kcal/mol)
0	200.62	A	5.7	0	226.1	A	9.8	0	34.26	S	10.1
30	241.32	A	2.9	30	246.9	A	5.0	30	52.11	S	7.0
60	180.75	A	6.6	60	243.9	A	2.1	60	30.25	S	6.3
90	170.2	A	5.2	90	248	A	4.1	90	31.14	S	6.8
120	146.58	A	5.8	120	247.8	A	2.2	120	30.37	S	4.0
150	143.29	A	6.3	150	250.5	A	0.0	150	32.08	S	2.8
180	150.02	A	7.7	180	246.4	A	0.7	180	38.22	S	4.6
210	184.28	A	11.3	210	247.2	A	4.8	210	25.23	S	6.4
240	179.34	A	15.1	240	352.7	S	10.8	240	106.4	A	9.2
270	115.24	A	9.0	270	289.5	S	13.3	270	111.4	A	11.2
300	117.66	A	4.9	300	309.1	S	14.9	300	109.5	A	11.6
330	123.77	A	3.9	330	3.533	A	15.3	330	52.25	S	17.8

Graph 5. Relative energy in solution for F.



Based on graph 5, five final geometries were chosen for total solvation optimization and NMR calculations and the coupling constants were collected and tabulated in Table 14. The final geometries obtained from the NMR calculations are shown in Figure 23.

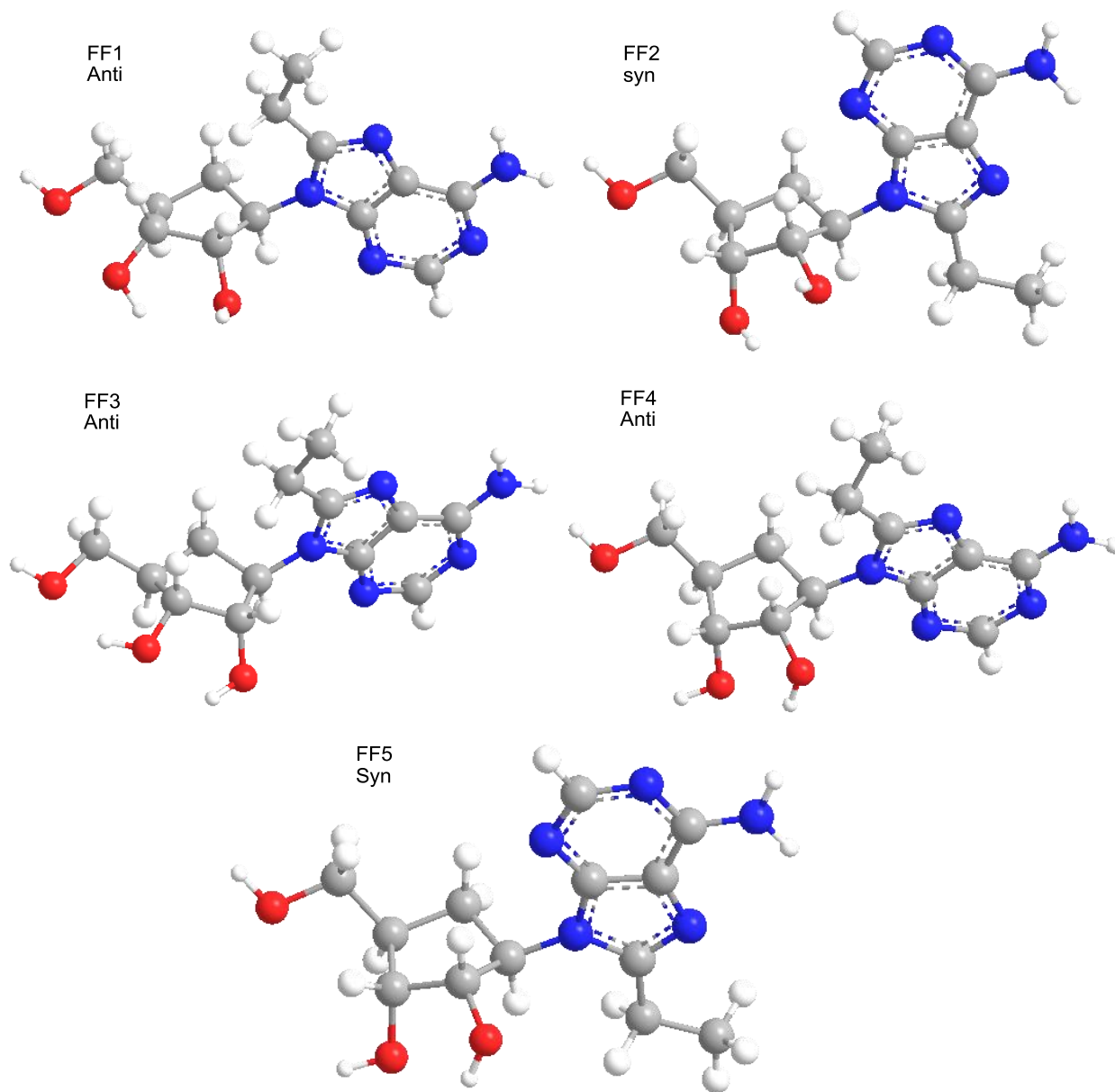


Figure 23. Final geometries for F after NMR calculations.

In addition to the theoretical calculated data, following the synthesis of 8-ethyl aristeromycin **2**, 1D and 2D NMR data were collected: ^1H NMR, ^{13}C NMR, COSY, HMBC and ROESY for the proper assignment of all the protons and carbons in the molecule. This was used to correlate experimental with theoretical as shown in Table 14. For the calculation of the coupling constant involving H2' i.e. 1'-2' and 2'-3', the ^1H NMR spectrum had an overlapping water peak (Figure 24), which led to acquiring the NMR at higher temperature to move the water peak and be able to calculate the coupling constants.

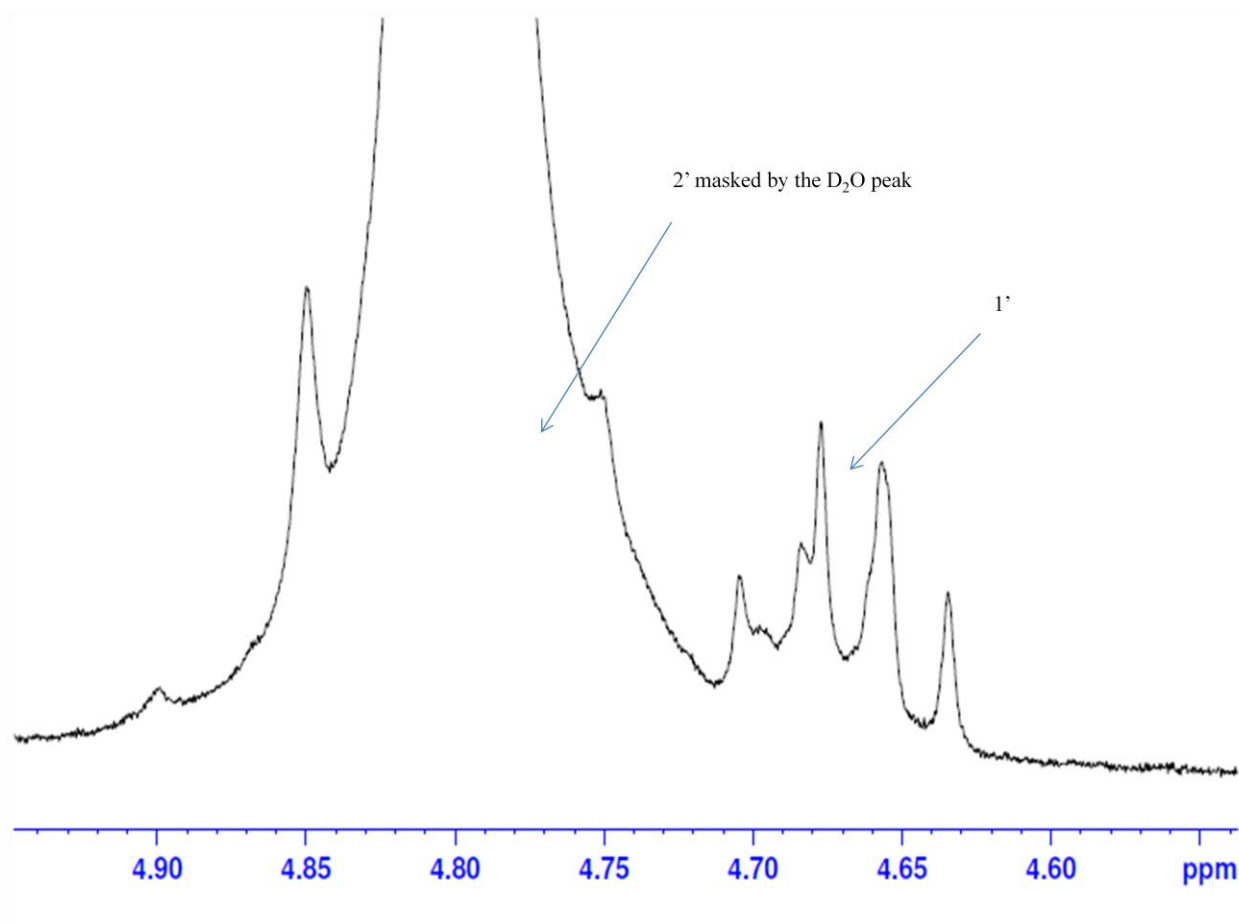


Figure 24. Portion of ^1H NMR spectrum of F in D₂O showing overlapping H2'.

The NMR of **F** was taken in D₂O to allow for minimum variations as possible from the theoretical study and it was run at 327 °K and the result is shown in Figure 25.

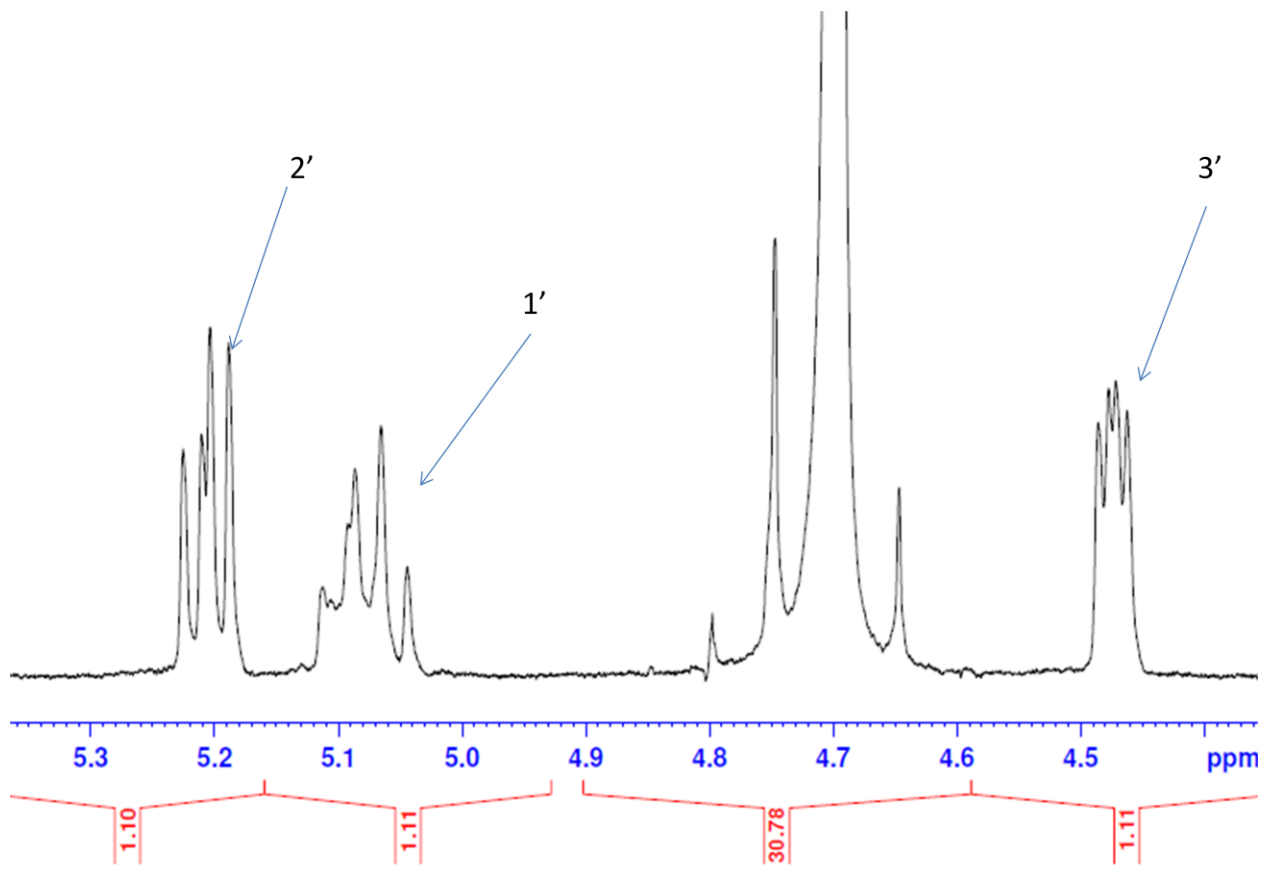
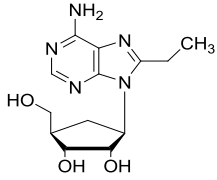


Figure 25. Portion of ¹H NMR spectrum of **F** in D₂O (327 °K) showing resolved peaks.

Table 14. A Comparison of experimental and theoretical spin-spin coupling constants for 8-ethylaristeromycin (F)

	$3J_{1'-2'}$	$J_{H2'-H3'}$	$J_{H3'-H4'}$	P	ν_{\max}	χ	ΔE^c	$C_{2'-endo}^d$	$\delta H_{2'}^e$
1-Exp.(D ₂ O)(327°K)	8.4	5.8	3.6			S		70.0	5.2
2-Exp(D ₂ O)(294°K)	9.2	N/A	3.2						4.7
Calc. ^a	F1	5.8	9.7	8.9	73.5	41.7	A	0.0	4.2
	F2	10.3	6.1	0.2	143.9	42.3	S	1.6	5.3
	F3	1.9	7.4	9.7	52.3	43.5	A	0.0	4.2
	F4	11.6	6.6	0.0	148.4	42.7	A	1.6	4.4
	F5	10.3	7.3	0.4	139.1	43.1	S	2.9	5.2
Linear Regression ^f	8.0	6.6	3.1					72.0	4.3
	0.4	0.8	0.5						

^aThe spin-spin coupling constant by *ab initio* calculation was done in aqueous solution. ^bThe value in parentheses is the difference between experimental data and linear regression results. ^c ΔE is the energy difference from the most stable conformer (kcal/mol). ^d $C_{2'-endo}$ is the relative population of the South conformer and is given by $[J_{H1'-2'}/(J_{H1'-2'}+J_{H3'-4'})]*100$. ^e $\delta H_{2'}$ is the chemical shift of the in ppm. ^fLinear regression equation for $1 = 0.37 \mathbf{F2} + 0.31 \mathbf{F3} + 0.24 \mathbf{F4}$

The data show agreement between the theoretical and the experimental NMR spin-spin coupling constants with a $\Delta 0.8$ Hz as the highest. Also, from experiment it shows that **F** prefers the $C_{2'-endo}$ with a population of 70 % and theoretical data shows preference for the $C_{2'-endo}$ as well with a population of 72 %.

Finally, the experimental chemical shift shows 5.2 ppm for H2' (at 327 °K) which according to the literature^{36,99} is a *syn* conformer, while it is 4.7 ppm (at 294 °K) where the theoretical one is 4.3 ppm which is closer to the *anti* conformation. Overall, there is satisfactory agreement between the theoretical study and the experimental study in terms of the coupling constants and the conformation of the five-membered ring.

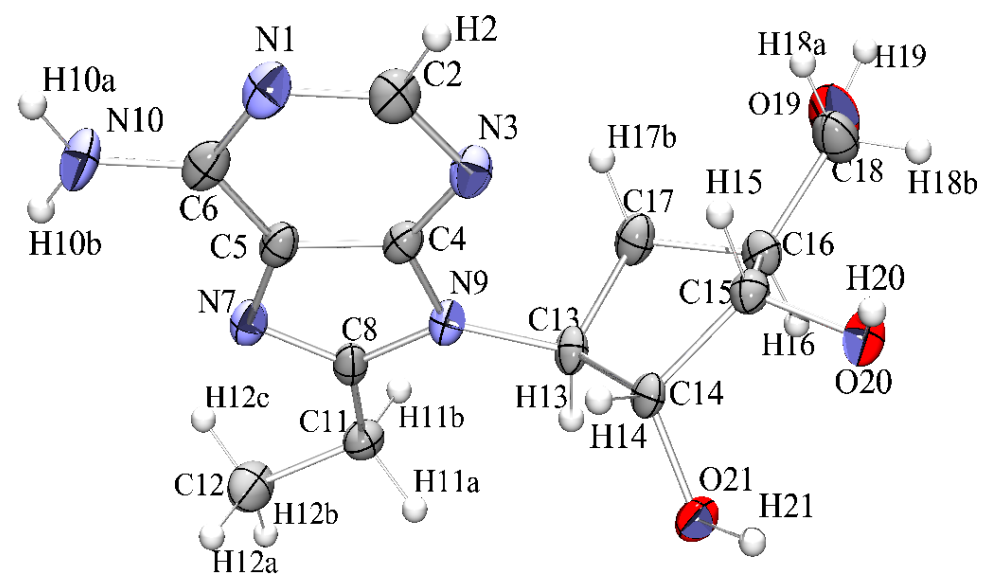


Figure 26. Structure of 2 from X-ray analysis.

The structure of target **2** has also been shown as the *syn* conformer via X-ray crystallography as shown in Figure 26.

Summary of results:

(i) In terms of the relationship between the *syn/anti* and *North/South* conformation:

The experimental coupling constants observed have been explained by the existence of two (for **A**, **B**, **C** and **D**) or more (three conformations in case of **E**) conformations in solution as shown by theoretical calculations. There is a correlation between *syn/anti* and pseudorotation as has been documented in the literature.⁴⁴ A *syn* conformation prefers a C2'-*endo* (South) and this was shown to be true through the studied compounds. For the *anti* conformers, both the C2'-*endo* and the C3'-*endo* are equally probable. This has been more evident with compound (**F**) where it showed three conformations, two of which are *anti/north* (31%) and *anti/south* (24%) which represents a nearly equal probability of N/S with the *anti* conformer. That is in addition to the *syn/south* conformer which is the major contributor to the observed experimental values, Figure 27.

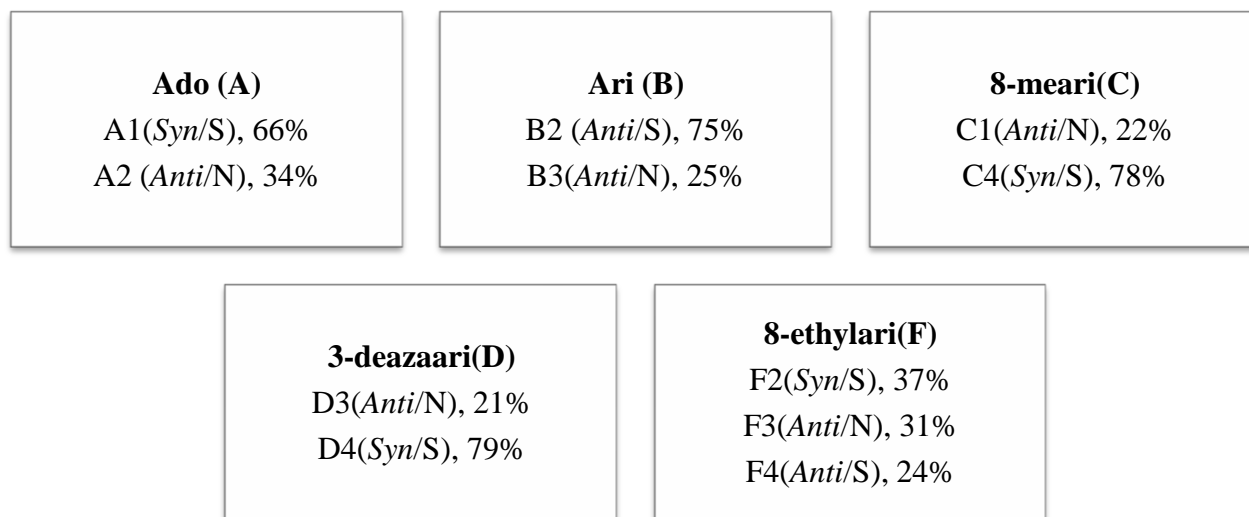


Figure 27. Summary of correlation study between theoretical and experimental data.

(ii) In terms of syn/anti conformations the 8-substitution:

Alkyl substitution at the 8-position produces a pronounced shift in equilibrium to the syn conformation yet the structure is explained by contributions from both conformations. Future biological activity studies could corroborate these findings for target molecules as well as give insight into the possibility of extrapolating the results to other carbocyclic nucleosides.

Conclusion

A theoretical methodology for explaining the conformational structural parameters of 8-substituted carbocyclic nucleosides have been investigated. In that direction, a series of optimizations have been carried out using the DFT level of theory to produce coupling constants for the optimized lowest energy conformations obtained. Tables 8-12 provide the calculated and experimental spin coupling constants of ${}^3J_{1'2'}$, ${}^3J_{2'3'}$ and ${}^3J_{3'4'}$ for 5 compounds. A theoretical calculation describes each compound in terms of two or more conformations as being the most probable conformations in solution. To obtain the best fit to experiment, linear regression statistics were then applied and contributions for each conformation were measured. The five compounds demonstrated a preference for the south conformation. A correlation between *syn* conformations and C2'-*endo* was found as well as an equal preference of the *anti* conformation for both the north/south. This suggests that antiviral activity could reside in the south conformation. Further biological studies could corroborate this finding.

In terms of the *syn/anti* relationship each compound is represented by an equilibrium that is shifted towards one conformation. For the 8-alkyl compound it was found that a preference for the *syn* conformation existed whereas unsubstituted aristeromycin showed a shift toward the *anti* conformation. Yet, in the end, the results for both the substituted and unsubstituted illustrated that *syn* and *anti* conformations were accessible. Thus, in regard to *syn/anti* conformational preference the results here are equivocal.

To avail authentic sample for the aforementioned NMR analyses, it was necessary to establish successful synthetic procedures for those molecules central to the investigation. For that purpose procedures were designed and accomplished via convergent methods involving (i) the construction of the purine bases from pyrimidine units, which required synthesis, and (ii) coupling the purines with appropriately designed and prepared cyclopentyl derivatives. The final products were obtained in overall reasonable yields and their structures verified by X-ray crystallography and a thorough NMR analysis using contemporary, multi-dimensional methods.

Experimental Details

General

Melting points were recorded on a Meltemp II melting point apparatus and the values are uncorrected. ^1H and ^{13}C NMR spectra were recorded on either a Bruker AV 250 spectrometer or a Bruker AV 400 spectrometer. All ^1H chemical shifts are reported in δ relative to the internal standard tetramethylsilane (TMS, δ 0.00). ^{13}C chemical shifts are reported in δ relative to CDCl_3 (center of triplet, δ 77.23) or relative to $\text{DMSO-}d_6$ (center of septet, δ 39.51). The spin multiplicities are indicated by the following symbols: s (singlet), d (doublet), t (triplet), q (quartet), quin (quintet), sex (sextet), sep (septet), m (multiplet) and br (broad). The reactions were monitored by thin-layer chromatography (TLC) using 0.25 mm Whatman Diamond silica gel 60-F254 precoated plates with visualization by irradiation with a Mineralight UVGL-25 lamp or exposure to potassium permanganate. Column chromatography was performed using Whatman silica, 230-400 mesh and 60 Å using elution with the indicated solvent systems. Yields refer to chromatographically and spectroscopically (^1H and ^{13}C NMR) homogeneous materials. All mass spectroscopic data (LC/MS) were collected using Waters Acquity UPLC and Q-Tof Premier Mass Spectrometer.

Methyl 2, 3-*O*-isopropylidene- β -D-ribofuranoside (11). Concentrated hydrochloric acid (10.0 mL) was added to a suspension of D-ribose (100 g, 0.67 mol) in acetone (420 mL),

methanol (420 mL), and 2, 2-dimethoxypropane (200 mL). The reaction was stirred at room temperature overnight and neutralized with pyridine. Water (1000 mL) and ether (300 mL) were added and the separated aqueous layer was washed with ether and ethyl acetate. The combined organic layers were washed with water, brine and dried over sodium sulfate. The solvent was evaporated by rotary evaporator and the residue was distilled in vacuum to give 104.5 g (77 %) of **11** as colorless oil. The NMR spectral data agreed with literature.⁷⁸

Methyl-5-deoxy-5-iodo-2,3-O-isopropylidene-β-D-ribofuranoside (12): A solution of **11** (90.92 g, 0.45 mol), imidazole (45.5 g, 0.67 mol) and triphenylphosphine (140.3 g, 0.5 mol) in toluene (500 mL) and acetonitrile (100 mL) was treated with iodine (135.8 g, 0.5 mol) portionwise. The reaction mixture was refluxed for 30 minutes and cooled to room temperature. The white precipitate was decanted and the remaining solution was diluted by ether. The organic phase was washed with 10% sodium thiosulfate solution, water and brine and dried over sodium sulfate. The residue after concentration was loaded on silica gel and eluted with hexane/ethyl acetate (15:1) to give 119.04 g (85.1 %) of **12** as colorless oil. The NMR spectral data agreed with literature.⁷⁸

(4R,5R)-2,2-dimethyl-5-vinyl-1,3-dioxolane-4-carbaldehyde (13). Activated powdered zinc (52.0 g, 0.8 mol) was added to **12** (50 g, 0.2 mol) in methanol (200 mL). The mixture was left at room temperature for 2 hours. After filtration, the filtrate was concentrated in vacuum around 20°C and the residue was loaded on a silica gel column and eluted with hexane /ethyl acetate (4:1) to afford 21.34 g (86%) of **13** as a colorless liquid. The NMR spectral data agreed with literature.⁸⁰

1-((4S,5R)-2,2-dimethyl-5-vinyl-1,3-dioxolan-4-yl)prop-2-en-1-ol (14). To a well stirred solution of **13** (4.1 g, 26.3 mmol) in THF (100 mL), was added vinyl magnesium bromide (1.0 M in THF, 31.5 mL, 31.5 mmol) dropwise between -20° and -30°C. The mixture was kept at that temperature for 2 hours and allowed to warm to room temperature. The mixture was quenched with saturated ammonium chloride solution and extracted with ethyl acetate. The combined organic layers were washed with brine and dried over sodium sulfate. Filtration, evaporation of the filtrate followed by column chromatography (4:1 hexane: ethyl acetate) gave 3.8 g (76%) of **14** as a colorless oil. The NMR spectral data agreed with literature.⁸¹

(3aR,6aR)-2,2-dimethyl-3aH-cyclopenta[d][1,3]dioxol-4(6aH)-one; ((4R,5R)-4,5-O-isopropylidene-2-cyclopentenone) (15). To a solution of the diene **14** (25 g, 135.7 mmol) in anhydrous methylene chloride (300 mL) was added Grubbs catalyst benzylidene bis (tricyclohexylphosphine) dichlororuthenium (1.2 g, 1.458 mmol) after the solution was flushed with nitrogen for 20 minutes. After stirring at room temperature for 12 hours, pyridinium chlorochromate (23.5 g, 271.4 mmol), and 4 Å molecular sieves (20 g) were added to the dark brown solution. The reaction mixture was stirred at room temperature overnight and filtered over silica gel pad with ethyl acetate. The filtrate was concentrated in vacuum and the residue was purified with column chromatography at afford 11.3 g (54%) of **15** as white crystals. The NMR spectral data agreed with literature.⁷⁹

(3aR,6R,6aR)-2,2-dimethyl-6-vinyldihydro-3aH-cyclopenta[d][1,3]dioxol-4(5H)-one (16). To a suspension of CuBr.Me₂S (166.7 mg, 0.8 mmol) in THF (120 mL) at -78 °C was added vinylmagnesium bromide (24.3 mL, 24.3 mmol) dropwise. The reaction mixture was

stirred for 20 minutes and HMPA (6.8 mL, 38.9 mmol) was added followed by a solution of cyclopentenone **15** (2.5 g, 16.2 mmol) and TMSCl (4.1 mL, 32.4 mmol) in THF (20 mL) dropwise. After the reaction was stirred for 3 hours at -78 °C, the mixture was warmed to 0 °C and quenched with a saturated solution of ammonium chloride. The reaction mixture was then stirred for 30 minutes and ethyl acetate was added (300 mL). The organic phase was separated and washed with water and brine, dried with MgSO₄. Solvent was evaporated in vacuo and the residue was purified by column chromatography (8:1 hexane: ethyl acetate) to give 2.18 g (74%) of **16** as a colorless liquid. The NMR spectral data agreed with literature.¹⁰⁰

(3aS,4S,6R,6aR)-2,2-dimethyl-6-vinyltetrahydro-3aH-cyclopenta[d][1,3]dioxol-4-ol

(17). To a suspension of lithium aluminum hydride (0.7 g, 17.8 mmol) in THF (50 mL) was added a solution of **16** (1.6 g, 8.9 mmol) in THF (20 mL) drop wise at 0 °C. The reaction mixture was stirred at room temperature for 4 hours and was quenched sequentially with water (0.6 mL), aqueous NaOH 15% (0.6 mL) and water (1.5 mL). After filtration, the filtrate was evaporated to give 1.5 g (92%) of **17** as a colorless liquid. The NMR spectral data agreed with literature.⁸¹

(3aS,4S,6aR)-2,2-dimethyl-4,6a-dihydro-3aH-cyclopenta[d][1,3]dioxol-4-ol (18). To a stirred solution of cyclopentenone **15** (1.0 g, 6.5 mmol) and CeCl₃.H₂O (2.4 g, 6.5mmol) in MeOH (50 mL) at 0 °C was added NaBH₄ (0.5 g, 13.0 mmol) portionwise. After stirring at room temperature for 1 h the mixture was neutralized with NH₄Cl, and extracted with CH₂Cl₂. The organic layers were combined, dried (anhydrous Na₂SO₄) and concentrated to give **18** as a colorless syrup (0.7 g, 68%). ¹H NMR (400 MHz, CDCl₃) δ 5.81 (s, 2H), δ 4.94 (d, 1H), δ 4.67

(t, 1H), δ 4.48 (m, 1H), δ 2.74 (d, 1H), δ 1.35 (s, 3H), δ 1.32 (s, 3H); ^{13}C NMR (100 MHz, CDCl_3) δ 136.5, 132.1, 112.5, 83.7, 77.3, 74.3, 27.8, 26.7.

6-chloropyrimidine-4,5-diamine (19). 1.5 g of 4,6-dichloropyrimidin-5-amine was dissolved in 25 mL MeOH and cooled to 0 °C for 30 min before being saturated with ammonia gas at the same temperature for 1 h. The solution was heated at 110 °C for 48 h in a sealed stainless steel Parr. The solvent was evaporated under reduced pressure and the residue was washed with EtOAc to give 1.2 g (90 %) of **19** as white crystals. ^1H NMR (400 MHz, DMSO): δ 7.637 (s, 1H, H-2), δ 6.757 (s, 2H, NH_2), δ 4.975 (s, 2H, NH_2), ^{13}C NMR (100 MHz, DMSO) δ 153.6, 145.8, 137.5, 123.2. ESI-MS calcd for $\text{C}_4\text{H}_5\text{N}_4$: $[(\text{M} + \text{H})^+]$: 145.0281, found: 145.0278

N-(4-amino-6-hydroxypyrimidin-5-yl) acetamide (20). 4, 5-Diamino-6-hydroxypyrimidine hemisulfate (1.9 g, 5.3 mmol) was added to a mixture of acetic acid (30 mL) and sodium acetate (0.8 g, 10.0 mmol) and left to reflux for 12 h. Excess acetic acid was evaporated under reduced pressure. 40 mL of acetic anhydride was added to the residue and refluxed for 4 h. The excess acetic anhydride was azeotropically evaporated with toluene. The residue was dissolved in 40 mL of 1.5 N NaOH and boiled for 20 min. The solution was acidified while hot with glacial acetic acid and cooled. The cooled solution gave 0.8 g (quantitative yield) of **20** as white crystals. ^1H NMR (400 MHz, DMSO): δ 11.75 (br s, 1H), δ 8.608 (s, 1H), δ 7.742 (s, 1H), δ 6.203 (s, 2H), δ 3.322 (br s, 1H), δ 1.93 (s, 3H); ^{13}C NMR (100 MHz, DMSO): δ 168.8, 159.2, 159.1, 146.9, 98.5, 22.8. ESI-MS calcd for $\text{C}_6\text{H}_6\text{N}_4\text{O}$: $[(\text{M} + \text{H})^+]$: 169.0731, found: 169.0714.

8-Methyl-6-chloropurine (21). To a solution of phosphorus oxychloride (35 mL), containing N, N-diethyl aniline (3 mL), was added compound **20** (2.3 g, 15.1 mmol) slowly. The mixture was refluxed overnight and the excess phosphorus oxychloride was distilled under reduced pressure. The residue was poured on cracked ice and the solution was made strongly basic with 10N potassium hydroxide and allowed to stand for 20 minutes. The solution was then extracted with ether (2x100 mL). The solution was then acidified to pH 4 with concentrated aqueous HCl and was continuously extracted with ether for 48 h. The organic layer was collected and evaporated under reduced pressure to yield **21** as yellow crystals. ¹H NMR (400 MHz, DMSO): δ 8.63 (s, 1H), 2.57 (s, 3H); ¹³C NMR (100 MHz, DMSO) δ 156.5, 152.6, 150.8, 149.0, 113.9, 15.1. ESI-MS calcd for C₆H₅N₄Cl: [(M + H)⁺]: 169.0281 found: 169.0270.

6-chloro-9-(2,2-dimethyl-6-vinyltetrahydro-3aH-cyclopenta[d][1,3]dioxol-4-yl)-8-methyl-9H-purine (22). To a solution of **17** (92.5 g, 13.6 mmol), triphenylphosphine (7.1 g, 27.3 mmol) and 6-chloropurine (3.0 g, 19.2 mmol) in THF (100 mL) was added DIAD (diisopropyl azodicarboxylate) (5.5 g, 27.3 mmol) dropwise at 0 °C. The reaction mixture was kept at 0 °C for 2 hours followed by stirring at 50 °C for 8 hours. The solvent was removed under reduced pressure and the residue was purified with column chromatography (hexane: ethyl acetate 4:1) to give (0.4 g, 55%) of **22** as yellow solid. ¹H NMR (400 MHz, CDCl₃): δ 8.51 (s, 1H), 5.86 (m, 1H), 5.11-5.01 (m, 3H), 4.63-4.57 (m, 2H), 2.83-2.74 (m, 2H), 2.64 (s, 3H), 2.19 (m, 1H), 1.46 (s, 3H), 1.14 (s, 3H). ¹³C NMR (100 MHz, CDCl₃) δ 155.2, 152.6, 150.6, 149.0, 137.4, 131.1, 116.1, 113.9, 83.7, 82.6, 61.5, 48.2, 35.2, 27.5, 25.0, 14.9. ESI-MS calcd for C₁₆H₁₉N₄O₂Cl: [(M + H)⁺]: 335.1275 found: 335.1271.

((3aR,4R,6R,6aS)-6-(6-chloro-8-methyl-9H-purin-9-yl)-2,2-dimethyltetrahydro-3aH-cyclopenta[d][1,3]dioxol-4-yl)methanol (23). To a suspension of **22** from above and sodium periodate (4.3 g, 20.2 mmol) in methanol (35 mL) and water (20 mL) was added OsO₄ (30 mg, 0.1 mmol) at 0 °C. The suspension was stirred for 2 hours at 0 °C and then for 3 h at room temperature. The suspension was filtered and the solid was washed with EtOAc. The combined filtrates were concentrated and the residue was diluted with water (20 mL) and extracted with EtOAc (3x40 mL). The combined organic layers were dried over MgSO₄. After filtration, the filtrate was evaporated at ambient temperature and dissolved in MeOH (40 mL). This solution was cooled to 0 °C and NaBH₄ (1.2 g, 30.8 mmol) was added portion wise. After 10 min, the solvent was removed by reduced pressure and the residue was neutralized by saturated ammonium chloride solution followed by extraction with EtOAc. The combined organic layers were washed with brine and dried over MgSO₄. After filtration, the solvent was removed under reduced pressure and the residue was purified via column chromatography using (hexane: EtOAc 1:2) to afford (0.4 g, 49%) of **23** as white solid. ¹H NMR (250 MHz, CDCl₃): δ 8.64 (s, 1H), 5.23 (t, *J*=10.4, 10 Hz, 1H), 4.80-4.70 (m, 2H), 3.89 (d, *J*=8.8 Hz, 2H), 3.49 (br s, 1H), 2.85 (m, 1H), 2.76 (s, 3H), 2.57-2.31 (m, 2H), 1.59 (s, 3H), 1.31 (s, 3H); ¹³CNMR (60 MHz, CDCl₃) δ 155.6, 152.6, 150.6, 149.3, 131.3, 113.6, 83.2, 81.9, 63.8, 62.9, 45.7, 32.1, 27.8, 25.2, 15.0. ESI-MS calcd for C₁₅H₁₉N₄O₃Cl: [(M + H)⁺]: 339.1224 found: 339.1222.

((4R,6R)-6-(6-amino-8-methyl-9H-purin-9-yl)-2,2-dimethyltetrahydro-3aH-cyclopenta[d][1,3]dioxol-4-yl)methanol (24): A solution of **23** (130 mg, 0.4 mmol) was dissolved in MeOH (20 mL) and was cooled to 0 °C for 30 min before being saturated with ammonia gas at the same temperature for 1 h. The solution was heated to 100 °C for 48 h in a

sealed stainless steel Parr. The solvent was removed under reduced pressure, and the residue purified by column chromatography (EtOAc/MeOH = 8:1) to give (100 mg, 82 %) as white solid. ¹H NMR (400 MHz, CDCl₃) 8.16 (s, 1H), 6.53 (s, 2H), 5.12 (t, *J* = 6.4, 6 Hz, 1H), 4.63 (dd, *J* = 4, 7.6 Hz, 1H), 4.64-4.58 (dddd, 1H), 3.81 (d, *J* = 5.2 Hz, 2H), 2.70 (q, 1H), 2.54 (s, 3H), 2.50-2.42 (m, 1H), 2.39-2.31 (m, 1H), 1.53 (s, 3H), 1.25 (s, 3H). ¹³C NMR (100 MHz, CDCl₃) δ 155.01, 151.58, 150.34, 149.53, 118.73, 112.95, 83.89, 82.56, 64.03, 62.80, 45.38, 32.18, 27.90, 25.30, 14.59.

(3R,5R)-3-(6-amino-8-methyl-9H-purin-9-yl)-5-(hydroxymethyl)cyclopentane-1,2-diol

(1). Compound **23** (110 mg, 0.3 mmol) was dissolved in a mixture of 1N HCl (6mL) and MeOH (6 mL). The mixture was stirred at room temperature for 3 h. The solution was then neutralized with weakly basic exchange resin (Amberlite IRA-67). Filtration followed with evaporation of solvent, the crude product was purified by chromatography (EtOAc/MeOH/NH₃:H₂O = 8:1:1) to give (70 mg, 73 %) of **1** as white crystals. ¹H NMR (400 MHz, DMSO-*d*₆) 8.04 (s, 1H), 7.03 (s, 2H), 4.85 (d, 1H), 4.76 (t, 1H), 4.67 (d, 1H), 4.60 (q, 1H), 4.53 (q, 1H), 3.84 9dd, 1H), 3.56 (quintet, 1H), 3.45 (quintet, 1H), 2.51 (s, 3H), 2.13-2.01 (m, 3H); ¹³C NMR (100 MHz, DMSO-*d*₆) δ 155.09, 151.06, 150.39, 149.38, 149.37, 149.36, 118.16, 73.16, 71.49, 63.36, 60.33, 45.68, 27.08, 14.4. ESI-MS calcd for C₁₂H₁₇N₅O₃: [(M + H)⁺]: 280.1410, found: 280.1401.

6-chloro-8-ethyl-9H-purine (28). To 16 ml of trimethyl orthopropionate was added **19** (0.98 g, 6.81 mmol) and the mixture was heated at 100 °C until clear. Formic acid (1 ml) was added dropwise and the solution refluxed overnight until the disappearance of starting material. The solution was evaporated and refluxed with 1.5 N NaOH for 1 h. The crude mixture was

evaporated and purified via column chromatography (EtOAc: MeOH = 15:1) to give (0.65 g, 58 %) of **28** as white solid. ^1H NMR (250 MHz, CDCl_3): δ 13.6 (br s, 1H, NH), δ 8.61 (s, 1H, H-2), 2.912 (q, 2H, CH_2), δ 1.321 (t, 3H, CH_3). ^{13}C NMR (60 MHz, CDCl_3): δ 161.0, 155.2, 150.4, 145.4, 129.5, 22.2, 11.3. ESI-MS calcd for $\text{C}_7\text{H}_8\text{N}_4\text{Cl}$: $[(\text{M} + \text{H})^+]$: 183.0437, found: 183.0439.

6-chloro-8-isopropyl-9H-purine (29). **19** (0.5 g, 3.5 mmol) was added to 1, 1, 1-trimethoxy-2-methylpropane (5.6 mL, 35 mmol) and the mixture was heated to 100 °C until it became almost clear. Formic acid (1 mL) was added dropwise and the solution was refluxed for 8 h. The solution was refluxed as such in 1.5 N NaOH for 1 h. The crude mixture was purified with column chromatography (EtOAc: MeOH = 15:1) to give (0.2 g, 32%) of **29** as a white solid and (0.5 g, 67%) of **31** as yellow oil.

6-chloro-8-isopropyl-9H-purine (29). ^1H NMR (400 MHz, CDCl_3) δ 13.59 (br s, 1H), δ 8.65 (s, 1H), δ 3.22 (sep, 1H), δ 1.36 (d, 6H); ^{13}C NMR (60 MHz, CDCl_3). ESI-MS calcd for $\text{C}_8\text{H}_{10}\text{N}_4\text{Cl}$: $[(\text{M} + \text{H})^+]$: 197.0594 found: 197.0587

8-isopropyl-6-methoxy-9H-purine (31). ^1H NMR (400 MHz, CDCl_3): δ 11.60 (br s, 1H), δ 8.37 (s, 1H), δ 4.08 (s, 3H), δ 2.49 (sep, 1H), δ 1.38 (d, 6H).

N-(4-amino-6-chloropyrimidin-5-yl) pivalamide (32). To a solution of **19** (1.0 g, 7.2 mmol) in dry toluene, pivaloyl chloride (1.2 mL, 8.6 mmol) was added dropwise. The solution was refluxed for 4 h. The solution was filtered and washed several times with cold toluene to yield (1.3 g, 80 %) of **32** as white solid. ^1H NMR (400 MHz, MeOD): δ 8.29 (s, 1H), 1.34 (s, 9H); ^{13}C NMR (100 MHz, MeOD): δ 181.5, 163.1, 156.4, 154.5, 15.6, 40.8, and 27.8. ESI-MS calcd for $\text{C}_9\text{H}_{14}\text{N}_4\text{OCl}$: $[(\text{M} + \text{H})^+]$: 229.0862, found: 229.0868.

8-tert-butyl-6-chloro-9H-purine (30). 0.3 g of **32** was refluxed in 1 N NaOH for 2 h. The solution was evaporated and the residue was purified with column chromatography EtOAc/MeOH = 15:1 to give 0.24 g (55%) of **30** as white solid. ^1H NMR (400 MHz, DMSO- d_6) δ 13.61 (br s, 1H), 8.66 (s, 1H), 1.42 (s, 9H); ^{13}C NMR (100 MHz, DMSO- d_6) δ 166.6, 154.8, 151.4, 147.5, 130.7, 34.4, 29.0. ESI-MS calcd for $\text{C}_9\text{H}_{11}\text{N}_4\text{Cl}$: $[(\text{M} + \text{H})^+]$: 211.0756, found: 211.0748.

6-chloro-9-((3aS,6aR)-2,2-dimethyl-6-vinyltetrahydro-3aH-cyclopenta[d][1,3]dioxol-4-yl)-8-ethyl-9H-purine (34). To a solution of **17** (0.4 g, 2.2 mmol), triphenylphosphine (1.4 g, 5.2 mmol) and **28** (0.5 g, 2.6 mmol) in THF (100 mL) was added DIAD (diisopropyl azodicarboxylate) (1.1 g, 5.2 mmol) dropwise at 0 °C. The reaction mixture was kept at 0 °C for 2 hours followed by stirring at 50 °C for 8 hours. The solvent was removed under reduced pressure and the residue was purified with column chromatography (hexane: ethyl acetate 4:1) to give **34** (1.3 g) as yellow solid contaminated with by-product of diisopropyl azodicarboxylate as confirmed by mass spectrometry and was used as such in the next step. ESI-MS calcd for $\text{C}_{17}\text{H}_{21}\text{N}_4\text{O}_2\text{Cl}$: $[(\text{M} + \text{H})^+]$: 349.1431, found: 349.1429.

((3aR,6aS)-6-(6-chloro-8-ethyl-9H-purin-9-yl)-2,2-dimethyltetrahydro-3aH-cyclopenta[d][1,3]dioxol-4-yl)methanol (35). To a suspension of **34** from above and sodium periodate (1.3 g 3.9 mmol) in methanol (35 mL) and water (20 mL) was added OsO_4 (30 mg, 0.1 mmol) at 0 °C. The suspension was stirred for 2 hours at 0 °C and then for 3 h at room temperature. The suspension was filtered and the solid was washed with EtOAc. The combined filtrates were concentrated and the residue was diluted with water (20 mL) and extracted with

EtOAc (3 x 40 mL). The combined organic layers were dried over MgSO₄. After filtration, the filtrate was evaporated at ambient temperature and dissolved in MeOH (40 mL). This solution was cooled to 0 °C and NaBH₄ (0.4 g, 5.9 mmol) was added portion wise. After 10 min, the solvent was removed by reduced pressure and the residue was neutralized by saturated ammonium chloride solution followed by extraction with EtOAc. The combined organic layers were washed with brine and dried over MgSO₄. After filtration, the solvent was removed under reduced pressure and the residue was purified via column chromatography using (hexane: EtOAc 1:2) to afford (0.4 g, 49%) of **35** as white solid. ¹H NMR (400 MHz, CDCl₃): δ 8.58 (s, 1H), 5.19 (t, *J* = 6.4, 6.4 Hz, 1H), 4.72-4.61 (m, 2H), 4.05 (q, 1H), 3.81 (d, *J* = 5.6 Hz, 2H), 2.97 (q, 2H), 2.68 (q, 1H), 2.42 (m, 1H), 2.29 (m, 1H), 1.51 (s, 3H), 1.42 (s, 3H), 1.24 (s, 3H); ¹³C NMR (100 MHz, CDCl₃) δ 159.9, 152.7, 150.7, 149.8, 113.7, 83.4, 82.4, 64.5, 62.8, 45.7, 32.4, 27.9, 25.3, 22.1, 12.2. ESI-MS calcd for C₁₆H₂₁N₄O₃Cl: [(M + H)⁺]: 353.1380 found: 353.1372.

((3aR,6aS)-6-(6-amino-8-ethyl-9H-purin-9-yl)-2,2-dimethyltetrahydro-3aH-cyclopenta[d][1,3]dioxol-4-yl)methanol (36). A solution of **35** (0.2 g, 0.5 mmol) was dissolved in MeOH (30 mL) and was cooled to 0 °C for 30 min before being saturated with NH₃ at the same temperature for 1 h. The solution was heated to 100 °C for 48 h in a sealed stainless steel Parr. The solvent was removed under reduced pressure, and the residue purified by column chromatography (EtOAc/MeOH = 8:1) to give **36** as a white solid. ¹H NMR (400 MHz, MeOD) δ 8.13 (s, 1H), 5.26 (t, 1H), 4.80-4.73 (m, 1H), 4.70-4.67 (q, 1H), 3.76 (dd, 1H), 3.71 (dd, 1H), 2.98 (q, 2H, CH₂), 2.69 (q, 1H), 2.41-2.29 (m, 2H), 1.55 (s, 3H), 1.43 (t, 3H), 1.29 (s, 3H); ¹³C NMR (100 MHz, MeOD) δ 156.3, 155.9, 152.6, 151.7, 119.3, 114.8, 84.0, 82.9, 64.3, 63.0, 47.4,

33.8, 27.9, 25.4, 22.0, 12.1. ESI-MS calcd for C₁₆H₂₃N₅O₃: [(M + H)⁺]: 334.1879, found: 334.1864.

(1R, 2S)-3-(6-amino-8-ethyl-9H-purin-9-yl)-5-(hydroxymethyl) cyclopentane-1,2-diol (2).

Compound **36** was dissolved in a mixture of 1N HCl (6mL) and MeOH (6 mL). The mixture was stirred at room temperature for 3 h. The solution was then neutralized with weakly basic exchange resin (Amberlite IRA-67). Filtration followed with evaporation of solvent, the crude product was purified by chromatography (EtOAc/MeOH/NH₃:H₂O = 8:1:1) to give (90 mg, 64 %) of **2** as white crystals. ¹H NMR (400 MHz, DMSO-d₆) δ 8.05 (s, 1H), δ 6.98 (s, 2H), 4.84 (d, J = 6.8, 1H), 4.75 (t, 1H), 4.69-4.63 (m, 2H), 4.53 (q, 1H), 3.87-3.84 (dd, 1H), 3.60-3.55 (quintet, 1H), 3.48-3.40 (quintet, 1H), 2.87 (q, 2H), 2.11-2.03 (m, 3H), 1.30 (t, 3H); ¹³C NMR (100 MHz, DMSO) δ 155.2, 153.6, 151.0, 150.4, 118.2, 72.9, 71.5, 63.3, 60.1, 45.6, 27.3, 20.7, 12.0. ESI-MS calcd for C₁₃H₁₉N₅O₃: [(M + H)⁺]: 294.1566, found: 294.1564.

6-Chloro-9-(2,2-dimethyl-4,6a-dihydro-3aH-cyclopenta[1,3]dioxol-4-yl)-8-methyl-9H-purine (37). To a solution of **18** (0.2 g, 1.4 mmol), triphenylphosphine (0.9 g, 3.4 mmol) and **21** (0.3 g, 1.7 mmol) in THF (100 mL) was added DIAD (diisopropyl azodicarboxylate) (0.7 mL, 3.4 mmol) dropwise at 0 °C. The reaction mixture was kept at 0 °C for 2 hours followed by stirring at 50 °C for 48 h. The solvent was removed under reduced pressure and the residue was purified with column chromatography (hexane: ethyl acetate 1:1) to give (0.5 g, 69%) of **37** as yellow oil. ¹H NMR (400 MHz, CDCl₃) δ 8.60 (s, 1H), δ 6.31-6.28 (dt, 1H), δ 5.84-5.82 (dd, 1H), δ 5.75-5.73 (dd, 1H), δ 5.58 (br s, 1H), δ 5.01 (d, J = 5.6 Hz, 1H), δ 2.77 (s, 3H), δ 1.52 (s, 3H), δ 1.39 (s, 3H); ¹³C NMR (100 MHz, CDCl₃) δ 154.8, 152.6, 150.9, 148.9, 137.3, 130.9,

128.9, 112.2, 85.6, 83.0, 66.8, 27.3, 25.6, 15.2. ESI-MS calcd for $C_{14}H_{15}N_4O_2Cl$: $[(M + H)^+]$: 307.0962 found: 307.0967.

9-(2,2-Dimethyl-4,6a-dihydro-3aH-cyclopenta[1,3]dioxol-4-yl)-8-methyl-9H-purin-6-ylamine (38). A solution of **37** (0.4 g, 1.3 mmol) was dissolved in MeOH (30 mL) and was cooled to 0 °C for 30 min before being saturated with ammonia gas at the same temperature for 1 h. The solution was heated to 100 °C for 48 h in a sealed stainless steel Parr. The solvent was removed under reduced pressure, and the residue purified by column chromatography (EtOAc/MeOH = 8:1) to give (0.3 g, 77%) of **38** as a white solid. 1H NMR (400 MHz, $CDCl_3$) δ 8.09 (s, 1H), δ 6.59 (s, 2H), δ 6.13-6.11 (dt, 1H), δ 5.69-5.67 (dd, 1H), δ 5.60-5.58 (dd, 1H), δ 5.38 (br s, 1H), δ 4.73 (d, 1H), δ 2.47 (s, 3H), δ 1.40 (s, 3H), δ 1.27 (s, 3H). ^{13}C NMR (60 MHz, $CDCl_3$) δ 154.7, 151.8, 150.6, 148.5, 136.1, 129.6, 118.1, 111.8, 85.3, 83.03, 66.0, 27.1, 25.3, 13.9. ESI-MS calcd for $C_{14}H_{17}N_5O_2$: $[(M + H)^+]$: 288.1461 found: 288.1476.

5-(6-Amino-8-methyl-purin-9-yl)-cyclopent-3-ene-1,2-diol (3). Compound **38** (0.2 g, 0.6 mmol) was dissolved in a mixture of 1N HCl (6mL) and MeOH (6 mL). The mixture was stirred at room temperature for 3 h. The solution was then neutralized with weakly basic exchange resin (Amberlite IRA-67). Filtration followed with evaporation of solvent, the crude product was purified by chromatography (EtOAc/MeOH/ $NH_3:H_2O$ = 8:2:1) to give (69.8 mg, 54 %) of **3** as white crystals. 1H NMR (400 MHz, $DMSO-d_6$) δ 8.01 (s, 1H), δ 6.98 (br s, 2H), δ 6.10-6.17 (m, 1H), δ 6.02 (dd, 1H), δ 5.35-5.32 (m, 1H), δ 5.05 (d, $J = 7.6$ Hz, 1H), δ 4.92 (d, $J = 5.6$ Hz, 1H), δ 4.50-4.46 (m, 1H), δ 4.43-4.38 (m, 1H), δ 2.51 (s, 3H); ^{13}C NMR (100 MHz, $DMSO-d_6$) δ 155.0,

151.37, 150.7, 149.0, 133.8, 133.6, 117.8, 75.5, 72.1, 64.6, 14.6. ESI-MS calcd for $C_{11}H_{13}N_5O_2$: $[(M + H)^+]$: 248.1147 found: 248.1148.

6-Chloro-9-(2,2-dimethyl-4,6a-dihydro-3aH-cyclopenta[1,3]dioxol-4-yl)-8-ethyl-9H-purine (39). To a solution of **18** (0.2 g, 1.3 mmol), triphenylphosphine (1.9 g, 3.1 mmol) and **28** (0.3 g, 1.5 mmol) in THF (100 mL) was added DIAD (diisopropyl azodicarboxylate) (1.0 mL, 3.1 mmol) dropwise at 0 °C. The reaction mixture was kept at 0 °C for 2 hours followed by stirring at 50 °C for 48 h. The solvent was removed under reduced pressure and the residue was purified with column chromatography (hexane: ethyl acetate 1:1) to give 0.7 g of **39** as yellow oil, contaminated with diisopropyl azodicarboxylate by-product, that was used without further purification in the next reaction. ESI-MS calcd for $C_{15}H_{17}N_4O_2Cl$: $[(M + H)^+]$: 321.1118 found: 321.1120.

9-(2,2-Dimethyl-4,6a-dihydro-3aH-cyclopenta[1,3]dioxol-4-yl)-8-ethyl-9H-purin-6-ylamine (40). A solution of **39** from the above step was dissolved in MeOH (30 mL) and was cooled to 0 °C for 30 min before being saturated with ammonia gas at the same temperature for 1 h. The solution was heated to 100 °C for 48 h in a sealed stainless steel Parr. The solvent was removed under reduced pressure, and the residue purified by column chromatography (EtOAc/MeOH = 8:1) to give (200 mg, 45 %) of **40** as a yellow oil. 1H NMR (400 MHz, MeOD) δ 8.01 (s, 1H), δ 6.06-6.04 (dt, 1H), δ 5.62 (d, 1H), 5.52 (d, 1H), δ 5.29 (br s, 1H), δ 4.08 (d, 1H), 2.92 (g, 2H), δ 1.43 (s, 3H), δ 1.38 (t, 3H), δ 1.31 (s, 3H). ^{13}C NMR (100 MHz, MeOD) δ 156.3, 155.7, 153.0, 152.4, 151.9, 147.5, 137.5, 131.4, 113.4, 87.2, 84.8, 67.7, 27.8, 25.9, 11.9. ESI-MS calcd for $C_{15}H_{19}N_5O_2$: $[(M + H)^+]$: 302.1617 found: 302.1615.

5-(6-Amino-8-ethyl-purin-9-yl)-cyclopent-3-ene-1,2-diol (4). Compound **40** was dissolved in a mixture of 1N HCl (6mL) and MeOH (6 mL). The mixture was stirred at room temperature for 3 h. The solution was then neutralized with weakly basic exchange resin (Amberlite IRA-67). Filtration followed with evaporation of solvent, the crude product was purified by chromatography (EtOAc/MeOH/NH₃:H₂O = 8:2:1) to give (80 mg, 46 %) of **4** as yellow crystals. ¹H NMR (400 MHz, CDCl₃) δ 8.05 (s, 1H), 6.21-6.17 (dt, 1H), 6.11-6.08 (dd, 1H), 5.52-5.47 (m, 1H), 4.67-4.65 (m, 2H), 4.48 (q, 2H), 1.44 (t, 3H); ¹³C NMR (100 MHz, MeOD) δ 156.7, 156.4, 152.8, 152.1, 135.4, 134.9, 77.2, 74.3, 66.5, 58.5, 18.5, 11.9. ESI-MS calcd for C₁₂H₁₅N₅O₂: [(M + H)⁺]: 262.1304 found: 262.1309.

6-Chloro-9-(2,2-dimethyl-4,6a-dihydro-3aH-cyclopenta[1,3]dioxol-4-yl)-8-isopropyl-9H-purine (41). To a solution of **18** (0.1 g, 0.4 mmol), triphenylphosphine (0.2 g, 0.9 mmol) and **29** (90.7 mg, 0.5 mmol) in THF (100 mL) was added DIAD (diisopropyl azodicarboxylate) (0.2 mL, 0.9 mmol) dropwise at 0 °C. The reaction mixture was kept at 0 °C for 2 hours followed by stirring at 50 °C for 48 h. The solvent was removed under reduced pressure and the residue was purified with column chromatography (hexane: ethyl acetate 1:1) to give 0.4 g of **41** as yellow oil. ¹H NMR (400 MHz, CDCl₃) δ 8.50 (s, 1H), δ 6.22-6.20 (dt, 1H), δ 5.72-5.67 (m, 2H), δ 5.45 (br s, 1H), δ 4.93 (d, 1H), δ 3.34-3.27 (sep, 1H), δ 1.45 (t, 9H), δ 1.32 (s, 3H); ¹³C NMR (100 MHz, CDCl₃) δ 162.9, 152.9, 151.0, 149.6, 137.6, 131.4, 129.1, 112.5, 86.1, 83.4, 66.8, 27.6, 25.8, 22.0, 21.5. ESI-MS calcd for C₁₆H₂₀N₄O₂Cl: [(M + H)⁺]: 335.1275 found: 335.1272.

9-(2,2-Dimethyl-4,6a-dihydro-3aH-cyclopenta[1,3]dioxol-4-yl)-8-isopropyl-9H-purin-6-ylamine (42). A solution of **41** (440 mg) was dissolved in MeOH (30 mL) and was cooled to 0

°C for 30 min before being saturated with ammonia gas at the same temperature for 1 h. The solution was heated to 100 °C for 48 h in a sealed stainless steel Parr. The solvent was removed under reduced pressure, and the residue purified by column chromatography (EtOAc/MeOH = 8:1) to give (120 mg, 82 % over 2 steps) of **42** as a white solid. ¹H NMR (400 MHz, CDCl₃) δ 8.14 (s, 1H), δ 6.19-6.17 (dt, 1H), δ 6.09 (s, 2H), δ 5.72-5.69 (m, 2H), δ 5.39 (br s, 1H), δ 4.96 (d, 1H), δ 3.21 (sep, 1H), δ 1.46 (s, 3H), δ 1.39 (d, 3H), δ 1.37 (d, 3H), δ 1.33 (s, 3H); ¹³C NMR (100 MHz, CDCl₃) δ 157.3, 154.9, 152.0, 151.0, 136.6, 130.0, 118.8, 112.1, 86.0, 83.5, 66.2, 27.5, 27.0, 25.7, 21.7, 21.6.

5-(6-Amino-8-isopropyl-purin-9-yl)-cyclopent-3-ene-1,2-diol (5). Compound **42** (120 mg, 0.4 mmol) was dissolved in a mixture of 1N HCl (6mL) and MeOH (6 mL). The mixture was stirred at room temperature for 3 h. The solution was then neutralized with weakly basic exchange resin (Amberlite IRA-67). Filtration followed with evaporation of solvent, the crude product was purified by chromatography (EtOAc/EtOH/NH₃:H₂O = 8:1:1) to give **5** as white crystals in quantitative yield. ¹H NMR (400 MHz, MeOD) δ 8.06 (s, 1H), δ 6.21-6.18 (dt, 1H), δ 6.08-6.06 (dd, 1H), δ 5.53 (d, 1H), δ 4.75 (t, 1H), δ 4.70-4.67 (dddd, 1H), δ 3.38 (sep, 1H), δ 1.46 (d, 3H), δ 1.40 (d, 3H); ¹³C NMR (100 MHz, MeOD) δ 158.8, 154.9, 151.2, 150.4, 134.0, 133.4, 117.8, 75.4, 72.8, 64.9, 26.4, 20.7, 20.6. ESI-MS calcd for C₁₃H₁₈N₅O₂: [(M + H)⁺]: 276.1461 found: 276.1461.

8-tert-Butyl-6-chloro-9-(2,2-dimethyl-4,6a-dihydro-3aH-cyclopenta[1,3]dioxol-4-yl)-9H-purine (43). To a solution of **18** (0.4 g, 2.2 mmol), triphenylphosphine (1.4 g, 6.5 mmol) and **30** (0.6 g., 2.7 mmol) in THF (100 mL) was added DIAD (diisopropyl azodicarboxylate) (1.1 mL,

6.5 mmol) dropwise at 0° C. The reaction mixture was kept at 0°C for 2 hours followed by stirring at 50 °C for 72 h. The solvent was removed under reduced pressure and the residue was purified with column chromatography (hexane: ethyl acetate 1:1) to give 0.1 g of crude **43** as yellow oil that was used as such in the next step. ESI-MS calcd for C₁₇H₂₂N₄O₂Cl: [(M + H)⁺]: 349.1431, found: 349.1422.

8-tert-Butyl-9-(2,2-dimethyl-4,6a-dihydro-3aH-cyclopenta[1,3]dioxol-4-yl)-9H-purin-6-ylamine (44). A solution of **43** from the above step 0.1 g was dissolved in MeOH (30 mL) and was cooled to 0 °C for 30 min before being saturated with ammonia gas at the same temperature for 1 h. The solution was heated to 100 °C for 48 h in a sealed stainless steel Parr. The solvent was removed under reduced pressure, and the residue purified by column chromatography (EtOAc/MeOH = 8:1) to give 40 mg of **44** with a yield of 51% over two steps as a white solid. ¹H NMR (400 MHz, CDCl₃): δ 8.18 (s, 1H), 6.24-6.20 (dt, 1H), 5.80-5.66 (m, 3H), 5.08 (d, 1H), 2.07 (s, 2H), 1.58 (s, 9H), 1.51 (s, 3H), 1.38 (s, 3H); ¹³C NMR (100 MHz, CDCl₃) δ 158.8, 154.9, 152.0, 147.9, 129.8, 112.1, 86.6, 83.5, 68.3, 60.7, 34.6, 30.0, 27.6, 25.8. ESI-MS calcd for C₁₇H₂₄N₅O₂: [(M + H)⁺]: 330.1930, found: 330.1906.

5-(6-Amino-8-tert-butyl-purin-9-yl)-cyclopent-3-ene-1, 2-diol (6). Compound **44** was dissolved in a mixture of 1N HCl (6mL) and MeOH (6 mL). The mixture was stirred at room temperature for 3 h. The solution was then neutralized with weakly basic exchange resin (Amberlite IRA-67). Filtration followed with evaporation of solvent, the crude product was purified by chromatography (EtOAc/EtOH/NH₃:H₂O = 8:1:1) to give **6** as white crystals. ¹H NMR (400 MHz, CDCl₃): δ 8.07 (s, 1H), 5.82 (dt, 1H), 5.73 (m, 1H), 5.03 (m, 2H), 4.92 (m,

1H), 3.96 (s br, 2H), 1.49 (s, 9H); ¹³C NMR (100 MHz, MeOD) δ 159.6, 155.2, 152.4, 151.3, 135.1, 133.0, 73.8, 73.7, 67.8, 34.4, 29.7, 22.7. ESI-MS calcd for C₁₄H₂₀N₅O₂: [(M + H)⁺]: 290.1617, found: 290.1600.

8-butyl-6-chloro-9H-purine (46). To a solution of **19** (0.5 g, 3.5 mmol) in dry toluene, valeroyl chloride (1.4 mL, 3.5 mmol) was added dropwise. The solution was refluxed for 4 h. The solvent was evaporated under reduced pressure. The residue was tested via mass spectroscopy and contained a mixture of both the monoacylated product **45** (major) as well as the bisacylated product. ESI-MS calcd for C₉H₁₄N₄OCl: [(M + H)⁺]: 229.0856, found: 229.0855.

The residue was refluxed in 1 N NaOH for 2 h. The solution was evaporated and the residue was purified with column chromatography EtOAc/MeOH = 15:1 to give (0.23 g, 31 %) of **46** as white solid. ¹H NMR (400 MHz, CDCl₃): δ 13.29 (s, 1H), δ 8.69 (s, 1H), δ 3.07 (t, 2H), δ 1.87 (quintet, 2H), δ 1.39 (m, 2H), δ 0.89 (t, 3H); ¹³C NMR (100 MHz, MeOD) δ 154.8, 152.9, 152.1, 150.8, 130.2, 30.1, 29.7, 22.5, 13.8. ESI-MS calcd for C₉H₁₂N₄Cl: [(M + H)⁺]: 211.0750, found: 211.0778.

8-butyl-6-chloro-9-((3aS,6aR)-2,2-dimethyl-4,6a-dihydro-3aH-cyclopenta[d][1,3]dioxol-4-yl)-9H-purine (47). To a solution of **18** (0.1 g, 0.7 mmol), triphenylphosphine (0.4 g, 1.7 mmol) and **46** (0.2 g., 0.9 mmol) in THF (100 mL) was added DIAD (diisopropyl azodicarboxylate) (0.2 mL, 1.7 mmol) dropwise at 0 °C. The reaction mixture was kept at 0 °C for 2 hours followed by stirring at 50 °C for 36 h. The solvent was removed under reduced pressure and the residue was purified with column chromatography (hexane: ethyl acetate 1:1) to give 0.1 g of crude **47** as yellow oil that was used as such in the next step ¹H NMR (400 MHz,

CDCl₃): δ 8.52 (s, 1H), 6.22-6.20 (dt, 1H), 5.82 (s, 1H), 5.82-5.67 (m, 2H), 5.41 (s, 1H), 2.95 (t, 2H), 1.83 (quin, 2H), 1.45 (s, 3H), 136 (q, 2H), 1.32 (s, 3H), 0.94 (t, 3H); ¹³C NMR (100 MHz, CDCl₃) δ 158.2, 152.4, 150.6, 149.0, 137.2, 128.7, 112.1, 85.6, 82.9, 74.0, 66.6, 29.7, 28.0, 27.1, 25.4, 22.4, 13.6. ESI-MS calcd for C₁₇H₂₂N₄O₂Cl: [(M + H)⁺]: 349.1431, found: 349.1422.

8-butyl-9-((3aS,6aR)-2,2-dimethyl-4,6a-dihydro-3aH-cyclopenta[d][1,3]dioxol-4-yl)-9H-purin-6-amine (48). A solution of **47** from the above step 0.1 g was dissolved in MeOH (30 mL) and was cooled to 0 °C for 30 min before being saturated with ammonia gas at the same temperature for 1 h. The solution was heated to 100 °C for 48 h in a sealed stainless steel Parr. The solvent was removed under reduced pressure, and the residue purified by column chromatography (EtOAc/MeOH = 8:1) to give (0.13 g, 25 % yield over two steps) of **48** as a white solid. ¹H NMR (400 MHz, CDCl₃): δ 8.15 (s, 1H), 6.20 (dt, *J* = 2.8, 1.8 Hz, 1H), 6.05 (br s, 2H), 5.72-5.69 (m, 2H), 5.37 (br s, 1H), 4.95 (d, *J* = 5.6 Hz, 1H), 2.84 (t, *J* = 8, 7.6 Hz, 2H), 1.77 (quin, 2H), 1.46 (s, 3H), 1.43 (q, 2H), 1.33 (s, 3H), 0.93 (t, *J* = 7.6, 7.2 Hz, 3H); ¹³C NMR (100 MHz, CDCl₃): δ 154.8, 152.9, 152.1, 151.0, 136.5, 130.0, 118.8, 112.1, 83.5, 86.0, 66.4, 30.2, 28.1, 27.5, 25.7, 22.9, 13.94. ESI-MS calcd for C₁₇H₂₄N₅O₂: [(M + H)⁺]: 330.1930, found: 330.1939.

(1S,2R)-5-(6-amino-8-butyl-9H-purin-9-yl)cyclopent-3-ene-1,2-diol (7). Compound **48** (70 mg) was dissolved in a mixture of 1N HCl (6mL) and MeOH (6 mL). The mixture was stirred at room temperature for 3 h. The solution was then neutralized with weakly basic exchange resin (Amberlite IRA-67). Filtration followed with evaporation of solvent, the crude product was purified by chromatography (EtOAc/EtOH/NH₃:H₂O = 8:1:1) to give **7** (120 mg) as white

crystals. ^1H NMR (400 MHz, CDCl_3): δ 8.08 (s, 1H), 6.19-5.97 (m, 4H), 5.42 (dd, $J = 2, 1.6$ Hz, 1H), 4.81-4.78 (m, 1H), 4.66 (t, $J = 6, 5.6$ Hz, 1H), 2.80 (br s, 1H), 2.78 (t, $J = 8, 5.6$ Hz, 2H), 2.58 (s, 1H), 1.71 (quintet, 2H), 1.35 (sextet, 2H), 0.88 (t, $J = 7.2, 7.2$ Hz, 3H); ^{13}C NMR (100 MHz, CDCl_3): δ 154.81, 152.89, 152.1, 151.0, 136.5, 130.0, 118.8, 86.1, 83.5, 65.3, 30.1, 27.8, 22.5, 13.8. ESI-MS calcd for $\text{C}_{14}\text{H}_{20}\text{N}_5\text{O}_2$: $[(\text{M} + \text{H})^+]$: 290.1617, found: 290.1616.

References

- (1) Garrett, R. H.; Grisham, C. M. *Principles of biochemistry: with a human focus*; Brooks/Cole Pub Co, 2001.
- (2) Neidle, S.; ScienceDirect *Principles of nucleic acid structure*; Elsevier, 2008.
- (3) Agrofoglio, L.; Suhas, E.; Farese, A.; Condom, R.; Richard Challand, S.; A. Earl, R.; Guedj, R. *Tetrahedron* **1994**, *50*, 10611.
- (4) Volpini, R.; Dal Ben, D.; Lambertucci, C.; Marucci, G.; Mishra, R.; Ramadori, A.; Klotz, K. N.; Trincavelli, M.; Martini, C.; Cristalli, G. *ChemMedChem* **2009**, *4*, 1010.
- (5) Cristalli, G.; Eleuteri, A.; Vittori, S.; Volpini, R.; Lohse, M. J.; Klotz, K. N. *Journal Of Medicinal Chemistry* **1992**, *35*, 2363.
- (6) Seley, K. L.; Mosley, S. L.; Zeng, F. *Organic Letters* **2003**, *5*, 4401.
- (7) Rodriguez, J. B.; Comin, M. J. *Mini Reviews in Medicinal Chemistry* **2003**, *3*, 95.
- (8) Borthwick, A. D.; Biggadike, k. *Tetrahedron* **1992**, *48*, 571.
- (9) Yuan, C.-S.; Liu, S.; Wnuk, S. F.; Robins, M. J.; Borchardt, R. T.; Clercq, E. D. In *Advances in Antiviral Drug Design*; Elsevier: 1996; Vol. Volume 2, p 41.
- (10) Shealy, Y. F.; Clayton, J. D. *Journal of the American Chemical Society* **1966**, *88*, 3885.
- (11) Kusaka, T.; Yamamoto, H.; Shibata, M.; Muroi, M.; Kishi, T. *The Journal of Antibiotics*, **1968**, *21*, 255.

- (12) Hayashi, M.; Yaginuma, S.; Yoshioka, H.; Nakatsu, K. *The Journal of Antibiotics* **1981**, *34*, 675.
- (13) Cools, M.; De Clercq, E. *Biochemical Pharmacology* **1990**, *40*, 2259.
- (14) Wolfe, M. S.; Borchardt, R. T. *Journal of Medicinal Chemistry* **1991**, *34*, 1521.
- (15) Borcharding, D. R.; Narayanan, S.; Hasobe, M.; McKee, J. G.; Keller, B. T.; Borchardt, R. T. *Journal Of Medicinal Chemistry* **1988**, *31*, 1729.
- (16) Guranowski, A.; Montgomery, J. A.; Cantoni, G. L.; Chiang, P. K. *Biochemistry* **1981**, *20*, 110.
- (17) De Clercq, E.; Cools, M.; Balzarini, J.; Marquez, V. E.; Borcharding, D. R.; Borchardt, R. T.; Drach, J. C.; Kitaoka, S.; Konno, T. *Antimicrobial Agents and Chemotherapy* **1989**, *33*, 1291.
- (18) Glazer, R. I.; Knode, M. C. *Journal of Biological Chemistry* **1984**, *259*, 12964.
- (19) Turner, M.; Yang, X.; Yin, D.; Kuczera, K.; Borchardt, R.; Howell, P. *Cell Biochemistry and Biophysics* **2000**, *33*, 101.
- (20) Cantoni, G. L. *Journal of Biological Chemistry* **1953**, *204*, 403.
- (21) Borchardt, R. T. *Journal of Medicinal Chemistry* **1980**, *23*, 347.
- (22) Banerjee, A. K. *Microbiology and Molecular Biology Reviews* **1980**, *44*, 175.
- (23) Mao, X.; Schwer, B.; Shuman, S. *Molecular and Cellular Biology* **1995**, *15*, 4167.
- (24) Lentz, S. R. *Life Sciences* **1997**, *61*, 1205.
- (25) McKeever, M. P.; Weir, D. G.; Molloy, A.; Scott, J. M. *Clinical Science* **1991**, *81*, 551.
- (26) Abeles, J. L. P. R. H. *Journal of Biological Chemistry* **1976**, *251*, 5817.
- (27) Palmer, J. L.; Abeles, R. H. *Journal of Biological Chemistry* **1979**, *254*, 1217.

- (28) Lee, K. M.; Choi, W. J.; Lee, Y.; Lee, H. J.; Zhao, L. X.; Lee, H. W.; Park, J. G.; Kim, H. O.; Hwang, K. Y.; Heo, Y.-S.; Choi, S.; Jeong, L. S. *Journal of Medicinal Chemistry* **2011**, *54*, 930.
- (29) Sumin Cai, Q.-S. L., Jianwen Fang, Ronald T. Borchardt,; Krzysztof Kuczera, C. R. M., and Richard L. Schowen *Nucleosides, Nucleotides and Nucleic Acids* **2009**, *28*, 485.
- (30) Liu, S.; Wolfe, M. S.; Borchardt, R. T. *Antiviral Research* **1992**, *19*, 247.
- (31) Wolfe, M. S.; Lee, Y.; Bartlett, W. J.; Borchardt, D. R.; Borchardt, R. T. *Journal of Medicinal Chemistry* **1992**, *35*, 1782.
- (32) Borchardt, D. R.; Scholtz, S. A.; Borchardt, R. T. *Journal of Organic Chemistry* **1987**, *52*, 5457.
- (33) Chiang, P. K., *Pharmacology and Therapeutics* **1998**, *77*, 115.
- (34) De Clercq, E. *Antimicrobial Agents and Chemotherapy* **1985**, *28*, 84.
- (35) Saenger, W.; Springer Advanced Texts in Chemistry. Springer-Verlag, New York, NY: 1984.
- (36) Rosemeyer, H.; Toth, G.; Golankiewicz, B.; Kazimierzuk, Z.; Bourgeois, W.; Kretschmer, U.; Muth, H. P.; Seela, F. *Journal of Organic Chemistry* **1990**, *55*, 5784.
- (37) Tvaroska, I.; Hricovíni, M.; Petráková, E. *Carbohydrate Research* **1989**, *189*, 359.
- (38) Blackburn, G. M. *Nucleic acids in chemistry and biology*; Royal Society of Chemistry, 2006.
- (39) Kilpatrick, J. E.; Pitzer, K. S.; Spitzer, R. *Journal of the American Chemical Society* **1947**, *69*, 2483.
- (40) Hall, L. D.; Steiner, P. R.; Pedersen, C. *Canadian Journal of Chemistry* **1970**, *48*, 1155.

- (41) Thibaudeau, C.; Chattopadhyaya, J. *Stereoelectronic effects in nucleosides and nucleotides and their structural implications*; Uppsala University Press Uppsala, 1999.
- (42) Altona, C.; Sundaralingam, M. *Journal of the American Chemical Society* **1972**, *94*, 8205.
- (43) Altona, C.; Sundaralingam, M. *Journal of the American Chemical Society* **1973**, *95*, 2333.
- (44) Saenger, W. *Principles of Nucleic Acid Structure*, C.R. Cantor (Ed.); Springer Advanced Texts in Chemistry. Springer-Verlag, New York, NY, 1984.
- (45) Westhof, E.; Röder, O.; Croneiss, I.; Lüdemann, H. D. *Zeitschrift für Naturforschung. Section C: Biosciences* **1975**, *30*, 131.
- (46) Davies, D. B.; Danyluk, S. S. *Biochemistry* **1974**, *13*, 4417.
- (47) Sundaralingam, M. *Annals of the New York Academy of Sciences* **1975**, *255*, 3.
- (48) Aoyagi, M.; Minakawa, N.; Matsuda, A. *Tetrahedron Letters* **1993**, *34*, 103.
- (49) Rhodes, L. M.; Schimmel, P. R. *Biochemistry* **1971**, *10*, 4426.
- (50) Stolarski, R.; Dudycz, L.; Shugar, D. *European Journal of Biochemistry* **1980**, *108*, 111.
- (51) Blackburn, B. J.; Grey, A. A.; Smith, I. C. P.; Hruska, F. E. *Canadian Journal of Chemistry* **1970**, *48*, 2866.
- (52) Rosemeyer, H.; Zulauf, M.; Ramzaeva, N.; Becher, G.; Feiling, E.; Mühlegger, K.; Münster, I.; Lohmann, A.; Seela, F. *Nucleosides, Nucleotides and Nucleic Acids* **1997**, *16*, 821.
- (53) Crimmins, M. T. *Tetrahedron* **1998**, *54*, 9229.
- (54) Ikehara, M.; Uesugi, S.; Yoshida, K. *Biochemistry* **1972**, *11*, 830.

- (55) Sarma, R. H.; Lee, C. H.; Evans, F. E.; Yathindra, N.; Sundaralingam, M. *Journal of the American Chemical Society* **1974**, *96*, 7337.
- (56) Bookser, B. C.; Matelich, M. C.; Ollis, K.; Ugarkar, B. G. *Journal Of Medicinal Chemistry* **2005**, *48*, 3389.
- (57) Van Aerschot, A. A.; Mamos, P.; Weyns, N. J.; Ikeda, S.; De Clercq, E.; Herdewijn, P. *A. Journal Of Medicinal Chemistry* **1993**, *36*, 2938.
- (58) Van der Werten, E. M.; Hartog-Witte, H. R.; Roelen, H. C. P. F.; von Frijtag Drabbe Künzel, J. K.; Pirovano, I. M.; Mathôt, R. A. A.; Danhof, M.; Van Aerschot, A.; Lidaks, M. J.; Ijzerman, A. P.; Soudijn, W. *European Journal of Pharmacology: Molecular Pharmacology* **1995**, *290*, 189.
- (59) Palczewski, K.; Kahn, N.; Hargrave, P. A. *Biochemistry* **1990**, *29*, 6276.
- (60) Hasobe, M.; McKee, J. G.; Borcharding, D. R.; Borchardt, R. T. *Antimicrobial agents and chemotherapy* **1987**, *31*, 1849.
- (61) Keller, B. T.; Clark, R. S.; Pegg, A. E.; Borchardt, R. T. *Molecular Pharmacology* **1985**, *28*, 364.
- (62) M. J. Frisch, G. W. T., H. B. Schlegel, G. E. Scuseria,; M. A. Robb, J. R. C., J. A. Montgomery, Jr., T. Vreven,; K. N. Kudin, J. C. B., J. M. Millam, S. S. Iyengar, J. Tomasi,; V. Barone, B. M., M. Cossi, G. Scalmani, N. Rega,; G. A. Petersson, H. N., M. Hada, M. Ehara, K. Toyota,; R. Fukuda, J. H., M. Ishida, T. Nakajima, Y. Honda, O. Kitao,; H. Nakai, M. K., X. Li, J. E. Knox, H. P. Hratchian, J. B. Cross,; V. Bakken, C. A., J. Jaramillo, R. Gomperts, R. E. Stratmann,; O. Yazyev, A. J. A., R. Cammi, C. Pomelli, J. W. Ochterski,; P. Y. Ayala, K. M., G. A. Voth, P. Salvador, J. J. Dannenberg,; V. G. Zakrzewski, S. D., A. D. Daniels, M. C. Strain,; O. Farkas, D. K. M., A. D.

- Rabuck, K. Raghavachari,; J. B. Foresman, J. V. O., Q. Cui, A. G. Baboul, S. Clifford,; J. Cioslowski, B. B. S., G. Liu, A. Liashenko, P. Piskorz,; I. Komaromi, R. L. M., D. J. Fox, T. Keith, M. A. Al-Laham,; C. Y. Peng, A. N., M. Challacombe, P. M. W. Gill,; B. Johnson, W. C., M. W. Wong, C. Gonzalez, and J. A. Pople,; Gaussian, I., Wallingford CT, 2004. **2004**.
- (63) Becke, A. D. *Physical Review A* **1988**, *38*, 3098.
- (64) Lee, C.; Yang, W.; Parr, R. G. *Physical Review B* **1988**, *37*, 785.
- (65) Tomasi, J.; Persico, M. *Chemical Reviews* **1994**, *94*, 2027.
- (66) Dunning, T. H. *Journal of Chemical Physics* **1989**, *90*, 1007.
- (67) Akdag, A.; Carver, C. M.; McKee, M. L.; Schneller, S. W. *Journal of Physical Chemistry A* **2002**, *106*, 11254.
- (68) Sun, G.; Voigt, J. H.; Filippov, I. V.; Marquez, V. E.; Nicklaus, M. C. *Journal of chemical information and computer sciences* **2004**, *44*, 1752.
- (69) Arpalahti, J.; D. Klika, K.; Sillanpaa, R.; Kivekas, R. *Journal of the Chemical Society, Dalton Transactions* **1998**, 1397.
- (70) Ciuffreda, P.; Casati, S.; Manzocchi, A. *Magnetic Resonance in Chemistry* **2007**, *45*, 781.
- (71) Stolarski, R.; Pohorille, A.; Dudycz, L.; Shugar, D. *Biochimica et Biophysica Acta (BBA) - Nucleic Acids and Protein Synthesis* **1980**, *610*, 1.
- (72) Miyashita, O.; Kasahara, F.; Kusaka, T.; Marumoto, R. *The Journal of Antibiotics* **1985**, *38*, 981.
- (73) Madhavan, G. V. B.; Martin, J. C. *Journal of Organic Chemistry* **1986**, *51*, 1287.

- (74) Montgomery, J. A.; Clayton, S. J.; Thomas, H. J.; Shannon, W. M.; Arnett, G.; Bodner, A. J.; Kion, I. K.; Cantoni, G. L.; Chiang, P. K. *Journal Of Medicinal Chemistry* **1982**, 25, 626.
- (75) Yang, M.; Zhou, J.; Schneller, S. W. *Tetrahedron Letters* **2004**, 45, 8981.
- (76) Ludek, O. R.; Marquez, V. E. *Synthesis* **2007**, 2007, 3451.
- (77) Rodriguez, J. B.; Marquez, V. E.; Nicklaus, M. C.; Mitsuya, H.; Barchi, J. J. *Journal Of Medicinal Chemistry* **1994**, 37, 3389.
- (78) Palmer, Andreas M.; Jäger, V. *European Journal Of Organic Chemistry* **2001**, 2001, 1293.
- (79) Jin, Y. H.; Liu, P.; Wang, J.; Baker, R.; Huggins, J.; Chu, C. K. *Journal of organic chemistry* **2003**, 68, 9012.
- (80) Paquette, L. A.; Bailey, S. *Journal of Organic Chemistry* **1995**, 60, 7849.
- (81) Yang, M.; Ye, W.; Schneller, S. W. *Journal of organic chemistry* **2004**, 69, 3993.
- (82) Grubbs, R. H.; Chang, S. *Tetrahedron* **1998**, 54, 4413.
- (83) Poeylout-Palena, A. A.; Testero, S. A.; Mata, E. G. *Journal of Organic Chemistry* **2008**, 73, 2024.
- (84) Hale, K. J.; Domostoj, M. M.; Tocher, D. A.; Irving, E.; Scheinmann, F. *Organic Letters* **2003**, 5, 2927.
- (85) Kurteva, V. B.; Afonso, C. A. M. *Chemical Reviews* **2009**, 109, 6809.
- (86) Hong, S. H.; Grubbs, R. H. *Journal of the American Chemical Society* **2006**, 128, 3508.
- (87) Casey, C. P. *Journal of Chemical Education* **2006**, 83, 192.
- (88) Schmalz, H.-G. *Angewandte Chemie International Edition in English* **1995**, 34, 1833.
- (89) Trnka, T. M.; Grubbs, R. H. *Accounts of Chemical Research* **2000**, 34, 18.

- (90) Lister, J. H. *Syntheses from Pyrimidines*; John Wiley & Sons, Inc., 2008; Vol. 24.
- (91) Montgomery, J. A. *Journal of the American Chemical Society* **1956**, 78, 1928.
- (92) Koppel, H. C.; Robins, R. K. *Journal of Organic Chemistry* **1958**, 23, 1457.
- (93) Mornet, R.; Leonard, N. J.; Theiler, J. B.; Doree, M. *Journal of the Chemical Society, Perkin Transactions 1* **1984**, 879.
- (94) Lister, J. H.; Fenn, M. D. *Synthesis from Pyrimidines*; John Wiley & Sons, Inc., 2008; Vol. 54.
- (95) Ueda, T.; Nomoto, Y.; Matsuda, A. *Chemical & Pharmaceutical Bulletin* **1985**, 33, 3263.
- (96) Kitade, Y.; Kozaki, A.; Miwa, T.; Nakanishi, M. *Tetrahedron* **2002**, 58, 1271.
- (97) Barton, D. H. R.; Hedgecock, C. J. R.; Lederer, E.; Motherwell, W. B. *Tetrahedron Letters* **1979**, 20, 279.
- (98) Hayakawa, H.; Haraguchi, K.; Tanaka, H.; Miyasaka, T. *Chemical & Pharmaceutical Bulletin* **1987**, 35, 72.
- (99) Rosemeyer, H.; Seela, F. *Journal of the Chemical Society, Perkin Transactions 2* **1997**, 2341.
- (100) Johnson, C. R.; Chen, Y. F. *Journal of organic chemistry* **1991**, 56, 3344.

Appendix

Data for linear regression calculation of AA:

```
#!/bin/ksh
```

```
#
```

```
touch EE.txt
```

```
for ((a=0.0; a<=1.0; a=a+0.01))
```

```
do
```

```
    b=$((1.0-$a))
```

```
    min1=$((7.8*$a+0.0*$b-6.1))
```

```
    echo $(( $min1*$min1 )) > MIN1
```

```
    min2=$((6.4*$a+6.1*$b-5.3))
```

```
    echo $(( $min2*$min2 )) > MIN2
```

```
    min3=$((-0.2*$a+7.8*$b-3.4))
```

```
    echo $(( $min3*$min3 )) > MIN3
```

```
if (( $a+$b <= 1.0 ))
```

```
then
```

```
    mint=$(( $min1*$min1 + $min2*$min2 + $min3*$min3 ))
```

```
echo $mint > MINT
```

```
echo $a > A
```

```
echo $b > B
```

```
paste A B MINT|awk '{printf ("%5.2f%5.2f%8.2f\n",$1,$2,$3)}' >> EE.txt
```

```
fi
```

```
done
```

```
/bin/rm MIN1 MIN2 MIN3 MINT A B
```